Thermal Indices and Thermophysiological Modeling for Heat Stress

George Havenith[*1] *and Dusan Fiala*[2]

ABSTRACT

The assessment of the risk of human exposure to heat is a topic as relevant today as a century ago. The introduction and use of heat stress indices and models to predict and quantify heat stress and heat strain has helped to reduce morbidity and mortality in industrial, military, sports, and leisure activities dramatically. Models used range from simple instruments that attempt to mimic the human-environment heat exchange to complex thermophysiological models that simulate both internal and external heat and mass transfer, including related processes through (protective) clothing. This article discusses the most commonly used indices and models and looks at how these are deployed in the different contexts of industrial, military, and biometeorological applications, with focus on use to predict related thermal sensations, acute risk of heat illness, and epidemiological analysis of morbidity and mortality. A critical assessment is made of tendencies to use simple indices such as WBGT in more complex conditions (e.g., while wearing protective clothing), or when employed in conjunction with inappropriate sensors. Regarding the more complex thermophysiological models, the article discusses more recent developments including model individualization approaches and advanced systems that combine simulation models with (body worn) sensors to provide real-time risk assessment. The models discussed in the article range from historical indices to recent developments in using thermophysiological models in (bio) meteorological applications as an indicator of the combined effect of outdoor weather settings on humans.
 Compr Physiol 6:255-302, 2016.

Introduction

Heat stress is a topic that has been important in an occupational, military operational, sports, and leisure context. Many incidents have been reported of heat illness in these settings, pushing forward research on the assessment of heat stress for the purpose of providing guidelines and limit values for the assessment of the risk (14). Also in the context of global warming, such risk assessment for occupational exposure and for the general public health has gained interest. Over the last 70+ years, a range of over 160 different climatic stress indices have been developed (42) of which over 100 are for heat stress (9, 81) (see Table 1). Many of these have seen only limited application since their inception while a few have become popular and are widely used. These indices vary substantially in their complexity and ease of use. Their popularity is in part determined by their simplicity, while the lack of use of some is related to them considering only part of human heat transfer.

The ideal heat-stress-assessment method will need to consider all aspects of heat generation inside the body and all pathways for heat exchange between the body and the environment. In other words, an ideal model does a full assessment of the human heat balance (99):

$$\text{Heat storage in the body} = \text{heat production} - \text{heat loss} \quad (1)$$

The amount of heat storage ("*S*") in the body and the rate at which this occurs then show the effect the climate combined with the work performed and the clothing worn (the external factors, representing the "stress") have on the physiological responses (the internal response, representing the "strain") experienced by the person. Heat production (metabolic rate "*M*") is defined by the work rate ("*W*") and the type of work (whether virtually all energy used is released as heat in the body (e.g., in walking on a level surface) or whether a part is released outside the body, for example, as mechanical energy in a cycle ergometer). Heat loss is defined by the components of heat exchange: conduction ("*K*"), convection ("*C*"), evaporation ("*E*"), respiration ("Resp"), and radiation ("*R*"). Rewriting Eq. (1) as:

$$S = M - (W + C + R + K + E + \text{Resp}) \quad (2)$$

All heat losses are driven by the, for each specific type of heat-exchange relevant, gradient in temperature (temperature of surfaces touching; ambient temperature and mean radiant temperature) or vapor pressure. Hence, for such a full model,

[*]Correspondence to g.havenith@lboro.ac.uk

[1]Environmental Ergonomics Research Centre, Loughborough Design School, Loughborough University, Loughborough, United Kingdom

[2]Ergonsim—Human Thermal Modelling, Marxzell, Germany

Published online, January 2016 (*comprehensivephysiology.com*)

DOI: 10.1002/cphy.c140051

Table 1 Historical Overview of Thermal Indices and Models for Heat-Stress Assessment; Collated and Supplemented from Belding (9; with Kind Permission of Charles C Thomas Publisher Ltd., Springfield, Illinois) Goldman (81; with Permission of Taylor & Francis) and de Freitas and Grigorieva (42; with Permission Int. J. Biometeorology)

Date	Index	Author(s)	Source	Description
1905	Wet-bulb temperature	Haldane (94)	*J Hygiene*, 5: 494, 1905	A better indicator of physiological effect than dry bulb temperature in hot, wet confined spaces
1916	Kata thermometer	Hill et al. (109)	*Phil Trans*, 207: 183, 1916	Rate of cooling of a previously warmed thermometer covered with a wetted wick is related to radiant, convective and maximal evaporative heat exchange
1923	Effective temperature (ET)	Houghton and Yaglou (114)	*J Amer Soc Heat Vent Eng*, 29: 515, 1923	Combinations of DB, WB, and velocity which yield equal sensations of comfort are assigned an ET equal to that of saturated, low V air which yields the same sensation
1937	Operative temperature (OT)	Winslow et al. (256)	*Amer J Physiol*, 120: 1, 1937	Uses heat transfer coefficients to reduce the effect of prevailing T_{rad}, T_a, and V to equivalent temperature if T_{rad} = Ta with minimum air movement
1945	Thermal acceptance ratio	Ionides et al. (122)	OQMG, Environ. Protection Report, Sept 17, 1945	Index defined as ratio = H_a/M; M is rate of body heat production, H_a is rate of acceptance of heat by environment for unclothed subjects with T_s = 36°C
1945	Index of physiological effect (I)	Robinson et al. (214)	*Amer J Physiol*, 143: 21	Combinations of T_a and T_{wb} at three levels of activity, which impose equivalent average demand in terms of elevation of HR, T_s, T_{re}, and sweat rate
1946	Corrected effective temperature (CET)	Bedford (8)	Med. Res. Council Memo 17, HMSO, London, 1946	Modifies ET scale, with 15 cm black globe temperature (T_g) for thermal radiation
1947	Probable 4-hour sweat rate (P4SR)	McArdle et al. (172)	Med. Res. Council R.N.P. Rep., 47: 391, 1947	Uses sweating to indicate physiological strain; predicts 4 h rate for combinations of M, T_g, T_{wb}, and V; clothing adjustment and computation method suggested later
1948	Resultant temperature (RT)	Missenard et al. (176)	Chaleur et Industrie, Jul-Aug 1948	Same basis as ET except exposures were longer and equilibrium obtained. Intended for rest only. Better estimation of effect of humidity than ET
1950	Craig index	Craig (33)	USA Chem. Corps Med. Div. Res. Rpt, 5, 1950	Modifies Robinson 1948 index of physiological effects so that $I = T + S + H/100$, where H = heart rate, $T = \Delta T_{re}$ in °C·h^{-1}, and S = sweat rate in kg h^{-1}
1955	Heat stress index (HSI)	Belding and Hatch (10)	*Heat Pip Air Cond*, 27: 129, 1955	Ratio between heat load ($M + R + C = E_{req}$) and evaporative capacity of environment (E_{max}; first use); uses coefficients of Nelson et al., Amer. *Physiol*, 151: 626, 1947
1957	Wet-bulb globe temp (WBGT)	Yaglou and Minard (271)	*AMA Arch Ind Health*, 16: 302, 1957	WBGT = 0·7 T_{wb} + 0·2 T_g + 0·1 T_{db}, where T_{wb} is nonaspirated, "natural" wet bulb
1957	Oxford index (WD)	Lind and Hellon (162)	*Appl Physiol*, 11: 35, 1957	WD = 0·85 T_{wb} + 0·15 T_{db}. Formula for deriving estimate of ET from T_a and T_{wb}
1957	Discomfort index (DI)	Thom (240)	*Air Cond Heat Vent*, 54: 73, 1957	Discomfort index, DI = 0·4 (T_{db} + T_{wb}) + 15
1958	Thermal strain index	Lee and Henschel (157)	Arid Zone Res, 10, UNESCO, Paris, 1958	Empirical equation involving R, C, M, clothing, and V. Similar to HSI
1962	Index of thermal stress	Givoni (74)	UNESCO Symposium on Arid Cond, India, 1962	Predicts sweat rate on basis of heat load, utilizing concept of efficiency of sweating or its reciprocal
1965	Heat strain predictive systems	Lustinec (in 81)	Thesis, Czech. Univivrsity, 1962	Predicts HSI under effects of variable clothing

Table 1 (*Continued*)

Date	Index	Author(s)	Source	Description
1966	New nomographs for HSI	McKars and Brief (173)	*Heat Pip Air Cond*, 38: 113, 1966; *J Occup Environ Med* 8.10: 557, 1966	Based on refined coefficients where $E_{req} = M + 17{\cdot}5\ (t_w - 95) + 0{\bullet}756\ V^{0.6}\ (T_a - 95)$: $E_{max} = 2.8\ VO^{0.6}\ (42 - VPa)$ in Btu, °F, fpm, and mmHg
1967	Effective radiant field	Gagge et al. (72)	*ASHRAE Trans*, 73: 1, 1967	Combines operative temperature and radiant heat
1970	Comfort vote & % dissatisfied	Fanger (53)	Thermal Comfort, Danish Tech. Press, 1970	Uses modified heat balance to predict comfort vote (PMV) and % predictably dissatisfied (PPD)
1970	Prescriptive zone	Lind (161)	*J Appl Physiol*, 28, 57, 1970	Uses inflection point of T_{re} increase.
1971	Humid operative temperature	Gagge (68)	*ASHRAE Trans*, 77: 247, 1971	Utilizes humid operative temperature (T_{oh}) to derive new T_{eff}, based on an interaction of constant skin wettedness loci with T_{db} for the 50% RH curve
1971	Wet globe temperature (WGT)	Botsford (18)	*AIHA J*, 32: 1, 1971	A copper sphere covered by a wetted black cloth provides one number for heat stress. Comparable to WBGT
1972	Predicted body temperature (Tre)	Givoni and Goldman (77)	*J Appl Physiol*, 38: 812, 1972	Utilizes function of $E_{req} - E_{max}$ to predict T_{re} response for given environment, clothing and work
1972	Skin wettedness	Kerslake (143)	Stress of Hot Environments, Cambridge University Press, 1972	Expression for skin humidity based on Gagge's concept of skin wettedness, *Amer J Physiol*, 120: 277, 1937
1973	Standard effective temperature (SET)	Gagge et al. (70)	Thermal Comfort Mod. Heat Stress, Proc. Build. Res. Estab. Conf., 1972	Translates the reference for effective temperature from the original 100% RH base to a subjectively more familiar 50% RH
1973	Predicted heart rate	Givoni and Goldman (78)	*J Appl Physiol*, 34: 201, 1973	Predicts HR response for given environment, clothing and work using predicted T_{re}; acclimatization modification added *J Appl Physiol*, 35: 875, 1973
1976	Heart rate	Dayal and Ramsey (81)	Proceedings of the 6th International Ergon. Congress, Maryland, 1976	Suggests using heart rate as an index of heat stress
1978	Skin wettedness	Gonzalez et al. (84)	*J Appl Physiol*, 44: 889, 1978	Measurement of skin wettedness by dew point sensors as index of physiological strain
1978	Fighter index of thermal stress (FITS)	Nunneley and Stribley (196)	*Aviat Space Env Med*, 1979	$FITS = 0{\cdot}828\ T_{wb} + 0{\cdot}355\ T_{DE} + 5{\cdot}04$ predicts plane cockpit conditions from ground readings
1982	Predicted sweat loss	Shapiro et al. (226)	*Eur J Appl Physiol*, 48: 83, 1982	Uses E_{req} and E_{max} to predict sweat rate
1985	Required sweating	Vogt, Malchaire (168, 248)	ISO 7933: 1989	Calculated sweat production for temperature regulation as an index of thermal stress and physiological strain; limits, based on heat storage, adjust exposure time
2001	PHS Index	Malchaire et al. (170)	*Ann Occup Hygiene* 45(2): 123-135.ISO 7933: 2004	Calculated sweat production for temperature regulation as an index of thermal stress and physiological strain; with prediction of rectal temperature development as strain indicator. Limits, based on heat storage, adjust exposure time
2002	Thermal Work Limit	Brake and Bates (19)	*Appl Occup Environ Hygiene*, 17(3): 176-186	Uses metabolic rate limit as indicator of stress based on heat balance requirements
2012	Universal Thermal Climate Index UTCI	Jendritzky et al. (123, 125)	Commission 6 ISB and WMO initiative. EU COST action project.*Int J Biometeorol*, 56(3): 421-428, 2012 (special issue on UTCI)	First thermal index based on a physiological simulation model, covering the whole climate range from heat to cold. Initially designed for weather information services and as parameter in epidemiological studies

which will be discussed in detail later one would need to know:

- ambient air temperature (T_a),
- temperature of surfaces in contact with the body,
- mean radiant temperature (including short and long wave radiation, T_{mrt}),
- ambient vapor pressure (P_a),
- air velocity ($m \cdot s^{-1}$)
- heat produced and released in body [metabolic rate (M) – externally released energy (W_{ext}), watt or $W \cdot m^{-2}$],
- resultant clothing insulation [the insulation in actual conditions incorporating effects of movement and wind (105); affecting all dry heat transfers, I_T], and
- resultant clothing vapor resistance (the vapor resistance in actual conditions incorporating effects of movement and wind (102); affecting evaporative heat transfer, R_{ET}].

Apart from the difficulty to measure all these parameters accurately, and in the last century the limited availability of cheap and compact computing power (for portable instruments), it may be understandable that this approach of a full analysis of the heat balance was not an option in many situations especially before the 1970s. Hence, most heat-stress models do not include all these factors and are thus simplified representations of the environmental stress, as opposed to models of physiological response, dealing with the strain induced by the climate. The models produced over the years range from equations that calculate an index value from only ambient temperature and humidity to complex computer models of human thermal physiology that simulate exposures to determine the expected physiological strain induced by the climate. Some have linked the observed index values to historical data on heat illness and in that way have established an empirical relation between index value and risk (empirical or direct model). The more complex indices typically calculate body heat-storage rate and physiological responses of which limit values are known from the physiological literature (analytical or rational model). This article will cover both types of heat stress models, empirical/direct, and rational/analytical. It will focus mainly on models that are still widely used, and in some cases give an example of the model type rather than discussing all variants. As such, a split is made between models used in occupational settings (industrial and military) and those that are used in a meteorological or epidemiological context. The first group tends to look at short-term imminent risk, often at high workloads and/or while wearing protective clothing, while the second focuses typically on perception of the circumstances and longer term risk on a population basis.

Industrial and Military Indices

For protection of workers in acute heat exposure, a number of indices, standards, and models have been developed that will be presented here. These are slightly different from those that were developed in a meteorological or epidemiological context. In the latter, the emphasis is on sensation (how does the condition feel) and population wide-risk assessment rather than individual or small group exposure.

Wet bulb globe temperature

Of all the empirical or direct indices reviewed by Goldman (81), only the WBGT, the Wet Bulb Globe Temperature Index, is still in widespread use for heat-stress management (personal communications with experts in ISO TC159/SC5/WG1). This method is formalized for industrial applications in an ISO and European standard, ISO 7243 [Hot environments—Estimation of the heat stress on working man, based on the WBGT-index (wet bulb globe temperature)] (117). For application in sports events, the method of use is defined in the American College of Sports Medicine position stand "Exertional Heat illness during training and competition" by Armstrong et al. (4). For military use, it is described in internal military reports of different countries (e.g., 43). The main differences between these application documents is the definition of the work load, each giving relevant examples in the limit tables for their own application area.

WBGT was developed as a control measure for heat stress in training camps in the United States military in the 1950s (for an extensive historical review, see Budd, 2008; 22). Large numbers of heat related casualties were reported in the 1940s and early 1950s. Between 1942 and 1945, heat-stroke incidence with lethal outcomes affected 197 soldiers. Surprisingly, this incidence was four times higher than observed in active service in hot deployment areas (32, 223). In 1952, 500+ cases of heat illness (mainly heat exhaustion) occurred at Paris Island (SC), and between 1951 and 1953 six recruits died from heat stroke (175). Initial attempts to control the heat exposures made use of ET, effective temperature, which uses ambient temperature and relative humidity as input parameters. This was followed by ETR, "effective temperature including a radiation component" (271), which had the practical complication of requiring a direct measurement of wind speed (no cheap instruments for this were available at the time) and a number of calculation steps, making it impractical for use by commanders in the field. Lacking a good and simple to use representation of the heat-load impact of solar radiation and of the cooling power of wind, researchers (271) looked at other combinations of climate parameters (test instruments) to construct a better or easier to use heat stress index and, in several iterations, came up with the WBGT index. This, together with a better enforcement of heat-stress-management strategies indeed reduced the incidence of heat illness (from 53 per 10,000 trainees per week in 1953 to below 10 in 1954 and 12 in 1955). Since those days, WBGT has seen little change

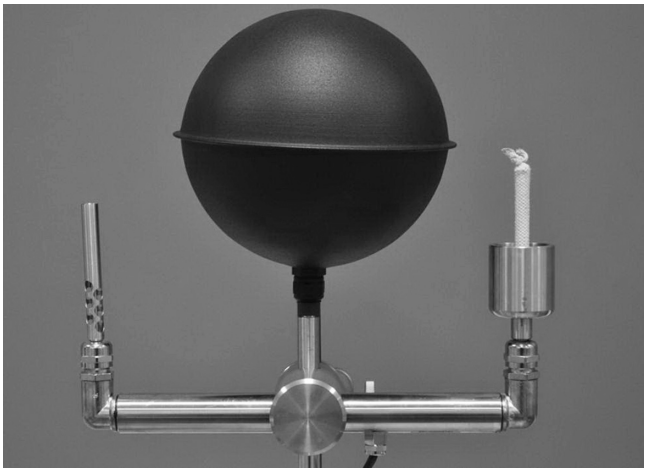

Figure 1 Official WBGT instrument according to ISO 7726 and ISO 7243, showing (left to right) shielded dry bulb, black globe (15 cm diameter), and natural wet bulb (wetted cotton wick over sensor with water reservoir below) sensors.

though attempts have been made to simplify the instrument, and to get a better incorporation of the effects of protective clothing (e.g., by trying to manipulate the sensor's color to account for different clothing colors or by changing weight factors to do this (22).

WBGT, is based on two, or in presence of solar radiation three, sensors (see Fig. 1). (i) A black globe (T_g), originally based on a black painted copper toilet cistern float of 15 cm diameter with a temperature sensor in its center; (ii) a natural wet bulb temperature (T_{nwb}), that is, a thermometer covered with a wet cotton wick suspended and exposed to the ambient wind and radiation; and (iii) a regular dry bulb thermometer, shielded from radiation. The black globe will have the same temperature as a dry bulb thermometer in the absence of solar or other radiation, for example, from hot objects, but with added heat radiation it will warm up above the air temperature, and when it is warmed up (and only then), it also is sensitive to the cooling power of any wind present (under a night sky, the value can be lower than ambient temperature, but that is outside the WBGT remit). The natural wet bulb temperature represents the cooling effect of evaporation from the wick. Thus, it is not only affected by the ambient relative humidity, but also by wind as that enhances evaporation. Finally, as it is not shielded, it will also be affected by any radiation present. The shielded dry bulb temperature (T_{db}) is only affected by ambient air temperature (though in practice, in extreme radiation conditions, the shield tends to warm up, causing the sensor to measure temperatures above the real T_a). The first two sensors thus combine the effects of radiation, air temperature, humidity, and wind. From these, WBGT is defined as:

$$\mathrm{WBGT} = 0.7T_{nwb} + 0.3T_g \quad (3)$$

And for conditions with solar radiation

$$\mathrm{WBGT} = 0.7T_{nwb} + 0.2T_g + 0.1T_{db} \quad (4)$$

In an ideal case, an instrument like WBGT should be affected by the climate in the same way as the human body is. Being sensitive to convection, conduction, evaporation, and radiation this index achieved good results in general, but it does have certain features that may cause it to deviate notably from a human's response to heat. For example, when there is no radiation, the globe takes on ambient temperature and is not sensitive to wind. The human skin, usually warmer than the environment temperature, will be sensitive to wind in that condition. Also, at 100% relative humidity, the wet bulb takes on ambient temperature, suggesting no evaporative heat loss is possible and it is insensitive to wind. Again, our skin is usually warmer than the environment and even if the environment is 100% humid, the vapor pressure on wet skin would be higher than that in the environment, resulting in evaporative mass and heat loss with sensitivity to wind. Such issues result in the two different equations for WBGT depending on the presence of solar radiation and also in different WBGT limit values for conditions with and without sensible air movement (see Tables 2 and 3). Using thermal models of the instrument and of human thermoregulation, Lotens (164) compared responses of the instrument with calculated heat-strain values for different climate types (wet, radiant, or high air temperature) all with equal WBGT. He observed different levels of heat strain at these equal WBGT conditions and found a lower sensitivity to wind for WBGT in low-radiation environments while in high-radiation environments, the sensitivity of WBGT for wind was higher than that of humans.

Clothing and the wet bulb globe temperature

ISO 7243 limits the application of WBGT to light clothing (0.6 clo insulation). This clearly restricts its usability and thus it is not surprising that for many industrial or military applications where protective clothing is worn researchers have come up with correction factors to WBGT for different clothing (5, 11, 12, 139) which amount up to 11°C shifts in the limit values. By exposing test participants in different protective clothing ensembles to a heat-stress protocol of increasing temperature or vapor resistance, Kenney et al. and Bernard et al.'s method looks for the inflection point in core temperature, that is, the point where core temperature cannot be controlled by the participant at the same level as before and starts to rise (140, 141). This deflection point shifts to lower temperatures or humidities when evaporative heat loss is attenuated by clothing, and thus this shift indicates the added load of the clothing and as such has been translated into a "WBGT penalty" (11, 12). This can practically be used in two ways with the same outcome: one is to add this penalty to the measured WBGT and use the standard reference values, the other is to lower the reference limit values by this clothing penalty, creating a clothing adjusted limit. Examples of proposed WBGT penalties for different types of clothing are given in Table 4.

This approach of a fixed correction factor has been criticized (169), stating that the effect of clothing varies in different climate types, so cannot be a fixed factor. Based on the

Table 2 WBGT Reference Limit Values from ISO 7243 (117)

Metabolic rate M ($W \cdot m^{-2}$)	Reference value of WBGT			
	Person acclimatized to heat (°C)		Person not acclimatized to heat (°C)	
0. Resting $M \leq 65$	33		32	
1. $65 < M \leq 130$	30		29	
2. $130 < M \leq 200$	28		26	
	No sensible air movement	**Sensible air movement**	**No sensible air movement**	**Sensible air movement**
3. $200 < M \leq 260$	25	26	22	23
4. $M > 260$	23	25	18	20

Note. The values given have been established allowing for a maximum rectal temperature of 38°C for the persons concerned.

physics of heat transfer, that criticism is correct, but on the other hand, when getting close to the WBGT limits the climate variation may diminish. The correction factor approach thus requires further evaluation for climates which differ from the ones used in Bernard et al.'s experimental conditions, for example, for high radiant loads. Also, it should be noted that WBGT is a rough screening index, and for screening such a simplification may be acceptable. For detailed analysis of protective clothing effects, more complex models would be needed though.

Table 3 ACSM Position Paper

Wet bulb globe temperature (WBGT)			Training and noncontinuous activity	
°F	°C	Continuous activity and competition	Nonacclimatized, unfit, high-risk individuals*	Acclimatized, fit, low-risk individuals*,†
≤50.0	≤10.0	Generally safe; EHS can occur associated with individual factors	Normal activity	Normal activity
50.1–65.0	10.1–18.3	Generally safe; EHS can occur	Normal activity	Normal activity
65.1–72.0	18.4–22.2	Risk of EHS and other heat illness begins to rise; high-risk individuals should be monitored or not compete	Increase the rest-work ratio. Monitor fluid intake.	Normal activity
72.1–78.0	22.3–25.6	Risk for all competitors is increased	Increase the rest-work ratio and decrease total duration of activity	Normal activity. Monitor fluid intake
78.1–82.0	25.7–27.8	Risk for unfit, nonacclimatized individuals is high	Increase the rest-work ratio; decrease intensity and total duration of activity	Normal activity. Monitor fluid intake
82.1–86.0	27.9–30.0	Cancel level for EHS risk	Increase the rest-work ratio to 1:1, decrease intensity and total duration of activity. Limit intense exercise. Watch at-risk individuals carefully	Plan intense or prolonged exercise with discretion; watch at-risk individuals carefully
86.1–90.0	30.1–32.2		Cancel or stop practice and competition	Limit intense exercise and total daily exposure to heat and humidity; watch for early signs and symptoms
>90.1	>32.3		Cancel exercise	Cancel exercise uncompensable heat stress‡ exists for all athletes

*While wearing shorts, T-shirt, socks, and sneakers.
†Acclimatized to training in the heat at least 3 weeks.
‡Internal heat production exceeds heat loss and core body temperature rises continuously, without a plateau.
Note. Differences of local climate and individual heat acclimatization status may allow activity at higher levels than outlined in the table, but athletes and coaches should consult with sports medicine staff and should be cautious when exceeding these limits. WBGT levels for modification or cancellation of workouts or athletic competition for healthy adults. Collated and adapted with permission by ACSM from Ref. 4.

Table 4 Clothing Correction Factors for WBGT Limit Values due to the Clothing's Limiting Effect on Sweat Evaporation (11, 12); Adapted with Permission from Annals of Occupational Hygiene, Oxford University Press

Ensemble	Comments	CAF from USF(°C-WBGT)	CAF from ACGIH(°C-WBGT)
Work clothes	Work clothes made from a woven fabric is the reference ensemble	0	0
Cloth coveralls	Woven fabric that includes FR treated cotton and Nomex	0	0
SMS nonwoven coveralls as a single layer	SMS is a nonproprietary process to make nonwoven fabrics from polypropylene	−1	0.5
Tyvek 1422A coveralls as a single layer	Tyvek is a proprietary fabric made from polyethylene. Tyvek 1422A has a somewhat higher CAF than 1424 and 1427, which were used for the TLV	2	1
Vapor-barrier apron with long sleeves and long length over cloth coveralls	The apron configuration was designed to protect the front of the body against spills from chemical agents	4	
Double layer of woven clothing			3
NexGen coveralls as a single layer	NexGen is a proprietary microporous fabric that is water-barrier, vapor-permeable. There is great variability in these types of fabrics and one CAF will not apply for another fabric	2.5	
Saratoga hammer protective clothing ensemble	Used by US military for chemical protective clothing	3	
Microporous coveralls (generic)	The CAFs of microporous barriers vary widely and the generic value represents a higher observed value in the range	6	
Vapor-barrier coveralls as a single layer	No hood. The real effect depends on the level of humidity and in many cases the effect is less	10	
Vapor-barrier coveralls with hood as a single layer	It was assumed that a hood would be worn with vapor-barrier coveralls	11	11
Vapor-barrier over cloth coveralls w/o hood and w/NP respirator		12	
Hood†	Wearing a hood of any fabric with any clothing ensemble	+1	
Full-face negative pressure respirator†	Military style respirator and should be a worst-case condition. The difference is not statistically or substantially different from 0	+0.3	

Use of wet bulb globe temperature without "correct" instrument

Though the WBGT instrument in its origin was relatively cheap to make, currently available units made to the original specifications tend to be costly ($500+ for a black globe). This, and the desire to make units smaller, faster responding, and more portable/manageable has led to the development of systems with smaller black globes (<10 cm), and systems that use relative humidity sensors instead of the natural wet bulb sensors. Going even further, some systems have been proposed (ACSM position statement, 4, 169, 278), that estimate WBGT solely from measured dry bulb temperature and relative humidity, while radiation is only assessed qualitatively based on time of day and cloud cover (64, 88). Moran et al. (179-182) in a series of studies considered a number of options to estimate WBGT without Globe Temperature, starting with a modified discomfort index

$$\mathrm{MDI} = 0.75T_{\mathrm{nwb}} + 0.3T_{\mathrm{a}} \quad (5)$$

later leading to a new environmental stress index,

$$\mathrm{ESI} = 0.63T_a - 0.03\mathrm{RH} + 0.002\mathrm{SR} + 0.0054\left(T_a \cdot \mathrm{RH}\right) - 0.073\left(0.1 + \mathrm{SR}\right)^{-1} \quad (6)$$

with T_a = air temperature, T_{nwb} = natural wet bulb temperature, RH = relative humidity, and SR = solar radiation ($W \cdot m^{-2}$). Though they achieved high correlations based on very large datasets (25k points) of weather data, for MDI the residual error was unevenly distributed and up to ±3°C, while for ESI r^2 was 0.92 for a validation dataset (0.98 for the development dataset), but with errors up to ±2°C [unfortunately no Standard Error of the Estimate (SEE) or limits of agreement (LoA) was reported for neither validation]. The high r^2 values show that the equations work for a lot of the conditions; however, it may be the critical ones where WBGT is substantially under or over estimated. Blazejczyk et al. (16) calculate WBGT based on air temperature and vapor pressure alone. Due to the complex interaction and impact of radiation, air speed, air temperature, and humidity on the WBGT sensors, the validity and reliability of such approaches across the whole four-dimensional (4D) climate spectrum however has been questioned (22,36,37), for example, showing large deviations at low air speeds. Mathematically, these predictions can even produce more than one solution for WBGT (13,36,37), which is practically unacceptable. Even the replacement of the large globe with a small one has received criticism (22). Despite the requirements for these sensors being defined in ISO 7726 ("Ergonomics of the thermal environment—Instruments for measuring physical quantities") (118) the same criticism, that sensors deviating from the original design are not necessarily validated across the whole 4D climate space before accepting them, is put forward (22). In addition, the implications regarding the different response times of different systems has raised concerns, as the original guidelines for WBGT limits are based on sensors with longer response times, therefore showing a different "averaging" response in fluctuating climates (22). The latter may not be an issue though if the data were regularly recorded using a data logger, allowing postprocessing. In the conclusion of their paper, d'Ambrosio Alfano et al. (37) however conclude: "the indirect evaluation of WBGT should clearly be avoided based on the ISO 7243 standard." In his review, Budd (22) strongly states with regards to using only air temperature and humidity to estimate WBGT that: "estimates of WBGT without Globe Temperature are clearly invalid and should never be referred to as 'WBGT'."

The conclusion must, therefore, be that nonoriginal WBGT instruments, especially those without a standard globe or natural wet bulb, should be treated with caution and require validation over the whole 4D climate space.

Heat stress index

With most of the heat stress indices based on specific instruments (Table 1) like botsball, WBGT, and Oxford index, it is typically assumed that in some way the heat exchange between these instruments and the environment resembles that of a human, and that therefore, the impact of the stress on the human has a strong correlation with the instrument's readout. As discussed earlier, this is often not the case (164) and corrections are needed when translating the instrument readout into terms of heat stress and strain as experienced by a human.

An alternative approach to avoid the above limitations is to actually calculate the heat exchange between a person and the environment, using the six basic parameters defining the climatic and personal conditions (ambient air temperature, radiant temperature, humidity, air speed, clothing, and metabolic rate). As discussed in the next sections, this approach resulted in a number of different simpler heat stress indices as well as more complex heat strain models, that is, predicting the human physiological response.

A well-known index that is based on human heat balance considerations is the Heat Stress Index, HSI, originally developed by Belding and Hatch (9, 10). Although HSI currently only sees limited use in the field, it is worthwhile discussing it as it forms the basis of many other, more recently developed rational indices. The underlying principle of HSI is the heat-balance equation and the calculation of its main components. Starting from the heat-balance equation, rearranged from Eq. (2):

$$M - W = C + R + K + E + \mathrm{Resp} + S \quad (7)$$

Assuming steady-state conditions (i.e., heat storage: $S = 0$), negligible mechanical work output efficiency ($W = 0$) and conduction ($K = 0$), and ignoring respiratory heat loss (Resp = 0) as this is typically low at high temperatures and humidities, the equation can be simplified and rearranged to calculate the required evaporation (E_{req}) for thermal balance, that is:

$$E_{req} = M - (C + R). \quad (8)$$

Assuming the metabolic rate is known [i.e., either measured via oxygen consumption or determined indirectly using techniques described, for example, in ISO 8996 "Ergonomics of the thermal environment—Determination of metabolic rate," (121)], the dry heat losses C and R can be calculated based on ambient temperature (T_a, °C), mean radiant temperature (T_{mrt}, °C), and air speed (v_a, $m \cdot s^{-1}$).

$$\begin{aligned} &\text{Convection } C = h_c(35 - T_a) \quad [\mathrm{Wm^{-2}}] \\ &\text{with } h_c = 7.6v_a^{0.6} \ [\mathrm{Wm^{-2}\,°C^{-1}}] \text{ (nude) or} \\ &\qquad h_c = 4.6v_a^{0.6} \ [\mathrm{Wm^{-2}\,°C^{-1}}] \text{ (clothed)} \end{aligned} \quad (9)$$

$$\begin{aligned} &\text{Radiation R} = h_r(35 - T_{mrt}) \quad [\mathrm{Wm^{-2}}] \\ &\text{with } h_r = 7.3 \ [\mathrm{Wm^{-2}\,°C^{-1}}] \text{ (nude) or} \\ &\qquad h_r = 4.4 \ [\mathrm{Wm^{-2}\,°C^{-1}}] \text{ (clothed)} \end{aligned} \quad (10)$$

In the original work (10), no differentiation was made between nude and clothed. Later, Hertig et al. introduced correction factors for heat loss through clothing compared to nude, which were between 0.4 (108, 149) and 0.3 (143). In the calculations for conductive and radiative heat loss, skin temperature was fixed at 35°C. However, by fixing the physiological response value, the HSI became a stress index rather than a strain index (143).

Having determined the evaporation rate required for thermal equilibrium, the next step was to compare this E_{req} to the maximal evaporation rate possible in the environment to determine whether the required balance can be achieved:

$$\begin{aligned} E_{max} &= h_e(5.6 - P_a) \quad [Wm^{-2}] \\ \text{with } h_e &= 117v^{0.6}\ [Wm^{-2}kPa^{-1}] \text{ (nude) or} \\ h_e &= 70v^{0.6}\ [Wm^{-2}kPa^{-1}] \text{ (clothed)} \\ &\text{with an upper limit for } E_{max} \text{ of } 390\ Wm^{-2} \end{aligned} \tag{11}$$

The upper limit is roughly equivalent to sweat evaporation of 1 L/h, considered the limit for an 8 h shift.

Finally, knowing the required and the maximal possible evaporation rates for the prevailing climate conditions, the HSI was calculated as the ratio between the two:

$$\text{HSI} = \frac{E_{req}}{E_{max}} \times 100 \tag{12}$$

The HSI values can range from below 0 (no evaporation needed with cooling present) via 0 (balance without evaporation) to 100 (balance at maximal evaporation) and above (evaporation does not reach the required amount).

In the latter case, heat balance is not achieved indicating the person would heat up. Assuming a maximal acceptable heat gain of 264 kJ of the body (a mean body temperature increase of about 1°C @ 75 kg) one can calculate the corresponding allowable exposure time (AET or often also referred as DLE: duration limited exposure) of:

$$\text{AET} = \frac{\left[\dfrac{264\ \text{kJ}}{1.8\ \text{m}^2 \cdot 60s.\ \text{min}^{-1}}\right]}{\left[E_{req} - E_{max}\right] Wm^{-2}} = \frac{2440}{E_{req} - E_{max}} \text{min} \tag{13}$$

where 1.8 m^2 is the average surface area of the human body. Interpretation of different HSI values is provided in Table 5.

Table 5 Interpretation of Heat Stress Index (HSI) Values

HSI	Effect of 8-h exposure
−20	Mild cold strain (e.g., recovery from heat exposure)
0	No thermal strain
10-30	Mild to moderate heat strain. Little effect on physical work but possible effect on skilled work
40-60	Severe heat strain, involving threat to health unless physically fit. Acclimatization required
70-90	Very severe heat strain. Personnel should be selected by medical examination. Ensure adequate water and salt intake
100	Maximum strain tolerated daily by fit acclimatized young men
Over 100	Exposure time limited by rise in deep body temperature

Required sweat rate index; ISO 7933 version 1989

Starting with the basic analytical model of the HSI, several attempts have been made to improve on the simplified heat balance calculation used. Givoni (74, 75) proposed the Index of Thermal Stress—an improved version of the HSI. The main conceptual addition was the translation of the required evaporation rate into a sweat rate for thermal equilibrium in summer clothing. Rather than converting sweat production into evaporation, this approach recognized that not all sweat may evaporate by calculating an evaporative efficiency.

Vogt et al. (248) introduced the required SWreq, providing a practical method of assessing heat stress and the dehydration risk. Rather than assuming respiratory losses, and external work efficiency to be zero, these components were now added to the model. Vogt et al. furthermore introduced a prediction equation for the mean skin temperature based on ambient temperature, radiation levels, vapor pressure, air velocity, metabolic rate, and clothing insulation. Following the extensive work by Libert (160) and Candas (25) on sweat production and evaporation, they too calculated an evaporative efficiency to convert the required evaporation rate into a required sweat rate (RSR).

As with the HSI, Vogt et al. started with the heat balance equation, equivalent to Eq. (7), but now cited as presented in their 1981 (248) paper:

$$M_n + W + E_e + E_i + E_{req} + R + C = 0 \tag{14}$$

where M_n is the net metabolic energy production, W = external mechanical work, E_e = respiratory evaporative heat loss, E_i = insensible skin evaporative heat loss by moisture diffusion, E_{req} = required sweating evaporative heat loss, R = radiant heat flux, and C = convective heat flux (all in $W \cdot m^{-2}$).

E_{req} represents the required evaporative heat loss to ensure heat balance of the body. As with HSI, if the actual heat loss by sweat evaporation (E_s) is lower than E_{req}, the body accumulates heat and body temperature rises. When E_{req} approaches E_{max}, [Eq. (11)], the skin wettedness will increase as not all sweat can evaporate (25, 74, 142, 160). The efficiency of sweating decreases when sweat starts to drip. Accordingly, the sweat efficiency, η (in $g \cdot m^{-2} \cdot s^{-1}$) is defined as the ratio of the actual sweat evaporation, E_s, and the calorimetric equivalent of sweat secretion:

$$\eta = \frac{E_s}{\lambda \times \text{Sweat rate}} = ae^{-b\omega} \tag{15}$$

with a and b being experimentally derived coefficients (248) [Vogt (248) suggests 6.3 and 2.3 for these], λ the latent heat of vaporization of water and ω the skin wettedness defined as:

$$\omega = \frac{E_{req}}{E_{max}} \tag{16}$$

This ratio defines the skin wettedness that is required to achieve the required evaporation rate as related to the maximal achievable evaporation rate. If $\omega > 1$ the exposure is unsafe, and, as with the HSI, safe exposure times are calculated from the difference ($E_{req} - E_{max}$), which represents the rate of heat storage within the body. This method for calculating the RSR was published as an ISO standard (ISO7933, 1989, [119]; now replaced by ISO 7933, 2004 [120])

For $\omega < 1$, the RSR to achieve thermal balance, S_r (in $g{\cdot}m^{-2}{\cdot}s^{-1}$), can be calculated by dividing E_{req} by $\eta \times \lambda$:

$$S_r = \frac{E_{req}}{\eta\lambda} \tag{17}$$

This value of the RSR itself can be used as strain index and can also be compared to the maximal sweat production that is deemed achievable for a person of a certain acclimatization status (S_p). If $S_r < S_p$, no problem is present, but if and when $S_r > S_p$, a heat balance cannot be achieved and safe exposure times need to be calculated. To link this to a dehydration rate, the hourly sweat secretion rate for the whole body is calculated as:

$$S_{hour} = 2.59\frac{E_{req}}{\eta} \tag{18}$$

where the constant is a lumped conversion factor of time and clothing surface area assuming light clothing (192,248). ISO 7933 (119) also provided limits values. These provide both a "warning" and a "danger" limit level for sweat rate for low and high work rates. In these limits, the standard differentiates between acclimatized and nonacclimatized workers. This gives the following sweat rate limits for the "danger" level: for low work rate (<65 $W{\cdot}m^{-2}$) in nonacclimatized people: 390 $g{\cdot}h^{-1}$ and in acclimatized people 780 $g{\cdot}h^{-1}$. For high work rate (>65 $W{\cdot}m^{-2}$), the limits are for nonacclimatized people: 650 $g{\cdot}h^{-1}$, and for acclimatized people 1040 $g{\cdot}h^{-1}$ (all for "danger"). The highest value is similar to the 1 $L{\cdot}h^{-1}$ limit defined earlier. However, while in case of HSI, the maximum rate of 8000 g/8 h work day was used, ISO 7933 (1989) defined a daily limit of 3250 and 5200 g for nonacclimatized and acclimatized workers, respectively, conservatively not taking rehydration into consideration as a safety measure.

After its publication, this standard was subjected to validation in several studies, and, although it represented an evident improvement on methods available to date, it was also criticized. Diverse papers compared various versions of the algorithms to calculate the SWreq to sets of experimental data (97,136,233) and identified limitations concerning the following issues: (i) the prediction equation for the skin temperature (e.g., the regression coefficient for the effect of clothing insulation was negative, being counterintuitive. This was caused by an "unbalanced" dataset in terms of climatic conditions, with radiation exposures causing this effect); (ii) the influence of the clothing on convective and evaporative heat exchanges; (iii) the combined effect of clothing and movements (not included); (iv) the increase of core temperature linked to the activity (independent of heat load); and (v) the prediction of the maximum allowable exposure durations (170). A European Union funded project (BMH4-CT96-0648) was then initiated to address these issues and improve on the quality of the ISO 7933 prediction, which led to a new version of the standard, the public health system (PHS) (170).

Predicted Heat Strain

Predicted heat strain: ISO 7933, version 2004

The EU-Biomed project, led by Malchaire (170) addressed a number of the shortcomings in ISO 7933-1989 (119) and produced a proposal for a new standard with the same number ISO 7933, but a different title: "Analytical determination and interpretation of heat stress using calculation of the predicted heat strain" (120). The development was based on a large dataset, collected from many different laboratories. In essence, this is still the same type of analytical index based on the heat balance analysis as the old 7933 was; however, it now also includes a prediction of the core temperature, which puts it closer to a physiological model (to be discussed later). However, it is important to note that there is no real physiological control and feedback function present in the algorithms. Major changes to the old standard regarding the calculation of the RSR include:

– a detailed representation of the convective respiratory heat loss (with both C_{res} and M in watts or in $W{\cdot}m^{-2}$) based on the work by Livingstone et al. (1994):

$$C_{res} = 1.52 \times 10^{-3} \times M \times (28.6 + 0.641 \times P_a - 0.885 \times T_a) \tag{19}$$

– a new expression for the respiratory evaporative heat loss (E_{res}) proposed by Varene (246):

$$E_{res} = 1.27 \times 10^{-3} M \times (59.3 + 0.53 \times T_a - 11.63 \times P_a) \tag{20}$$

– a new formula to predict skin temperature (174), for clothed subjects (Icl ≥ 0.6 clo):

$$t_{sk\ clothed} = 12.2 + 0.020 \times T_a + 0.044 \times T_{mrt} + 0.194 \times P_a - 0.253 \times v_a + 0.00297 \times M + 0.513 \times T_{re} \tag{21}$$

– and for nude subjects (Icl ≤ 0.2 clo):

$$t_{sk\ nude} = 7.2 + 0.064 \times T_a + 0.061 \times T_{mrt} + 0.198 \times P_a - 0.348 \times v_a + 0.616 \times T_{re} \quad (22)$$

with T_{sk} = mean skin temperature; T_a = ambient temperature (°C), T_{mrt} = mean radiant temperature (°C); P_a = ambient vapor pressure (kPa); v_a = air velocity ($m \cdot s^{-1}$); T_{re} = rectal temperature (°C); and M = metabolic rate (W).

For clothing insulation (I_{cl}) between 0.2 and 0.6 clo, a linear interpolation between both models is used:

$$T_{sk} = T_{sk\ nude} + 2.5 \times \left(T_{sk\ clothed} - T_{sk\ nude}\right) \times (Icl - 0.2) \quad (23)$$

Exponential averaging for the skin temperature and the sweat rate

Being a heat-balance-based standard without any real physiological control components, the old RSR standard assumed that new physiological steady states are reached instantaneously when the boundary conditions (BCs) change. So for example, when the work rate and the heat-stress level increase, a new sweat rate would be achieved instantaneously. Similarly, stopping exercise or any other heat load would instantly stop sweating—even though in reality the person would continue to be hyperthermic, and respond by a continued elevated latent heat loss. Though this simplification is of limited relevance for longer term constant load exposures, it makes the approach inappropriate for the prediction of responses to intermittent exposures and work-rest cycles. In real life, there is always a delay before the new steady-state conditions are achieved. With this respect also, the rate of heat accumulation is assumed to remain the same during the whole exposure, while in reality, it obviously tends toward 0 causing the body core temperature to approach an equilibrium state.

Further modifications to the model were made as to predict the sweat rate, skin, and rectal temperatures at any time instant by taking into account a person's thermal history, that is, any past exposures. For this purpose, a first-order system approach was employed (168, 170):

$$V(t) = V_0 + \Delta V \times \left[1 - e^{\left(\frac{-t}{\tau}\right)}\right] \quad (24)$$

where

- $V(t)$ is the value at time t
- V_0 is the initial value
- ΔV is the increase of parameter V in the new condition ($V_0 + \Delta V$) being therefore the new equilibrium value
- t is time
- τ is the time constant (in min)

Time constants (τ) around 3 min for skin temperature and 10 min for sweat rate have been suggested (170). This also implies that the model has to be calculated iteratively, as the slower rise in sweat rate also affects the storage of heat within the body.

Mean body temperature

Rather than using a fixed weighting core-skin temperature ratio of 0.7/0.3 for calculating the mean body temperature:

$$T_b = (1 - \alpha) \times T_{re} + \alpha \times T_{sk} \quad (25)$$

The ratio used in the new standard can vary between 0.9/0.1 and 0.7/0.3 (core/skin) for the vasodilated and vasoconstricted skin, respectively (30, 71, 137, 236).

The paper by Colin et al. (30) suggests that this coefficient is not simply a function of the vasodilatation status and skin blood flow, but also varies with heat storage, and thus, indirectly, with the rectal temperature. Therefore the model assumes that for:

$$\text{for} \quad T_{re} \le 36.8°C: \quad \alpha = 0.3$$
$$\text{and} \quad T_{re} \ge 39°C: \quad a = 0.1$$

For core temperature between $36.8°C < T_{re} < 39°C$ α varies between 0.3 and 0.1 according to: $\alpha = 0.3 - 0.09\ (T_{re} - 36.8)$.

Distribution of the heat storage in the body

As in the new ISO7933 model, skin temperature is estimated [see Eq. (21)], and heat storage is calculated, mean body temperature change can be determined from these, and subsequently, with knowledge of the skin/core distribution factor, a core temperature change can then be derived from these.

As T_{sk} and T_{co} are different from T_{sk0} and T_{co0}, the skin-core weighting ratio changes continuously [see Eq. (25)]. Also, the increase in skin temperature during the last minute interval relates directly to the outer surface of the skin but progressively affects the whole skin layer of thickness α.

The proposed model assumes that, inside this skin layer, the temperature varies linearly from T_{sk0} to T_{co0} initially and from T_{sk} to T_{co} at the end of the minute.

The core temperature T_{co} at time i can thus be calculated using the following expression:

$$T_{co} = \frac{1}{1 - \frac{\alpha}{2}} \left[\frac{dS_i}{c_p W_b} + T_{co0} - \frac{T_{co0} - T_{sk0}}{2}\alpha_0 - T_{sk}\frac{\alpha}{2}\right] \quad (26)$$

where:

- c_p is the specific heat of the body ($J \cdot kg^{-1} \cdot °C^{-1}$) and W_b the body mass (kg) and T_{co} have to be determined iteratively knowing that α varies as a function of T_{co} as indicated before.

In addition, the standard calculates a rectal temperature from this "deep" core temperature [Eq. (26)] to allow a comparison with field data and existing exposure limits.

Evaporative efficiency

As described in the previous section, not all sweat may evaporate, especially in humid air scenarios. In such conditions, the RSR would be higher than the required evaporation rate according to Eq. (16). As in the older version of the model, the lower limit for η was set at 0.5, when the skin wettedness ω reaches its saturation, that is 1, an anomaly occurs. Any increase of the air humidity reduces E_{max} causing also the predicted sweat rate to decrease [Eq. (16)]. This is evidently incorrect and unrealistic (146, 277). Therefore, in the newer model, the skin wettedness can exceed unity (which may be interpreted as a growing sweat layer thickness on the skin):

$$\eta = 1 - \frac{w^2}{2} \quad \text{for} \quad w \le 1 \tag{27}$$

$$\eta = \frac{(2-w)^2}{2} \quad \text{for} \quad 1 < w \le 1.7 \tag{28}$$

$$\eta = 0.05 \quad \text{for} \quad w > 1.7 \tag{29}$$

As before, the predicted evaporation rate remains estimated using ω (limited to w_{max}):

$$E_{pred} = w\,E_{max} \tag{30}$$

while the predicted sweat rate is a function of η calculated earlier:

$$SW_{pred} = E_{pred}/\eta \tag{31}$$

With all these additions [for a full list please refer to Malchaire (170)], this new PHS version of ISO7933 (120) is a predictor of heat strain rather than just heat stress. By adding empirical knowledge on time courses of sweating and body temperature, the analytical model used now produces a physiological parameter (core temperature/rectal temperature) for the evaluation of the heat stress and strain.

The model was evaluated extensively against large datasets obtained from many (mainly European) laboratories and field studies (168,170). A limited number of studies have evaluated the standard since, and its use so far seems to be limited.

Empirical modeling of heat strain

In addition to the heat stress indices and strain indices discussed earlier, another approach has been followed that is best described as empirical modeling of heat strain. This approach which mainly stems from USARIEM (199, 200) has used data from many heat exposures to create prediction equations for the development of heart rate, rectal temperature, sweat rate, and water loss for exercise in various warm and hot environments.

Rectal Temperature Prediction

Givoni and Goldman (77) started this line of work in 1972 with prediction equations for equilibrium rectal temperature that was calculated based on a number of heat-exchange parameters (77, 200):

$$\begin{aligned} T_{ref} &= 36.75 + 0.004\cdot(M - W_{ext}) + 0.0011\cdot H_{(R+C)} \\ &\quad + 0.8e^{[0.0047\cdot(E_{req}-E_{max})]} \quad (^\circ C) \\ &= \begin{bmatrix}\text{Metabolic}\\ \text{contribution}\end{bmatrix} + \begin{bmatrix}\text{Dry heat}\\ \text{exchange}\end{bmatrix} + \begin{bmatrix}\text{Evaporative heat}\\ \text{exchange}\end{bmatrix} \end{aligned} \tag{32}$$

For M, in watts, the prediction equation for metabolic rate based on work by Givoni et al. (76) and by Pandolf et al. is used (197, 198)

$$\begin{aligned} M_{walking} &= 1.5W + 2.0(W+L)\left(\frac{L}{W}\right)^2 \\ &\quad + \eta(W+L)\left[1.5(v_w)^2 + 0.35G\cdot v_w\right] \end{aligned} \tag{33}$$

for speeds below 2.2 m·s^{-1}; Where M = metabolic rate (watt); W = nude body mass (kg); L = clothing and equipment weight (kg); σ = terrain factor (1 for black top surface; 1.1 dirt road; 1.2 light brush; 1.3 hard packed snow; 1.5 heavy brush; and 2.1 loose sand to 4.1 for 35 cm soft snow); v_w = walking speed (m·s^{-1}); and G = grade/inclination (%).

Or, for running, the modified equation by Epstein et al. (52) for speeds between 2.2 and 3.2 m·s^{-1} for which a correction for the grade was not deemed necessary.

$$\begin{aligned} M_{running} &= M_{walking} - 0.5\cdot(1 - 0.01\cdot L)\cdot \\ &\quad \left(M_{walking} - 15\cdot L - 850\right) \text{ (watt)} \end{aligned} \tag{34}$$

For W_{ext}, and the other components, Givoni and Goldman (77) suggest:

$$W_{ext} = 0.098\cdot G(W+L)v_w \tag{35}$$

$$H_{(R+C)} = \frac{6.45\cdot \text{body surface area}\cdot\left(T_a - \overline{T}_{skin}\right)}{I_T} \tag{36}$$

With I_T the total clothing insulation in clo units (1 clo = 0.155 m^2·°C·W^{-1}).

For $T_a \ge 30$°C [for temperatures between 15 and 30°C, it is suggested to use a value of 30°C as in that range the core temperature is not affected by the ambient temperature (77)]

$$E_{req} = (M - W_{ext}) + H_{(R+C)} \quad \text{(watt)} \tag{37}$$

$$E_{max} = 14.21\frac{i_m}{I_T}A_{D\_eff}\left(P_{sk} - \frac{RH}{100}P_{a,sat}\right) \quad \text{(watt)} \tag{38}$$

where i_m = clothing permeability index (N.D.); A_{D_eff} = effective surface area for evaporation (m^2); P_{sk} = water vapor

pressure at skin (mmHg); RH = relative humidity (%) and $P_{a,sat}$ = saturated water vapor pressure at air temperature (mmHg).

Givoni and Goldman (77) also provide equations for estimating the time course of the core temperature before reaching the equilibrium value given earlier, which required separate equations for rest, exercise and recovery. In their validation, they use a number of data sets, indicating an explained variance of the prediction equation in the range of 92% to 96% for the data that was used to develop the equations, and going down to 69% to 92% for independent datasets. Lowest values were obtained for data sets where tolerance times were very limited.

Heart rate prediction

For prediction of the equilibrium heart rate, Givoni and Goldman (78) first calculate an "index of the equilibrium heart rate level":

$$I_{HR} = 0.4M + \left(\frac{2.5}{I_T}\right)(T_a - 36.) + 80e^{0.0047(E_{req}-E_{max})} \quad (39)$$

With I_T (in clo) and the other components as described earlier. Then, heart rate is predicted as:

$$\text{for } 0 < I_{HR} < 225 : HR_f = 65 + 0.35(I_{HR} - 25) \quad (40)$$

$$\text{for } I_{HR} \geq 225 : HR_f = 135 + 42\left[1 - e^{-(I_{HR}-225)}\right] \quad (41)$$

using a lower limit for HR_f of 65 bpm in the case of cold exposure. The authors also give equations for the time course of heart rate in reaching a new equilibrium value. In the validation, they observe good agreement for their tested conditions with an r^2 of 94% and a standard error of the prediction of 6 bpm.

Sweat rate prediction

Finally, an empirical prediction of the sweat rate was produced in the same laboratory by Shapiro et al. (226), which can also be used to look at water requirements in heat exposure:

$$\text{Sweat loss} = 27.9\frac{E_{req}}{(E_{max})^{0.455}} \quad (g\,m^2\,h^{-1}) \quad (42)$$

with E_{req} and E_{max} in $W{\cdot}m^{-2}$ [note: it was in watts in equations (37) and (38)] and limited to $50 < E_{req} < 360\ W{\cdot}m^{-2}$ and $20 < E_{max} < 525\ W{\cdot}m^{-2}$.

This was evaluated between 20 and 54°C in a wide humidity range and with different clothing. Later, this was evaluated for outdoor conditions (225). Independent evaluations (29) indicate that this equation often overpredicts sweating rates, with overestimations up to 100% during higher exercise intensities, but also underestimations up to 80% in cool environments (86). This has initiated new research, and more recently Gonzalez and co-workers (85, 86) updated this work and the new equation became:

$$\text{Sweat loss} = 147 + 1.527 \cdot E_{req} - 0.87 \cdot E_{max}\ (g \cdot m^2 \cdot h^{-1}) \quad (43)$$

This equation ($r^2 = 0.78$; SEE = $\pm 181\ g{\cdot}m^{-2}{\cdot}h^{-1}$) was found to take into account effects of heavy work, clothing factors, and body armor effects, longer exposure times (2-8 h), residual errors inherent in the original equation to predict sweat loss, and is not gender specific.

Though this equation looks simple, one should remember that the calculation of E_{req} requires a substantial amount of input data, which may limit its application by a nonspecialist audience (86 reevaluated Shapiro's equation, for example, with updated clothing values and found a substantial impact of this on the outcomes). The main reason for updating the original equation by Shapiro et al. was the presence of a risk of hyperhydration (29) if their numbers were used to drive water uptake behavior.

It should be noted that the main applications of such equations are in the area of military logistics (calculation water provision requirements), public health scenarios, or for example, in preparations and logistics for large running events (86). They are not reliable enough for individual control of hydration (86).

Since the publication of equation (43), several studies have evaluated and adapted it for application in different conditions, like solar exposures (87) and high-altitude treks (88), with good results.

Physiological models

Mathematical modeling of human thermoregulation goes back some 70 years. Physiological models for the prediction of thermal strain combine models of the environmental heat exchange with models of the human body as "passive system," and cybernetic models of the active control system, that is, the central nervous system. It is mainly the latter that discriminates these models from pure heat balance models such as HSI, and PHS discussed earlier.

Physiological models range from simple to sophisticated, according to the realism of the body implementation, the types of physiological sensors involved, and the sophistication of the active system (165). Models evolved from single, homogeneous single-node approaches, via two-node models accounting for the body core and shell (7, 67, 69, 272) into multilayered representations of the human body. The latter were represented either as single (typically concentric) cylinders or as composites of cylinders of various sizes representing individual body elements, "connected" with each other by blood circulation (e.g., 2, 60, 63, 66, 91, 116, 149, 156, 228, 235, 239, 260, 261, 271), Figure 2.

Multisegmental models typically include explicit simulation of the heat and mass transport and regulatory processes

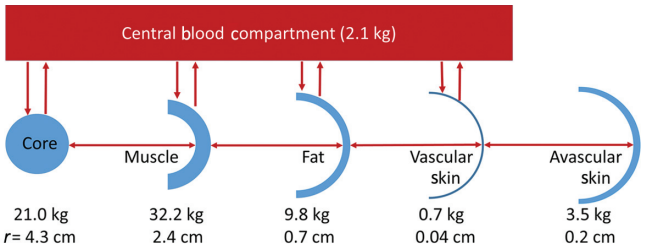

Figure 2 Cross-section of cylindrical model containing five concentric annular tissue compartments; dimensions shown are for reference individual (70 kg, 1.8 m^2). Kraning and Gonzalez (150), redrawn with permission J. Therm. Biology.

within tissues (55, 58, 60, 63, 234, 235, 260, 261) taking into account characteristics of the human body including body anatomy/shape, size and mass, heat capacities, layering of fat, muscle and other tissues, etc.

Perhaps, the most prominent example of a simpler model is the Gagge et al. (67) two node model, simulating the body core and shell as connected to a simple regulatory controller. Although comfort research was the original aim, this model has ever since been used successfully (with various modifications) also as a heat-strain-assessment tool (96,97,165). In the heat, due to the high blood perfusion of all body segments, spatial variation between segments is typically much lower than in the cold (91,97) and thus models require fewer segments, making such a two node model application feasible. Lotens (166) modified Gagge's two node model in that he split the single shell node in four sections based on two parameter combinations: clothed and unclothed and irradiated and not irradiated by a directional radiation source (e.g., the sun). However, his major extension of the Gagge model consisted of adding a sophisticated clothing heat-transfer model (see Fig. 3), which aside from usual heat- and vapor-transfer phenomena also included processes like condensation, reevaporation, and regain.

Compared to single or two-compartment models, multisegmental models simulate the human body in greater detail predicting both overall and local responses. Tissue layers and their physical and physiological properties are deduced from anatomical data including skin, fat, muscles, and inner organs. Environmental heat exchanges are calculated taking into account human-typical inhomogeneities such as nonuniform clothing, nonuniform skin temperatures, and regulatory responses or asymmetric environmental conditions.

Wissler (257, 264) started in 1959, modeling digits, with the expansion of Pennes' 1948 landmark paper (202) on the interaction of blood flow, metabolic heat generation and (radial) heat dissipation within tissues, producing the "bioheat equation." Pennes presented an analytical (steady-state) solution of the bioheat equation for the forearm only which was expanded upon to full body models by Wissler (258-260) and Wyndham and Atkins (268). Stolwijk (235) used six compartments (head, trunk, arms, legs, hands, and feet) of four layers each with an additional central blood compartment, resulting in a total of 25 nodes. This model was refined and expanded by

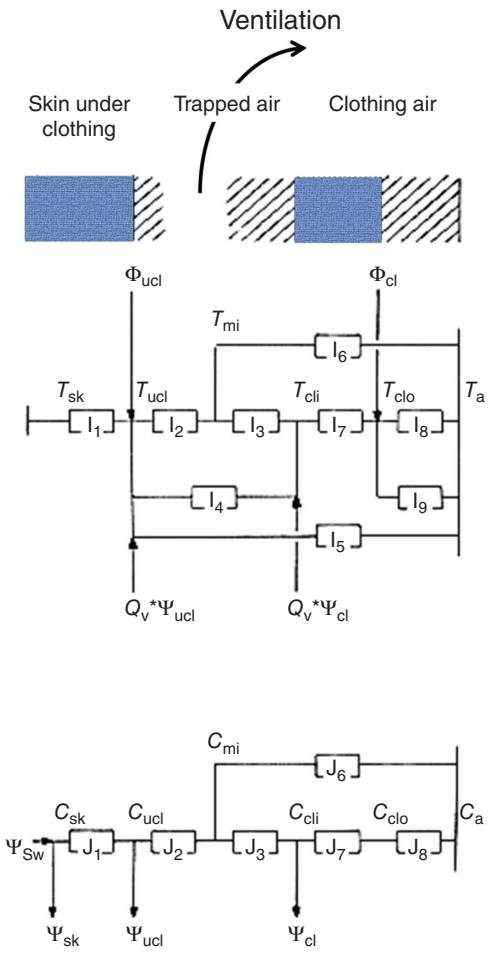

Figure 3 Schematic representation of the Lotens clothing model, showing the four clothing/air layers and the related network of heat and vapor resistances for conduction, radiation, and convection (166). Reproduced with permission from author (copyright holder).

Gordon (91) to nine compartments composed of eight tissue materials. Wissler's model consisted of 15 anatomical body regions: head, thorax, abdomen, and proximal, medial, and distal segments of the arms and legs. This further developed toward a detailed multicompartment model including physiological control functions, multidimensional heat transfer, etc. (261), requiring a vast amount of computing power and time. More recently Hensley et al. (107) extended the model with more compartments to represent glabrous skin of hands and feet with up to 6300 tissue nodes for the body as a whole (see Fig. 4).

Werner and Buse (254) gave up the idealized cylindrical symmetry in favor of a three-dimensional (3D) digital representation of the human body including individual organs. The focus of their work was detailed analysis of temperature profiles within the (passive) human body in the state of thermal neutrality, that is, in absence of any thermoregulatory reactions.

Nelson et al. (189) developed another detailed 3D human body model based on the *Brooks Man* anatomical data set,

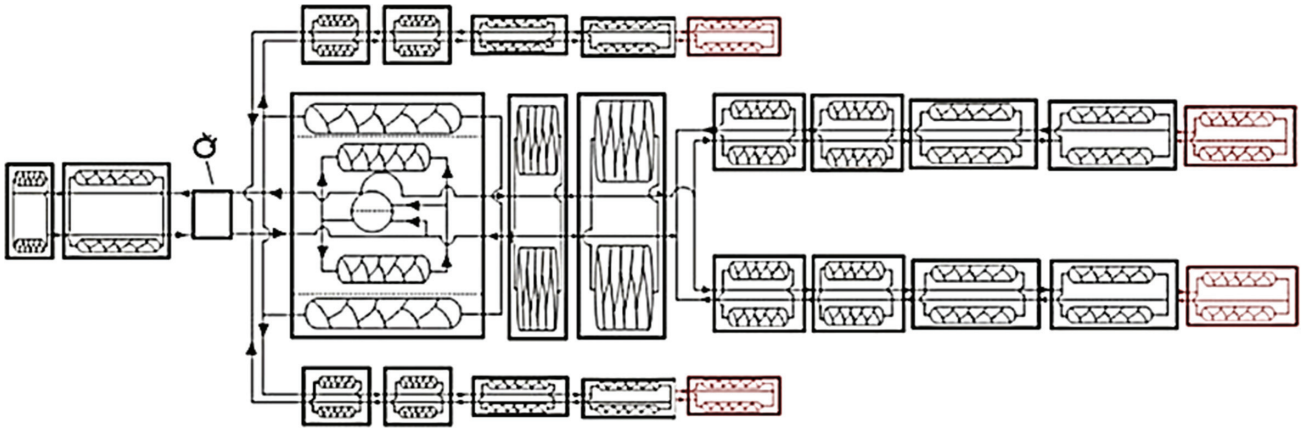

Figure 4 Graphical representation of the classic Wissler model that terminates at the wrists and ankles. Each of the 25 elements consists of 21 radial layers and 12 angular segments. The new model has four additional elements for two hands and two feet that are highlighted in red. Hensley et al. (107), reproduced with permission Journal of Biomechanical Engineering.

consisting of 1.3×10^8 tissue elements. In contrast to Werner, Nelson et al. incorporated an active system simulator based on work of Fiala et al. (63) to predict tissue temperature profiles and regulatory responses to conditions of mild hyperthermia with focus on thermal dosimetry applications and the assessment of exposures to nonionizing radiation sources.

The bioheat equation, which blood perfusion term is based on Fick's first principle, has been subject to critical discussion (28, 241, 267) and has seen various improvements (28, 49, 138, 227). Also, alternative models of microvascular structures have been proposed (6,129,250,251). However, Pennes' traditional bioheat equation has become the preferred approach in whole body models due to its simplicity and accuracy that is comparable with more detailed models requiring comprehensive data on the vascular architecture of tissues (3,27).

As in case of passive system models different approaches at different levels of complexity have been employed and developed to simulate the active human thermoregulatory system. In simpler models, the role of (sudomotor and vasomotor) thermoregulatory responses are only considered in the calculation of the heat balance of the skin (67, 69, 166).

Early models by Machle and Hatch (167), Kerslake and Waddell (144), Wyndham and Atkins (268) were in fact passive systems only with no real control loop between body temperature and effectors (blood flow, sweating) present. It was not until the early sixties that actual physiological regulatory functions were introduced by Crosbie et al. (35). In the first models, a mean body temperature was the input variable, but later modelers also included central, muscle and skin temperatures as separate afferent signals (234) while Gordon (91) employed the skin heat flux as a punitive signal to simulate human responses to cold stress conditions.

The regulatory controllers typically represent a system of temperature sensors either in the brain only, or in the brain and the skin or even further distributed across the body, that are connected to an integrating system, located primarily in the hypothalamus, which sends out efferent signals to activate vasomotor and sudomotor systems or shivering in muscles (Fig. 5). In most models, the strength of the efferent signals depends on the comparison between the integrated afferent signals and a reference value, that is, these models work with the set point concept, similar to a room thermostat. This concept refers to the reciprocal activity behavior of different types of receptors in their "operational range", that is, the decrease in activity of a sensor type is associated with an increase in activity of the other sensor type (106). In terms of cybernetics, this opposing behavior is capable of creating set points; a concept which has found application in many engineered models of the human thermoregulatory system (17), matching the traditional physiological "unified controller" paradigm (216).

As the set point controllers could not explain or simulate all responses observed in real life, for example, they would not normally produce a body temperature that is related to the workload intensity in compensable climates, others (253) produced models without set points (Fig. 6). Such models achieve temperature stability ("balance point," 216) by combining various overlapping and opposing effector controls. These do exhibit steady-state core temperatures (253) that are related to the workload as observed by Lind (161, 162). Few models include a direct metabolic afferent input (147) to the control system, but most only use body temperatures as the main inputs. Such an afferent metabolic input may be relevant to, for example, the control of sweating, as one of the features of many models is that they tend to predict body core temperature to come back to baseline after exercise much faster than in real life data as the initially high body temperatures after exercise keep sweating high in the models. In real data, despite a still raised body temperature (131) one typically sees a faster drop of sweat generation after exercise than in the models, which may be caused by the drop of a metabolic input to the sweat system (147) after cessation of exercise. Also Mitchell (177), Gisolfi and Robinson (73) and Robinson et al. (213) suggested a quickly rising effect of exercise on

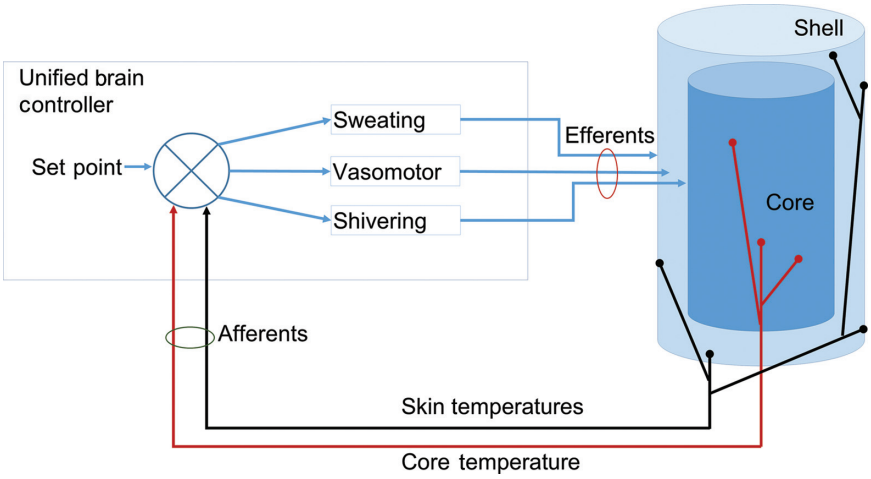

Figure 5 Schematic representation of feedback control system of thermoregulation using a two compartment (core, skin) representation of the body. In this "set point" concept, an individual unified controller is assumed to be present.

the gain of the sweat control allowing a faster start of sweating before body temperatures change significantly. Nevertheless, temperature-only-based active systems have generally received more experimental support and acceptance among physiologist and modelers.

Compared to models of sweat regulation, which are often rather simple, the control of blood flow shows a number of different interpretations. These range from using regression models of variable skin conductance (implicitly depending on skin blood flow; 268), or applying nonlinear (bang-bang/on-off) controllers (145) to more complex models of blood pressure control and arterial resistance instead of direct flow control (115) and the inclusion of differentiation of control between glabrous and nonglabrous skin (107).

Stolwijk (234, 235) developed a comprehensive, widely accepted model of the active system that has been source of motivation for refinements and further-development to

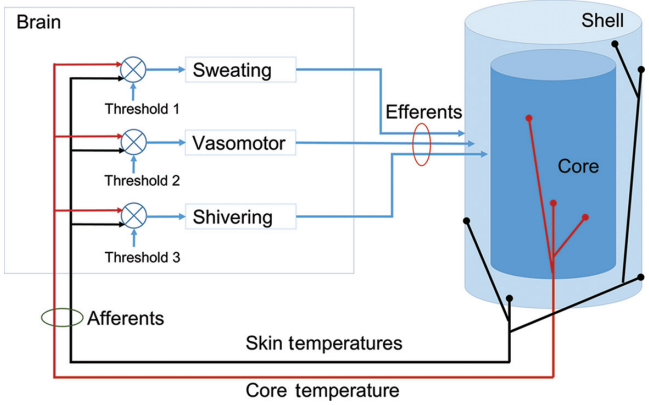

Figure 6 Schematic representation of feedback control system of thermoregulation using a two compartment (core, skin) representation of the body. This model contains thresholds for individual effector systems, which in combination lead to an overall body "balance point" (253), rather than being controlled by an individual set point value.

date. Although this set point and temperature-based system is essentially linear, it also includes nonlinear components. Sweat rate, vasoconstriction, vasodilation, and shivering are regulated by algorithms of similar type to those in other models, though also the rate of temperature change is included as a further input signal (235). The importance of such temperature transients was emphasized by Mitchell et al. (178), confirmed by Libert et al. (159) and in later models (261,263) more explicitly processed. The basic principles of Stolwijk's active system model were also adopted by others. Fiala et al. (63,65) simulated sets of experiments from literature to determine the involvement of different afferent signals in individual regulatory responses. Rather than using postulative methods, meta-regression analysis was employed to define a statistically founded, set point temperature-based nonlinear system that also includes dynamic sensory components, that is, rates of change of skin temperature.

In terms of popularity and application, the two models originating from the J.B. Pierce laboratories, building on data collected by Ethan Nadel, Bruce Wenger, Duncan Mitchel, Michael Roberts and their coworkers, that is, the Gagge and the Stolwijk model have probably seen the largest follow up, as other models (e.g., Wissler, used in complex diving and hyperbaric conditions, 262) were often considered too complex or requiring too much computing power, at some point running a network with each individual segment on a dedicated PC. The multi segment Stolwijk model (234, 235) was produced for NASA providing a basis for the simulation of thermoregulation in space travel. A model that has gained popularity over the last decade in a range of applications is the Fiala Thermal Physiology and Comfort (FPC) model (for a review see, e.g., 58). The model has not only been used in indoor and car climate applications (34, 61), but also for weather "interpretation" (56), in heat-strain modeling (59), in the control of "physiological" responses of thermal manikins (204, 206), and in medical research (46, 224). The main

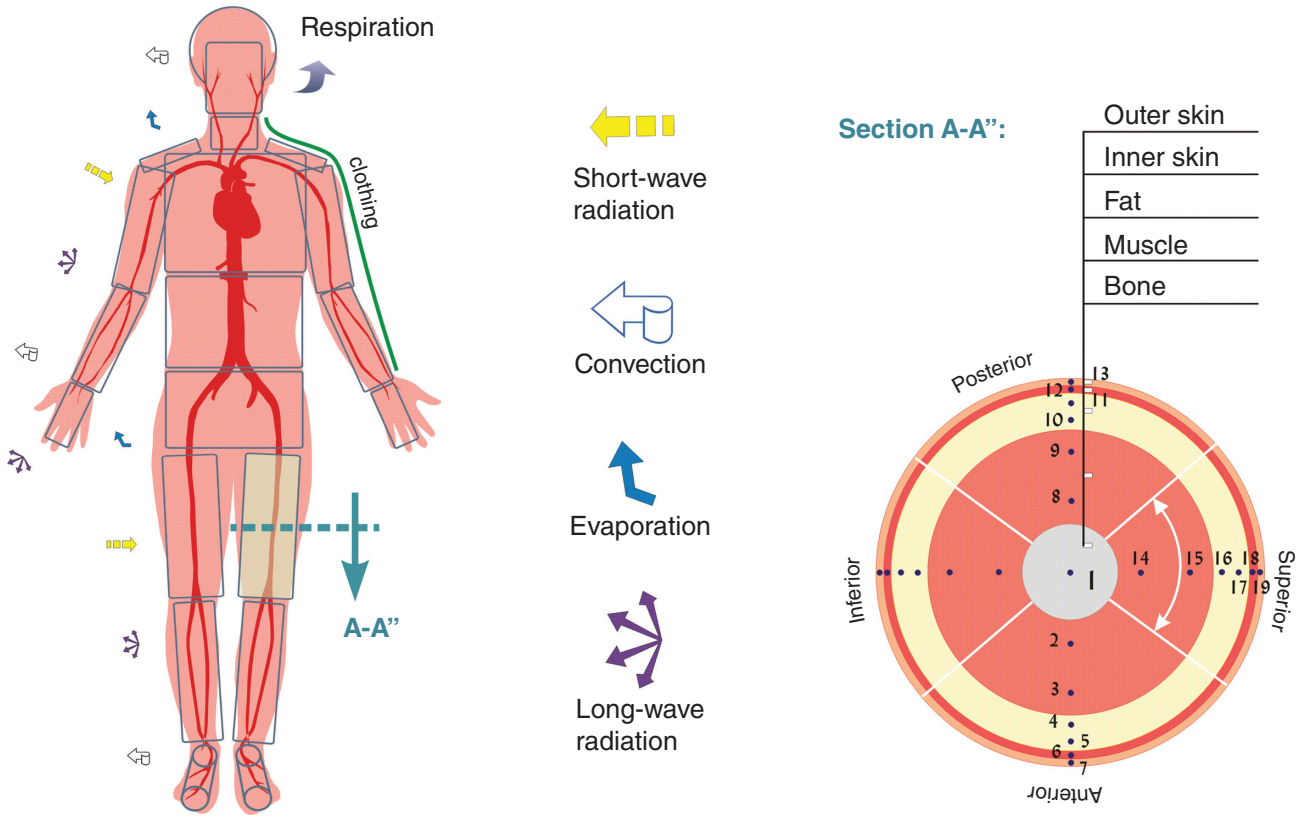

Figure 7 Schematic diagram of the FPC human body model with segmental, spatial, tissue, and nodal subdivisions. Reproduced from (55) with approval of the copyright holder.

principles of this model are similar to the ones discussed earlier. This model is thus used here for more in-depth discussion as a recent representative of the multinode thermophysiological models which are based on a very similar first-principles modeling approach.

Example for a multinode model approach

Human body and tissue heat transfer (the passive system) The human body is modeled as (cylindrical and spherical) body compartments built of concentric tissue layers (section A-A″ in Fig. 7) with distinct thermal and physiological properties (56, 60, 65). Skin is modeled as an inner cutaneous layer representing the blood-perfused cutaneous plexus, and the outer skin which contains sweat glands but no thermally significant blood vessels. Body elements are subdivided also into tangential sectors to enable adequate modeling of exposures to asymmetric boundary conditions (e.g., frontal or lateral directional radiation).

The standard model simulates an average person whose overall body characteristics and local body element dimensions resemble a 50 percentile subject as observed in anthropometric field surveys (90,186,187,201). In the chosen example, this so-called “‘reference” human anthropometry model represents a (35 years old, unisex) 169.7 cm tall person, weighing 71.4 kg that features a skin surface area of 1.83 m^2, body fat content of 22.6%, and an average body density of 1.05 g/cm^3 (55, 58).

Heat transport within tissues is modeled using the Pennes' general bioheat differential equation (202) extended for heat dissipation in spheres:

$$\rho c \frac{\partial T}{\partial t} = k\left(\frac{\partial^2 T}{\partial r^2} + \frac{\omega}{r}\frac{\partial T}{\partial r}\right) + q_m + c_{bl}\,\rho_{bl}\,w_{bl}\,(T_{bla} - T) \qquad (44)$$

where ρ, c, and k represents tissue density ($kg \cdot m^{-3}$), heat capacitance ($J \cdot kg^{-1} \cdot K^{-1}$), and conductivity ($W \cdot m^{-1} \cdot K^{-1}$), respectively. T is the tissue temperature (°C), t time (s), r radius (m); ω a geometry factor (ω = 1: polar, ω = 2: spherical coordinates for the head), q_m metabolic heat generation ($W \cdot m^{-3}$), ρ_{bl} blood density ($kg\ m^{-3}$), w_{bl} blood perfusion rate ($m^3 \cdot s^{-1} \cdot m^{-3}$), c_{bl} heat capacitance of blood ($J \cdot kg^{-1} \cdot K^{-1}$), and T_{bla} (°C) arterial blood temperature.

The q_m-term in Eq. (44) is a sum of the local tissue's thermoneutral basal metabolic rate, $q_{m,bas,0}$ ($W\ m^{-3}$) and any additional heat gain, Δq_m ($W\ m^{-3}$):

$$q_m = q_{m,bas,0} + \Delta\, q_m \qquad (45)$$

Δq_m includes variations in basal metabolism due to changes in tissue temperature deviating from its local set point, T_0, in conditions of thermal neutrality (see later). In

muscles, additional heat may be induced by exercise, $q_{m,ex}$, or by regulatory shivering, $q_{m,sh}$, that is, the local portions of the respective overall quantities:

$$\Delta q_m = q_{m,bas,0}\left(2^{\frac{T-T_0}{10}} - 1\right) + q_{m,ex} + q_{m,sh} \quad (46)$$

Similarly to q_m, local tissue blood perfusion rates, w_{bl}, are defined as a sum of the thermoneutral basal rate $w_{m,bas,0}$ ($m^3 \cdot s^{-1} \cdot m^{-3}$) and variations Δw_{bl} ($m^3 \cdot s^{-1} \cdot m^{-3}$):

$$w_{bl} = w_{bl,bas,0} + \Delta w_{bl} \quad (47)$$

the latter being proportional to changes in the local metabolic rate: $\Delta w_{bl} = 0.93 \Delta q_m$ (234, 235). The largely variable blood flows of the cutaneous plexus are subject to central nervous system regulation. The resultant blood perfusion rate w_{bl} within the skin in Eq. (44) is provided as a local portion of the overall peripheral vasomotion response—modulated by local changes in skin temperature (56):

$$w_{bl} = \frac{w_{bl,bas,0} + a_{dl}\,{}^{DL}/_{\rho_{bl}\, c_{bl}\, V}}{1 + a_{cs} CS\, e^{-DL/80}} \times 2^{\frac{T_{sk}-T_{sk,0}}{10}} \quad (48)$$

DL and CS are the overall regulatory responses of vasodilatation and constriction, respectively, as predicted by the thermoregulatory system model, a_{dl} and a_{cs} are the corresponding distribution coefficients (56), V is tissue volume, and T_{sk} and $T_{sk,0}$ the actual and the reference local skin temperature, respectively.

In the numerical model, tissue layers are discretized as tissue nodes using a numerical form of Eq. (44) which employs a (forward) finite-difference *Crank-Nicholson* scheme (60). This is applied to each tissue node of the numerical model using appropriate material properties, nodal heat generation, and blood perfusion rates. The set of tissue node equations constitutes a system of coupled linear equations to be solved for each time and iteration step of a simulation (60). Solving the whole body matrix for the (undressed) reference person exposed to thermoneutral, steady state (still air) environmental conditions of 30°C, 50% RH results in a mean skin temperature of 34.3°C and body core temperatures of 37.0°C in the head core (hypothalamus) and 36.9°C in the abdomen core (rectum). The cumulated physiological data replicate a reclining subject with an overall basal body metabolism of 75.5 W, basal evaporation rate (insensible perspiration/diffusion through the skin) from the skin of 19 W, and basal cardiac output of 4.9 L min^{-1}.

Thermoregulatory System (Active System)

The thermoregulatory system model predicts the four essential overall responses of the central nervous system: constriction, CS, dilatation, DL, of cutaneous blood flows, shivering, SH, and sweat moisture excretion, SW (63). The overall responses are distributed over body regions and may be altered locally by autonomic regulation as local skin and tissue temperatures deviate from their respective set points—the so-called Q10-effect (56). A schematic diagram of the FPC Model of the thermoregulatory system is provided in Figure 8.

The thermoregulatory model is based on simulation and analysis of experimental exposures to steady state and transient environments ranging from cold stress to heat stress conditions and physical activities from reclining to heavy exercise. Individual afferent signals involved in regulatory processes and their quantitative contributions to generating overall responses were determined by regression analyses of measured and simulated data (63). The system coefficients and the actual control equations resulted from meta-regression analysis as nonlinear functions of the respective punitive signals, Figure 9.

With the coefficients listed in Table 6 the following nonlinear relationship predicts each of the four overall responses, F:

$$F = \langle A_1 \tanh\left[A_2(T_{sk,m} - T_{sk,m,0}) + A_3\right] + A_4\rangle (T_{sk,m} - T_{sk,m,0}) + \langle B_1 \tanh\left[B_2(T_{hy} - T_{hy,0}) + B_3\right] + B_4\rangle (T_{hy} - T_{hy,0}) + C\Delta T_{sk,m}\dot{T}^{-}_{sk,m} + D \quad (49)$$

where $\Delta T_{sk,m}$, T_{hy}, $T_{sk,m,0}$, and $T_{hy,0}$ are the sensitivity-weighted mean skin temperature, head core (hypothalamus) temperature, and the corresponding set points, respectively (63). The $d\dot{T}^{-}_{sk,m}/dt$ term represents negative rates of change of the mean skin temperature as a punitive signal governing the dynamics of regulatory responses against cold, that is, SH and CS during conditions of fast body cooling.

In the model, shivering has a theoretical maximum of 350 W while vasoconstriction and sweat rate are limited by an upper limit of 600 and 1800 g/h, respectively (63). The overall responses are distributed over body regions and are also subject to local autonomic regulation assuming a local response may about double by a 10 K increase in local tissue/skin temperature (158, 185, 235):

$$Q_{10} = 2^{\left[\frac{(T_{sk}-T_{sk,0})}{10}\right]} \quad (50)$$

Blood Circulation

Blood circulation plays a vital role in the human heat transfer. The blood perfusion term of the bioheat Eq. (44) accounts solely for heat exchange in capillary beds. In the FPC Model also, countercurrent heat exchanges between pairs of adjacent arteries and veins are considered (60). The model of the blood circulatory system incorporates a central blood pool (heart) and predicts local arterial and venous blood temperatures for individual body compartments.

In the circulatory process, each body element is supplied with arterial blood from the central pool. Before perfusing local tissues, blood is "conditioned" by countercurrent bloodstreams of adjacent veins. Arterial blood then perfuses tissues exchanging heat in the capillary beds where, according to Eq. (44), it reaches equilibrium with local tissues. Depleted

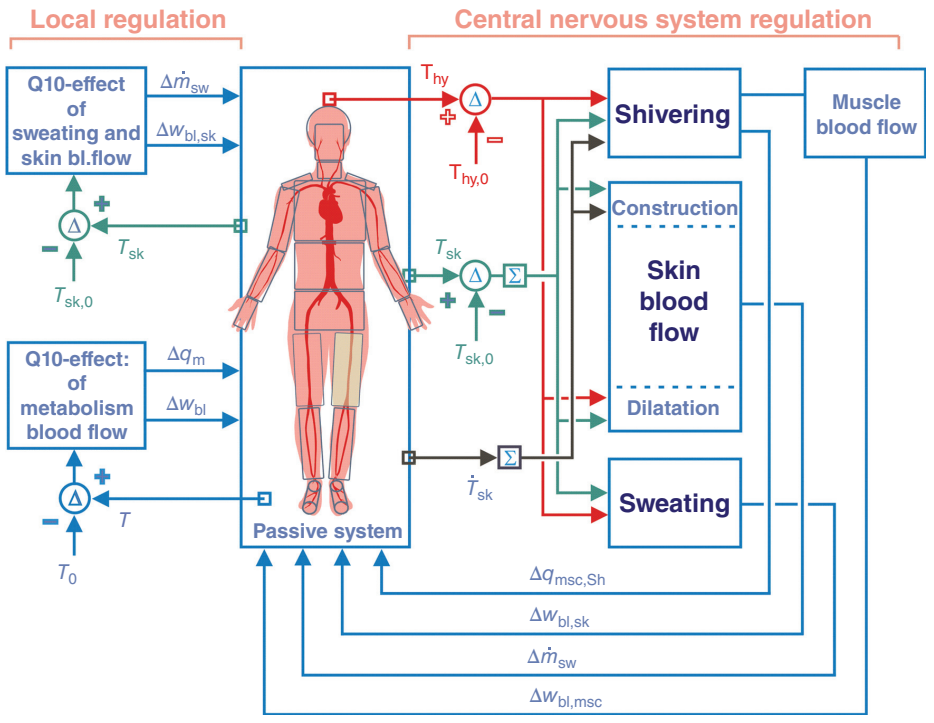

Figure 8 Schematic diagram of the FPC Model of human thermoregulation: feedback system with local skin and tissue temperatures, head core (hypothalamus) temperature, and the rate of change of skin temperature as punitive signals. Set point temperatures $T_{sk,i,0}$, $T_{i,0}$, and $T_{hy,0}$ refer to the body's thermoneutral state at 30°C room temperature. Reproduced from (55) with approval of the copyright holder.

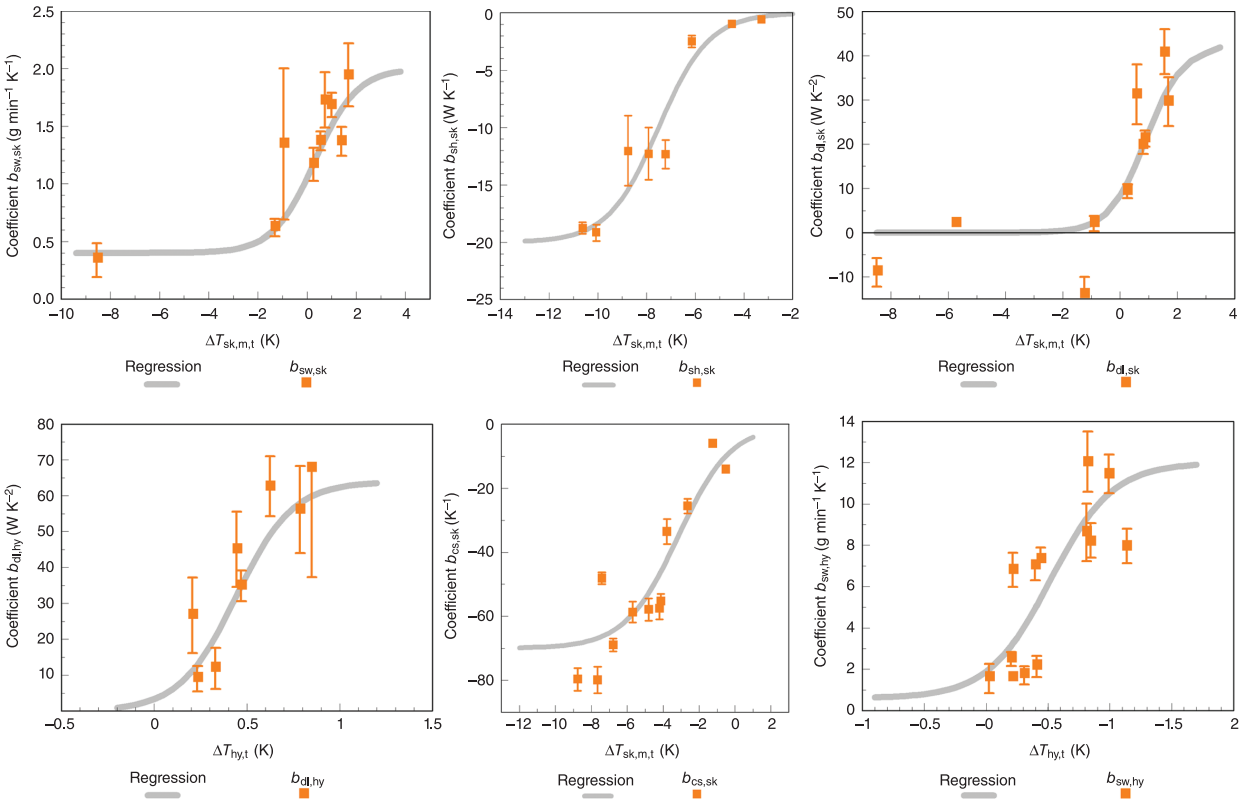

Figure 9 Control equation coefficients as nonlinear functions of temperature input signals from the body core and the skin. Reproduced from (63) with kind permission from Springer Science + Business Media.

Table 6 Thermoregulatory System Coefficients; Each column gives values for specific responses in Eq. (49)

Coefficient	SH (W)	CS (–)	DL (W/K)	SW (g/min)
A_1	10.0	35.00	21.0	0.80
A_2	0.48	0.34	0.79	0.59
A_3	3.62	1.07	−0.70	−0.19
A_4	−10.0	−35.0	21.0	1.20
B_1	0.00	0.00	32.0	5.70
B_2	0.00	0.00	3.29	1.98
B_3	0.00	0.00	−1.46	−1.03
B_4	−27.9	0.00	32.0	6.30
C	1.70	3.90	0.00	0.00
D	−28.6	0.00	0.00	0.00

Abbreviations: SH, shivering; CS, vasoconstriction; DL, vasodilation; SW, sweating.

blood is then collected in veins being rewarmed by countercurrent heat exchange with adjacent arteries as it flows back to the central pool. Finally, venous blood from the whole body is mixed in the central blood pool to constitute a new central blood pool temperature.

Considering the countercurrent heat exchange between adjacent vessels, the heat loss from an artery equals to the heat gain of the adjacent vein. Assuming mass continuity in blood vessels, the decrease in arterial blood temperature, $T_{blp} - T_{bla}$ is thus equivalent to the increase in venous blood temperature, $T_{blvx} - T_{blv}$, after passing the countercurrent heat exchanger:

$$\sum_{i}^{\text{nodes}} \rho_{bl}\, c_{bl}\, w_{bl,i}\, V_i \left(T_{blp} - T_{bla}\right) = \sum_{i}^{\text{nodes}} \rho_{bl}\, c_{bl}\, w_{bl,i}\, V_i \left(T_{blvx} - T_{blv}\right) \tag{51}$$

where T_{blp} (°C) is the central blood pool temperature, V_i (m^3) tissue nodal volume, and T_{blv} (°C) and T_{blvx} (°C) is the body element's venous temperature before and after passing the countercurrent heat exchanger, respectively. The net heat exchange between adjacent vessels, Q_x (W) may also be expressed as (91):

$$Q_x = h_x \left(T_{bla} - T_{blv}\right) \tag{52}$$

where h_x ($W{\cdot}K^{-1}$) is a body element's countercurrent heat-exchange coefficient (56). Since Eq. (44) assumes that capillary blood reaches equilibrium with the surrounding tissues, T_{blv} yields:

$$T_{blv} = \frac{\sum_{i}^{\text{nodes}} T_i\, w_{bl,i}\, V_i}{\sum_{i}^{\text{nodes}} w_{bl,i}\, V} . \tag{53}$$

With the aforementioned equations, the arterial blood temperature, T_{bla}, of a body element then results in:

$$T_{bla} = \frac{T_{blp} \sum_{i}^{\text{nodes}} w_{bl,i}\, V_i}{\frac{h_x}{\rho_{bl}\, c_{bl}} + \sum_{j}^{\text{nodes}} w_{bl,i}\, V_i} + \frac{\frac{h_x}{\rho_{bl}\, c_{bl}} \sum_{i}^{\text{nodes}} T_i\, w_{bl,i}\, V_i}{\sum_{j}^{\text{nodes}} w_{bl,i}\, V_i \left(\frac{h_x}{\rho_{bl}\, c_{bl}} + \sum_{j}^{\text{nodes}} w_{bl,i}\, V_i\right)} \tag{54}$$

The blood pool temperature, T_{blp}, is a function of local tissue temperatures from all body parts:

$$T_{blp} = \frac{\sum_{k}^{\text{b.elem.}} \left(\frac{\sum_{i}^{\text{nodes}} w_{bl,k,i}\, V_{k,i}}{\frac{h_{x,k}}{\rho_{bl}\, c_{bl}} + \sum_{i}^{\text{nodes}} w_{bl,k,i}\, V_{k,i}} \times \sum_{i}^{\text{nodes}} T_{k,i}\, w_{bl,k,i}\, V_{k,i} \right)}{\sum_{k}^{\text{b.elem.}} \left[\frac{\left(\sum_{i}^{\text{nodes}} w_{bl,k,i}\, V_{k,i}\right)^2}{\frac{h_{x,k}}{\rho_{bl}\, c_{bl}} + \sum_{i}^{\text{nodes}} w_{bl,k,i}\, V_{k,i}} \right]} . \tag{55}$$

Environmental Heat Exchange

As discussed in the sections on analytical heat balance models (RSR) before, humans exchange bodily heat by convection, respiration, and skin moisture evaporation with the ambient air, by long-wave radiation with surrounding surfaces, short-wave irradiation from high-intensity sources, and/or by conduction with surfaces in direct contact with the body surface. Environmental heat losses may vary considerably over the body typically due to nonuniform clothing, locally varying environmental conditions or physiological responses. In the model, environmental heat loss asymmetries are thus accounted for by establishing local heat and mass balances at each body sector. The resultant heat exchange between a body sector and the environment is then a sum of the individual heat loss components [equivalent to Eqs. (7) and (14), but here in engineering symbols]:

$$q_{sk} = q_{cv} + q_{rl} + q_{rs} + q_{ev} + q_{cn} \tag{56}$$

where q_{sk} ($W{\cdot}m^{-2}$) is the total heat loss from a skin sector, q_{cv} ($W{\cdot}m^{-2}$) heat loss by free and forced convection, q_{rl} ($W{\cdot}m^{-2}$) long-wave radiation, q_{rs} ($W{\cdot}m^{-2}$) short-wave irradiation, q_{ev} ($W{\cdot}m^{-2}$) sweat moisture evaporation and skin moisture diffusion, and q_{cn} ($W{\cdot}m^{-2}$) heat conduction. The calculation of the individual heat loss components in the FPC Model is detailed elsewhere (55,56, 152) but follows the same principles as discussed earlier in this article.

In hot conditions—the focus of this contribution—the evaporation of sweating is the most critical heat-transport mechanism. Unlike some other models (e.g., 235), the rate of sweat evaporation is not dealt with as a direct response

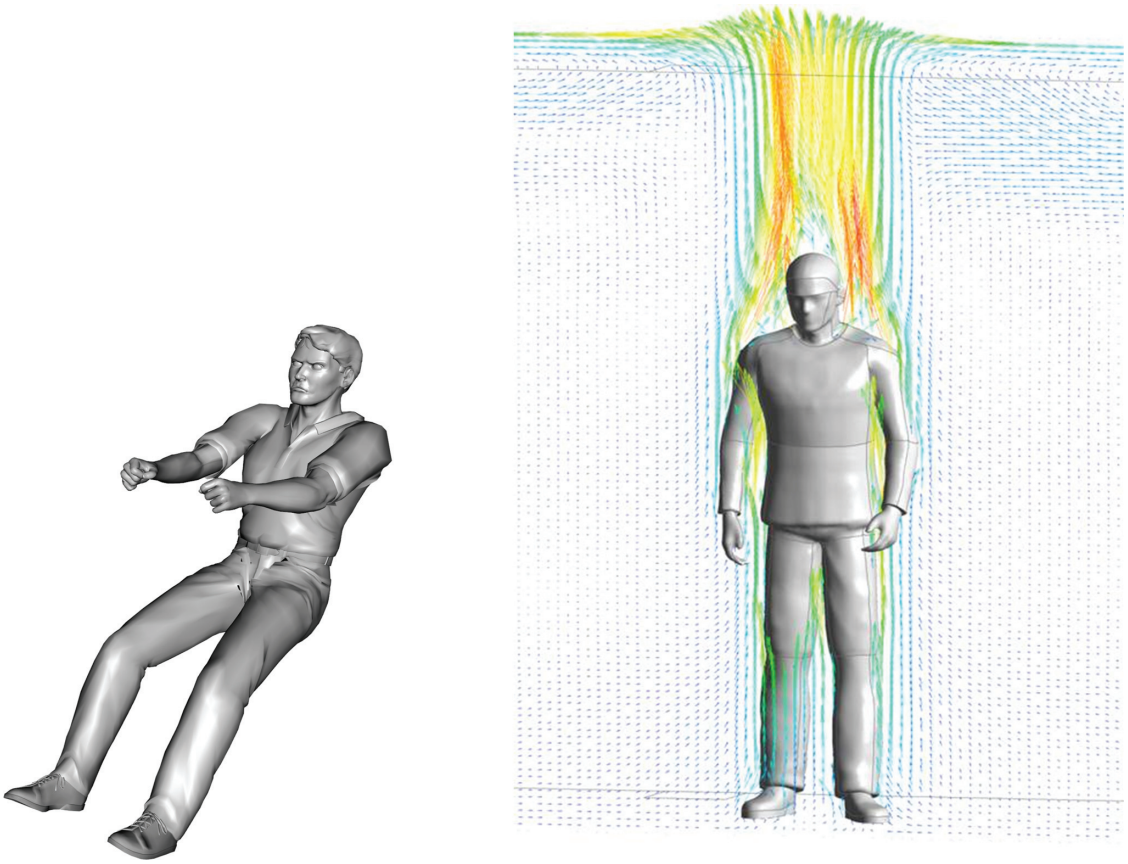

Figure 10 3D geometry models for detailed human heat-transfer analysis using a combination of a thermophysiological model with computational fluid dynamics simulations.

of the thermoregulatory system in the FPC Model. Rather, the amount of regulatory sweating that actually evaporates depends on the local evaporative potential and the evaporative resistance of the clothing (56):

$$\frac{P_{sk} - P_a}{R_{cl,e,t}} = \lambda_{H_2O} \frac{dm_{sw}}{dt} + \frac{p_{osk,sat} - P_{sk}}{R_{sk,e}} \quad (57)$$

where P_{sk}, P_a (Pa) is the partial water vapor pressure at the skin surface and of the ambient air, respectively, $P_{osk,sat}$ (Pa) the saturated partial vapor pressure within the outer skin layer; λ_{H_2O} ($J \cdot kg^{-1}$) heat of water vaporization, dm_{sw}/dt ($kg \cdot s^{-1} \cdot m^{-2}$) local regulatory sweat moisture production, and $R_{sk,e}$ is skin moisture permeability. $R_{cl,e,t}$ is the total regional evaporative resistance of any (multilayered) clothing covering a body sector (55, 82) that can also consider wind penetration effects (101).

The maximum evaporation rate from a body sector is achieved when P_{sk} reaches its saturation $P_{sk,sat}$. In that event, any excessive sweating, dm_{acc}/dt ($kg \cdot s^{-1} \cdot m^{-2}$), may accumulate on the skin surface:

$$\frac{dm_{acc}}{dt} = \frac{dm_{sw}}{dt} - \frac{P_{sk,sat} - P_a}{R_{cl,t,e}\lambda_{H_2O}} \quad (58)$$

assuming quantities exceeding 35 $g \cdot m^{-2}$ will run off (130).

Under real-world conditions, environmental heat transfer processes may be very complex and often heat losses to the environment have to be either measured directly or simulated by means of sophisticated numerical simulation models such as CFD codes using detailed 3D human geometry models (Fig. 10). Diverse industrial applications require detailed analysis of the complex human-environment heat and mass transport processes, for example, to aid the design of comfortable and energy efficient vehicles and buildings (61, 64, 163, 274). Such specialist simulation systems, that couple CFD and/or detailed thermal simulation of cars with mathematical models of human thermoregulation, synergize the predictive capabilities of the individual submodels and advance our ability to predict the complex thermal interactions between the temperature-regulated human body and the thermal environment. Examples of models used in that way are presented by references 34, 184, 207, 238, and 239, 270.

Developed coupled systems include, for example, physical thermal manikins with "physiological intelligence" (58, 204, 206, 207, 219), numerical simulation of human-environment thermal interactions (34, 275) including those where there is a risk of skin burn (252), dynamic thermal and comfort simulation of cars (61, 163, 238, 239), and directional IR-radiation scenarios (274). More recent work includes the development of

monitoring and warning systems that use wearable sensors to predict noninvasively internal temperature and heat stress levels in people working in hot industrial environments (55, 57, 59) that is discussed further later.

Model Validation

The standard model has been subject to diverse general and application-specific validation tests. The studies included climate chamber experiments with exposures to wide-ranging steady state and transient environmental and personal conditions (63), indoor climate and occupant comfort conditions in buildings (62), rapid transients in cars (61), a variety of asymmetric radiation scenarios (58, 151-153, 208), exposures to (uncompensable) heat stress (57, 59, 208), etc. An international large-scale validation study, conducted as part of an EU research project, also included wind tunnel experiments and field studies with exposures to uncontrolled and extreme outdoor weather conditions (205). Generally, the various validation studies revealed consistent predictions in line with experimental observations with respect to thermoregulatory and perceptual responses, mean and local skin temperatures and internal temperatures for the analyzed range of environmental temperatures between −17°C and 50°C, relative humidities 20% and 98%, radiant temperatures up to +93°C and radiant asymmetries up to 100 K, average wind velocities between 0.0 and 22 m/s, clothing insulations between $0 < I_{cl} < 2.2$ clo, and activity levels between 0.8 and 13 met. Mean and local skin temperatures agreed with experimental observations typically within a root mean square deviation, RMSD, of 1.0 and 2.0 K, respectively, body core temperatures within 0.3 K, shivering and sweating responses within 30 W. Details of the individual results and comparisons with measured data are discussed in the respective publications and (55, 58). The performance of the individualized model and in conjunction with noninvasive body core temperature assessment is discussed in the respective sections further later.

Individualizing physiological models

Mathematical models of human thermal response are widely used, for example, to predict the risk of exposures, or define limits and preventive measures such as use of protective clothing, changes to environmental conditions, etc. A general problem with the prediction of the human thermal response has been the large interindividual variability in the strain responses to identical stress. The reasons include differences in physical fitness, acclimatization status, hypertension, age, gender, ethnicity, anthropometric and body composition properties, etc. (98, 100).

Most existing models are population based. As such they are limited to prediction of the average-population response (often young, fit males, due to the type of validation datasets available) which may involve risks to individuals who do not fall within the range of a "typical" person. Since the late 1990s, several efforts have been made to "individualize" models, for example, by Havenith (98, 100), Zhang et al. (275), van Marken-Lichtenbelt et al. (245), Takada et al. (237), Yokota et al. (272, 273), Wölki et al. (265, 266), Zhou et al. (276), and Novieto (194, 195). Most of these focus on a number of personal characteristics, where anthropometrics are most popular, that is, adjustments to the passive system such as body (segment) sizes, fat content, etc. Some of these authors have introduced changes to the active system, that is, modified the control equations for sweating, blood flow and/or shivering, or employed the so-called "Monte Carlo" approach for the simulation of individual variations on a population basis (83, 273). Although many papers on the individualization of models are published, few provide the quantitative information in terms of equations or code used to represent and simulate the individual, perhaps due to the commercial interests in such models. Rather individualization approaches have been discussed in general terms with model validation presented as the main focus of the publications.

For modelers of individual differences, the challenge is to define, despite the complexity of the subject area, an easy-to-use individualized model that requires a minimum of inputs, and these should be easy to measure, readily available personal data (59, 98). The latter refers to the importance to make such a model attractive for use in practice rather than in scientific study only.

According to Havenith et al. (98, 100), among the many personal parameters four factors play the main roles in the individual heat-stress response: physical fitness (work capacity), acclimatization, and anthropometric and morphological body properties. Other factors such as age and gender are considered of secondary importance as they lose influence when observed data is corrected for the effect of the maximum aerobic power, VO_{2max}, and body-fat content (98, 100, 103, 104). The following section describes the various aspects of individualized response models, based mainly on work published by Havenith et al. (98, 100) and Fiala et al. (55, 59) as these provided more explicit information. Where available, also work from other authors is included. The modeling approaches and implications for human temperature and regulatory reactions to warm and hot conditions are discussed using the multisegmental FPC model introduced above, which accounts for personal variations in anthropometric and morphological body properties, as well as the four individualization factors noted earlier.

Individualizing the passive system

Anthropometry model Most models allow some input of anthropometry, typically body mass and height or body surface area which influence the basal metabolic rate, exercise metabolic rate (in weight bearing activity), and the size of the body surface offered to heat exchange with the environment. More sophisticated versions use such input to determine also local body characteristics such as segment lengths and circumferences, like the "body builder" approach by Zhang et al. (275). A good example with specific detail is

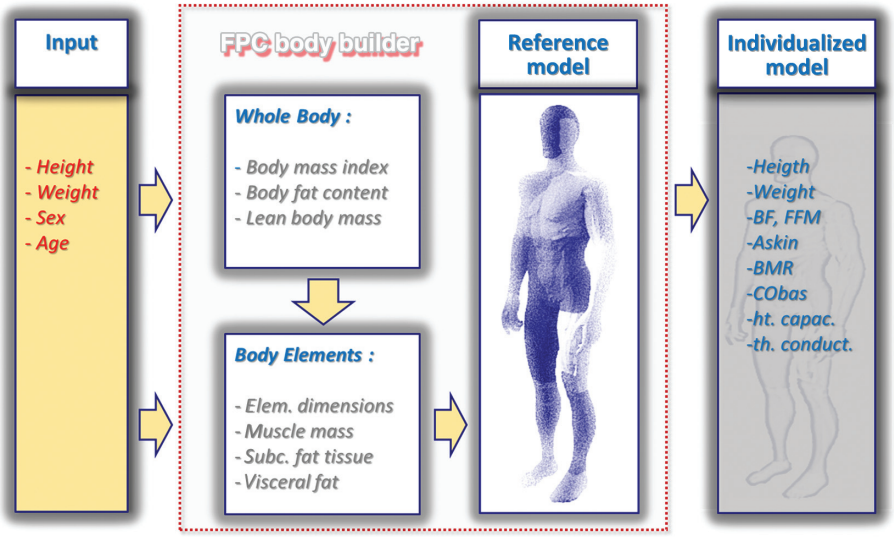

Figure 11 Schematic diagram of the calculation process constituting the scalable FPC Human Anthropometry model. Reproduced from (55) with approval of the copyright holder.

provided by Fiala et al. (55). They produced a scalable human anthropometry model, based on published, large population anthropometric data from three sources. (i) NASA (186, 187) collected data of anthropometric (civilian and military) field studies conducted around the world between 1940 and 1975 providing information on stature, weight, age, ethnicity, and local body dimensions of male and female subjects. (ii) Gordon et al. (90) produced a large-scale survey conducted 1987 to 1988 to obtain anthropometric data of 2208 female and 1774 male different ethnic-origin military personnel aged between 17 and 51 years. (iii) Paquette et al. (201) conducted a study between 2006 and 2008 that employed 3D-scanning techniques to survey 2811 male and 651 female active duty and reserve military personnel. Based on the extensive anthropometric data, a scalable model was defined that requires solely four basic individual parameters as input to simulate a person: body height, mass, age, and gender. This information is used to calculate the overall and local dimensions and body composition characteristics of a person. The procedure is outlined schematically in Figure 11 and is detailed further in the text.

The procedure employs a *Reference Model* of human anthropometry which forms the basis upon which the personal anthropometric characteristics of the person to be simulated are modeled. To obtain a representative model averages from the aforementioned anthropometric surveys were derived for male and female subjects to represent a 50-percentile (35-year-old) man and woman (59), that is, stature of 176.5 cm, 79.9 kg weight (25.6 kg/m^2 body mass index), and 162.9 cm, 62.9 kg (23.7 kg/m^2) respectively, reproducing well also other public data on 50-percentile persons (190).

The reference anthropometry humanoid used to simulate average-population responses is therefore 169.7 cm high and "weighs" 71.4 kg (BMI = 24.8 kg/m^2). A comparison of the resultant relative body element lengths of this *Reference Model* with field survey data (90, 186, 187, 201) and data employed in a biomechanical model of Daanen and Heerlen (38) are provided in Table 7.

Body elements of the *Reference Model* are "scaled" based on the four overall input parameters characterizing the person. The length of extremities is computed for males and females from the length of the *tibia*, *femur*, *humerus*, and *ulna* bones:

$$L = a_1 H + a_0 \tag{59}$$

where L is the length of the bone in cm, H the body height in cm, and a_1 and a_0 are the corresponding regression coefficients (186). The length of the remaining cylinder-shaped body elements is scaled in proportion to changes in the stature while the trunk is sized to retain the body height of the individual to be simulated.

The length of the main sections of the stature are compared with the corresponding measured data obtained from the CEASAR anthropometric survey (39, 212) for male subjects grouped in ten height categories (from 155 to 202 cm average height) in Figure 12.

A similar modeling approach, though with less detailed analysis was applied by Zhang et al. (275). They used data from Tilley and associates (242) who determined gender specific body segment proportions in relation to the body height, with, for example, men having a slightly longer chest, calf and foot, and females having a longer pelvis region.

Individualized models based on anthropometric data statistics should be updated to capture the continuous changes in population anthropometrics or ethnic groups studied, such

Table 7 Comparison of Relative Body Part Lengths of the *Reference Model* with the Corresponding Published Data from Different Sources

Body part	*Reference model* %	Daanen (38) %	Ansur I (90) %	Ansur II (201) %	NASA (186, 187) %
stature	100.0	100.0	100.0	100.0	100.0
Head + neck	13.9	17.4	13.5	13.7	14.5
Trunk	39.2	28.0	39.0	38.9	38.7
Head-trunk	53.1	50.3	52.5	52.6	53.1
Upper arm	19.0	17.4	19.5	18.9	18.4
Lower arm	15.6	15.7	15.2	15.2	15.9
Upper leg	20.4	24.0	20.5	20.5	20.2
Lower leg	22.7	25.1	23.2	23.2	22.9
Ankle (height)	3.7				3.7

Note. Adapted from (55) with approval of the copyright holder.

as the overall increase in body height or body weight. Additional data may be obtained from ASTM and ISO standards on this topic.

Body composition, resting metabolic rate and surface area In addition to anthropometry, body composition is a further factor to consider to adequately represent a person in a thermoregulatory simulation model. In the FPC model, the reference was defined to simulate an "average" human with respect to body height, mass, tissue density, fat content, skin surface area, basal metabolic rate, cardiac output, and the dimensions and weight of body parts. A comparison of the relative weights of different body parts with measured quantities is provided as percentages of the body weight in Figure 13.

The overall body-fat content of male and female subjects is either user-defined input (based on actual measurements) or is calculated according to Han and Lean (95) using the body mass index and age of the simulated person:

$$\mathrm{BF}\,(\%) = c_{\mathrm{bf,b}} \cdot \mathrm{BMI} + c_{\mathrm{bf,a}} \cdot \mathrm{age} + c_{\mathrm{bf,0}} \qquad (60)$$

where BF is the body fat content in % body weight, BMI body mass index in kg/m^2; the age of the person is in years. The coefficients $c_{\mathrm{bf,b}}$, $c_{\mathrm{bf,a}}$, and $c_{\mathrm{bf,0}}$ with 1.330, 0.236, and −20.20 for male and 1.210, 0.262, and −6.70 for female subjects, respectively, indicate significant differences in the body-fat content among sexes (95).

Zhang et al. (275), given that body fat measurement requires skills and equipment, also used an approximation rather than measurement of body fat in their "body builder." Firstly, they link the body fat content to body density, using the classical Siri equation:

$$\mathrm{BF}(\%) = 100\left(4.95 \times 10^{-3}/\rho - 4.5\right) \qquad (61)$$

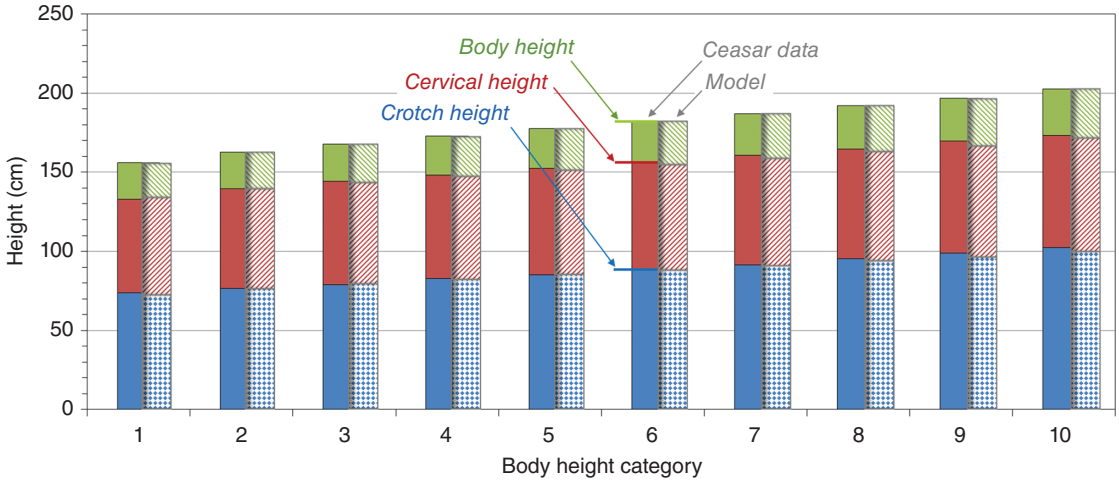

Figure 12 Comparison of predicted body part lengths forming the stature with data obtained for male subjects from the CEASAR Project (39, 212) for 10 body height categories (59). Reproduced from (55) with approval of the copyright holder.

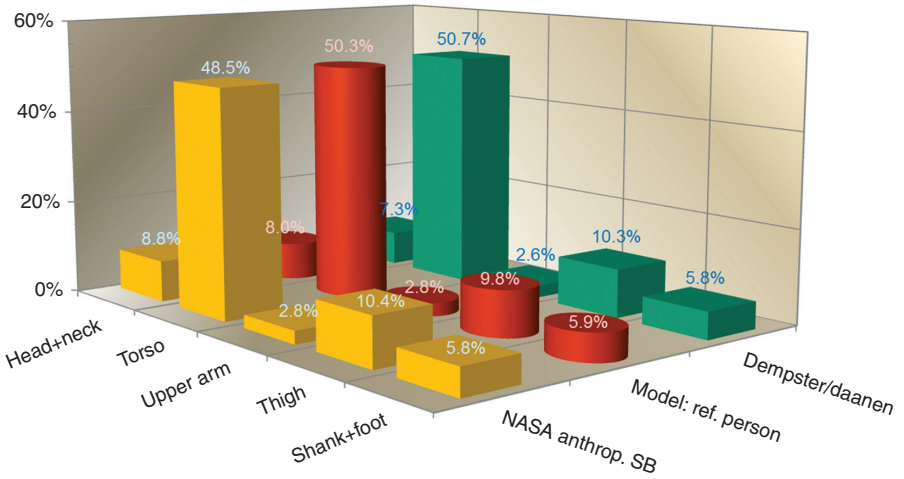

Figure 13 Relative weight of body parts: comparison of the *Reference Model* with measured data (38, 186). Reproduced from (55) with approval of the copyright holder.

[with ρ = body density (kg·m^{-3})] while the body density is deducted from height and body circumference measurements from Hodgdon and Beckett (110):

$$\begin{aligned}\rho\ \text{males} &= 10^3\left\{-\left[0.19077\cdot{}_{10}\log(C_u - C_n)\right]\right.\\ &\quad\left.+\left[0.15456\cdot{}_{10}\log(100\cdot H\right]+1.0324\right\}\\ \rho\ \text{females} &= -\left[0.35004\cdot{}_{10}\log(C_m - C_h - C_n)\right]\\ &\quad+\left[0.22100\cdot{}_{10}\log(100\cdot H\right]+1.29579\end{aligned}\quad(62)$$

With ρ = body density (kg·m^{-3}), H = height (m), C_u = body circumference at level of umbilicus, C_m = minimal abdominal width midway between xyphoid and umbilicus, C_n, C_b, C_h = circumferences of neck, biceps, and hip (all in cm). Van Marken Lichtenbelt et al. (245) applied data specific to a Dutch population (247) to a Fiala model using the formula:

$$\text{BF}(\%) = 1.20\cdot\text{BMI} + 0.23\cdot\text{age} - 10.8\cdot\text{sex} - 5.4 \quad (63)$$

where age is in years, BMI = body mass index and sex = 1 for males; 0 for females, while Zhou et al. adjusted the same model (59, 60) to a Chinese population, calculating the body-fat percentage as:

$$\text{BF}(\%) = 1.38\cdot\text{BMI} + 0.25\cdot\text{age} - 12.1\cdot\text{sex} - 8.1 \quad (64)$$

with age in years, sex = 1 for males; 0 for females; based on work by Deurenberg et al. (44).

Various studies using magnetic resonance imaging revealed that especially in males a notable portion of body fat is retained within the abdomen as abdominal subcutaneous adipose tissue (ASAT) and visceral adipose tissue (VAT). In the FPC model, VAT is determined based on the work of Kuk et al. (154) who investigated the influence of age and sex on VAT and ASAT in 483 young and older male and female subjects covering a wide range of body mass indexes.

Taking into account the functional relationship between waist circumference, overall body fat content and age, according to Han and Lean (95) the amount of the VAT yields:

$$\begin{aligned}\text{VAT} &= \text{BF}\left(c_{\text{vat,bf0}} + c_{\text{vat,bfa}}\,\text{age}\right)\\ &\quad + c_{\text{vat,aa}}\,\text{age}^2 + c_{\text{vat,a}}\,\text{age} + c_{\text{vat,0}}\end{aligned}\quad(65)$$

where VAT is visceral fat tissue in kg and BF body fat content in % body weight. The coefficients $c_{\text{vat,bf0}}$, $c_{\text{vat,bfa}}$, $c_{\text{vat,aa}}$, $c_{\text{vat,a}}$, and $c_{\text{vat,0}}$ are gender specific with 0.459, 0.003, 0.0003, −0.071, and 12.892 for males and −0.005, 0.003, 0.0008, −0.076, and 0.529 for females, respectively.

The abdominal subcutaneous fat content is computed similarly based on experimental results of Kuk et al. (154) and Han and Lean (95):

$$\text{ASAT} = c_{\text{as,b}}\,\text{BF} + c_{\text{as,a}}\,\text{age} + c_{\text{as,0}} \quad (66)$$

where ASAT is the amount of abdominal subcutaneous fat in kg. The coefficients $c_{\text{as,b}}$, $c_{\text{as,a}}$, and $c_{\text{as,0}}$ were obtained as 0.194, 0.020, and −1.400 for males and 0.251, 0.055, and −3.387 for females, respectively.

The aforementioned information is used in the FPC model to compute the local adipose and fat-free mass portions. The iterative procedure distributes adipose tissues by scaling local subcutaneous fat layers based on relative tissue proportions in body elements defined by the *Reference Model*. This approach recognizes that while the largest portion of body fat is contained in central body parts, the remainder is distributed with successively decreasing amounts over proximal limbs toward outer extremities and the head (51).

The adjusted local properties are then "mapped" onto individual body parts of the *Reference Model* resulting in an updated numerical representation of the passive system. Figure 14 (left), compares the model's resultant total body fat

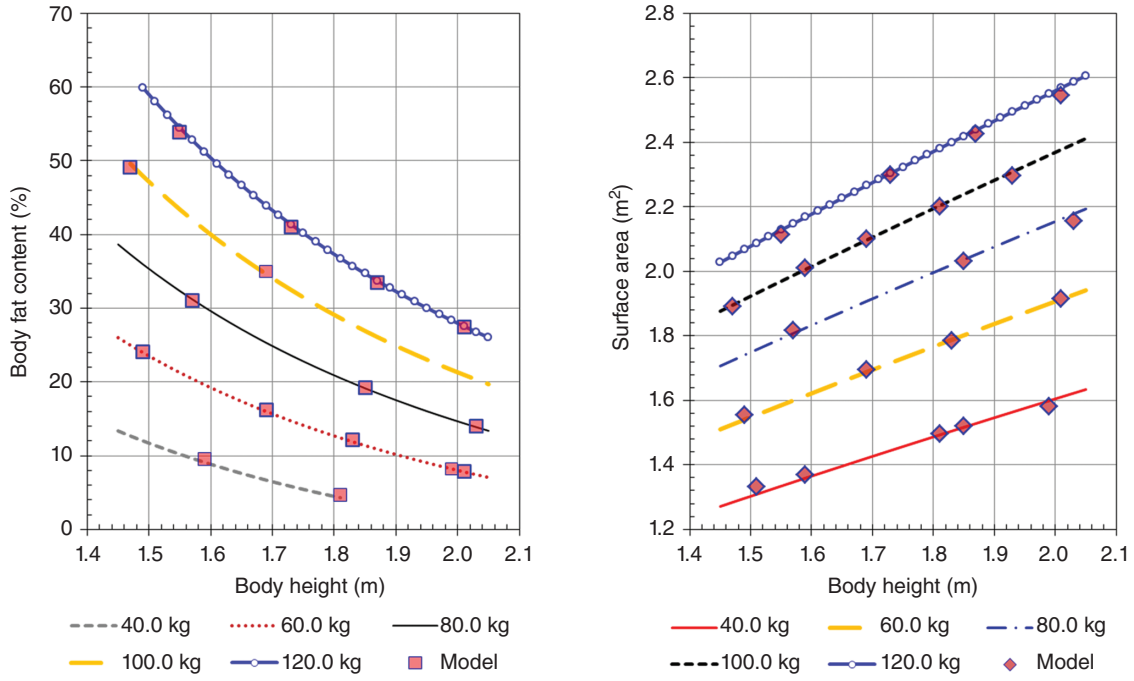

Figure 14 The model's body fat content (left) and total skin surface area (right) as functions of the body height and weight obtained for (35 years old) male subjects compared with experimentally based data (47, 95). Reproduced from (55) with approval of the copyright holder.

content after iterative scaling and integration with experimentally based values (95) over a wide range of body height and fat content combinations.

Yokota et al. (273), followed a completely different anthropometric individualization approach. Considering the correlations of body fat content with height and mass ($r = -.03$ and $+0.70$, respectively), they employed the population based distribution of weight to determine the statistical distribution in body fat for their Monte Carlo-based approach. Rather than modeling specific individuals, this approach provides a statistical distribution of the impact of anthropometrics on thermal strain.

It should be noted that the scaling processes not only alter anthropometric and morphological body characteristics but may inherently change also further body properties which are no model input, such as the basal metabolic rate and skin surface area. According to WHO (255), the basal metabolic rate of males and females is proportional to the body mass though with significant differences among sexes (62):

$$\begin{aligned}\text{BMR (watt)} &= 11.574 \cdot (0.048 \cdot \text{mass} + 3.653 \text{ for men})\\ \text{BMR (watt)} &= 11.574 \cdot (0.034 \cdot \text{mass} + 3.538 \text{ for women})\end{aligned} \quad (67)$$

with mass in kg. Van Marken Lichtenbelt et al. (245) used these formulae to calculate BMR directly. In the FPC model, BMR is not directly calculated but varies as a result of body scaling reproducing the WHO data within 5% relative error for both sexes. Zhang et al. (275) used a model by Mifflin et al. to calculate the basal metabolic rate from fat free mass:

$$\text{BMR (watt)} = 0.04884 \cdot (19.7 \cdot \text{fat free mass} + 413) \quad (68)$$

while Zhou et al. (276) used a specific equation for Chinese individuals:

$$\begin{aligned}\text{BMR (watt)} = 0.011574 \cdot (58 \cdot \text{mass} + 1741 \cdot \text{Height}\\ - 14 \cdot \text{age} - 470 \cdot \text{sex} + 227)\end{aligned} \quad (69)$$

where mass is in kg, height in m, sex = 0 for males and 1 for females [note: (i) inconsistent use of sex coding by Zhou et al. in Eqs. (64) and (69)]. (ii) The BMR equations were converted to watts from the original papers for easier comparison—resulting in differences of less than 3 W for an average man).

Another important body characteristic which influences the human heat exchange with the environment and thus has implications also for temperature regulation is the overall skin surface area. The model's resultant skin surface area, determined by the segment scaling calculations is compared with the Dubois body surface area (47) for different combinations of body height and weight in Figure 14 (right). Most other authors directly use the Dubois and Dubois calculation of the skin surface area from body mass and height (275) or use equations derived for different ethnic groups (276). Skin surface areas for the reference persons in the different models vary from 1.71 m^2 (female) over 1.85 m^2 (unisex humanoid)

to 1.98 m^2 (male, 69) to 1.55 and 1.71 for a Chinese females and males, respectively (88).

With most studies that use body mass and height to calculate the surface area, the effect of altering the body density (due to different adiposities) on the surface area at a given body weight is ignored. An analysis of this effect (98), showed that for a body mass of 75 kg, a change in fat content (replacing muscle) of 10% of total mass results in a change of the body surface area of around 1.9%. Hence, this is a relevant factor, especially when, for example, obesity effects are studied. For studies within athletic or active military populations this effect may have less relevance due to the smaller range in adiposity in these populations.

Other individual characteristics considered include, for example, skin absorptivity (88) [based on data from Houdas and Ring (113) for absorptivity in different wavelengths of black and white skin and midway interpolation for brown skin], counter current blood vessel length and heat exchange (88), tissue thermal capacity, and conductance (59, 88, 100).

For models with few compartments (e.g., only two radial nodes as in the Gagge model), heat flows do not pass from one tissue type compartment to the next, as there is only the core and skin compartment of "lumped" tissue. In that case, the tissue core to skin conductance needs to be defined as an active component that is influenced by activity level (e.g., muscle insulation changes with activity), representing the combined conductive and convective heat-transfer components of multilayer models in a single number. Figure 15 illustrates this approach, creating an overall core to skin conductivity based on passive insulation of the subcutaneous fat layer, a variable insulation of the muscle layer based on activity level and a variable convective flow of the core to skin blood flow (98). The individual's body fat as well as fitness and acclimatization will therefore all affect the core to skin "conductivity" value.

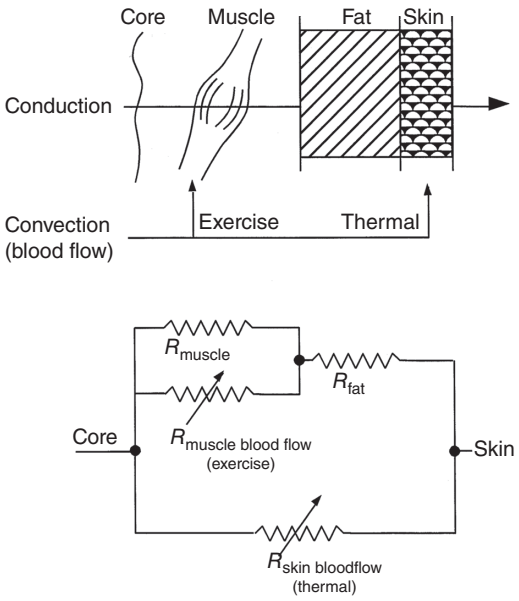

Figure 15 Representation of the core to skin heat resistance network to represent individual differences in anthropometrics and blood circulation in a two radial node model (98, 100). Reproduced with permission of the copyright holder (G. Havenith).

Individualizing the active system

Of the above noted four main personal factors, individualized passive system models can account solely for the impact of the body's anthropometry and morphology including related parameters, for example, changes in the body surface area, body fat content, total body mass (i.e., body heat capacity), and surface-to-body-mass ratio. The remaining two personal characteristics, that is, physical fitness and acclimatization are dealt with by individualizing active system models. The direct input parameters and other parameters that indirectly affect personal thermoregulatory responses and their integration in a model are depicted in Figure 16 (59, 98, 100).

According to Havenith (98, 100) and Fiala et al. (59) the effect of physical fitness can be dealt with using the maximum aerobic power of the individual, $VO_{2,max}$ ($mL \cdot kg^{-1} \cdot min^{-1}$) as a direct input into the model. Though "fitness" is a concept encompassing many different aspects of health, work capacity, training, etc., for the purpose of heat-stress response modeling, the actual aerobic power seems to be the most relevant factor, as it also incorporates information on the cardiovascular reserve during work (98, 104). To incorporate this factor in simulation models, the difference between the individual and the average maximum aerobic power of an average-fit person (40 $mL \cdot kg^{-1} \cdot min^{-1}$) is calculated as a measure of the individual fitness (a fitness scaling factor to be applied to the *Reference Model*), *fit* ($mL \cdot kg^{-1} \cdot min^{-1}$):

$$\text{fit} = VO_{2,max} - 40 \tag{70}$$

where $VO_{2,max}$ may vary between $20 < VO_{2,max} < 60$ $mL \cdot kg^{-1} \cdot min^{-1}$ from unfit to trained individuals, respectively. Any quantities exceeding these margins are set equal to the respective limit in the model.

The acclimatization status, accl, is taken as a function of the number of acclimatization days (each with at least 90 min exposure to the heat-stress conditions studied, 98), n_{acd}:

$$\text{accl} = 1 - e^{(-0.3 \times n_{acd})} \tag{71}$$

The number of acclimatization days is the second direct input parameter into the FPC model and can vary between: $0 < n_{acd} < 14$ days (98). The shape of the curve (98) was based on work by Givoni and Goldman (79).

Having analyzed the literature on effects of training and acclimatization on sweating and blood flow (SKBF), in terms of changes to set points and gains, Havenith (98,100) based his individualized model concept on the assumption that changes in regulatory action due to physical fitness or acclimatization elicit a downward shift of the thermoregulatory set point

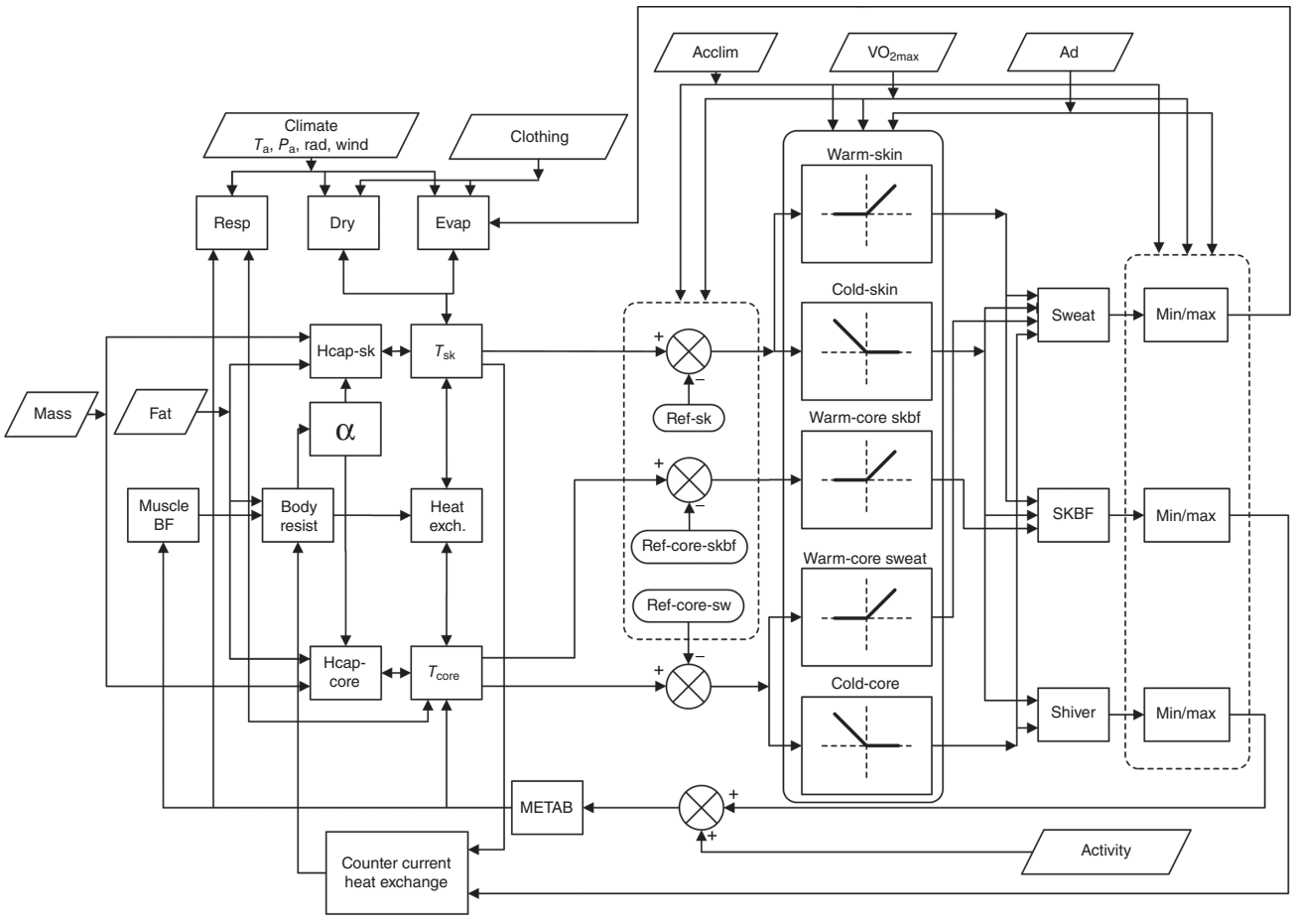

Figure 16 Input parameters into the thermoregulatory system model to simulate responses of individuals: direct model input and variations of body configuration as indirect input (98, 100). Reproduced with permission from Journal of Applied Physiology.

temperature in the head core, that is, the hypothalamus temperature, $\Delta T_{hy,set}$ (°C), in the physiological model:

$$\Delta T_{hy,set} = -\left(0.1 \times \frac{fit}{10} + 0.25 \times accl\right) \quad (72)$$

The new set point temperature, $T_{hy,set}$ (°C), thus yields:

$$T_{hy,set} = T_{hy,set,0} + \Delta T_{hy,set} \quad (73)$$

If both fit and accl are zero also $\Delta T_{hy,set}$ becomes zero and the original set point temperature applies resulting in $T_{hy,set,0} = 37.0$°C for an average-fit, unacclimatized person. The shift of the set point temperature for sweating and skin blood flow causes a shift of the onset of sweating and SKBF toward lower body core temperatures as can be seen in Figure 17A.

The sweating response of an acclimatized and/or nonstandard-fit person is furthermore affected by a gain factor, $g_{sw,f+ac}$:

$$g_{sw,f+ac} = \left(1 + 0.35 \times \frac{fit}{20}\right)(1 + 0.15 \times accl) \quad (74)$$

The $g_{sw,f+ac}$ factor increases the sensitivity of sweating to afferent signals from the head core by multiplying the (standard-person) SW—response to obtain the individualized response SW_{f+ac} (98, 100):

$$SW_{f+ac} = SW \times g_{sw,f+ac} \quad (75)$$

This results in a steeper increase of regulatory sweating as the body core temperature, the fitness and acclimatization levels rise (Fig. 17).

In the standard FPC thermoregulatory system model, there is an upper limit SW_{max} of 30 g min^{-1} sweat production for a standard person. This upper limit is multiplied by a factor $f_{sw,max}$:

$$f_{sw,max} = 1 + 0.25 \times \frac{fit}{20} + 0.25 \times accl \quad (76)$$

to obtain the individual maximum sweat rate, $SW_{max,f+ac}$ (g min^{-1}) of (55)

$$SW_{max,f+ac} = SW_{max} \times f_{sw,max} \quad (77)$$

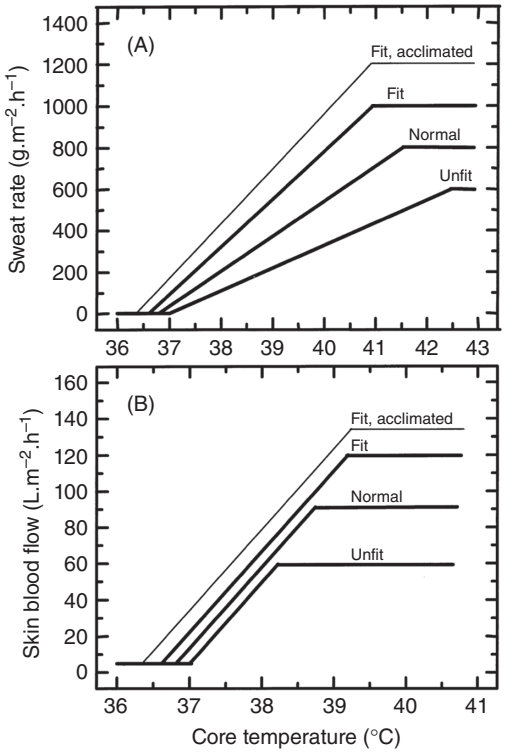

Figure 17 Schematic representation of control function for skin blood flow and sweat rate with effect of fitness and acclimatization causing shifts in thresholds and gain values (98, 100). Reproduced with permission from Journal of Applied Physiology.

The impact of the aerobic fitness and acclimatization status on skin blood flow is obtained in the same way as the sweating response, that is, using the afferent signal $\Delta T_{hy} = T_{hy} - T_{hy,set}$ from the head core and a modified set point temperature, $T_{hy,set}$ (Fig. 17B). This signal is used with the control equation for predicting the central effector output of vasodilatation, DL ($W \cdot K^{-1}$) (55, 218).

The maximum skin blood flow is not a constant but varies with the intensity of the exercise performed (218). For a given activity level, the individual maximum SKBF, that is, individual maximum blood perfusion rate $w_{bl,sk,max,f+ac}$ ($m^3 \cdot s^{-1} \cdot m^{-3}$) is derived from the standard model maximum rate $w_{bl,sk,max}$ for an average-fit, unacclimatized subject using the factor $f_{SKBF,max}$ (55):

$$w_{bl,sk,max,f+ac} = w_{bl,sk,max} \times f_{SKBF,max} \quad (78)$$

where the factor $f_{SKBF,max}$ is a function of the personal aerobic fitness and acclimatization status, as indicated in Eq. (76).

Schematic representation of the effect of these parameters, fitness and acclimatization, on sweat rate and skin blood flow is shown in Figure 17.

Most of the other individualized models have followed similar approaches to determine the changes in their control characteristics. While Havenith (98,100) and Fiala (55) chose to represent sex and age through other physiological parameters like fitness and body composition, Zhou et al. (276) linked their cardiac output control parameter (CO) directly to the individual's sex and age:

$$CO = 0.024 \cdot \text{body mass} - 0.057 \cdot \text{age} - 0.305 \cdot \text{sex} + 4.544 \quad (79)$$

With mass in kg, age in years and sex = 0 for men and 1 for women. Zhang et al. (275) individualized their cardiac output based on body type (ectomorph vs. endomorph) in five steps with an increase of 35% from extreme endomorph to ectomorph. Studying age effects, Novieto (194) defined the ageing person in terms of decreasing body weight, surface area, basal metabolic rate, and cardiac output, but higher body fat, and then used an optimization procedure to determine the best fit coefficients for the regulation of sweating, shivering, vasodilation, and constriction based on a number of datasets. Takada et al. (237) used a similar optimization procedure, and identified six coefficients related to blood flow and sweating in a two node model. In their research, they fitted these six parameters to each individual separately in their dataset, with a total of 1,260,000 possible parameter combinations [Takada et al. (237)].

It should be noted that optimization procedures can differ substantially on principles used. For example, Havenith (98, 100), Fiala et al. (55, 59), and most of the early modelers like Stolwijk (235) developed control equations/models from the physiological literature directly, expressing control parameters in terms of threshold and gains based on literature data. Examples of a different approach are, for example, those followed by Takada and Novieto, following a parameter optimization procedure. The latter cases, with about 30 coefficients to be optimized (194,195), or six coefficients optimized to each individual participant's dataset (237), provides usually a better fit, but may be more limited in its application, as the parameters determined may not have a relation with the underlying physiological control. For example, Takada et al. (237) used the six parameters to optimize the response of only four individual subjects in the following equations:

$$\text{Sweat rate (kg m}^{-2}\text{ s}^{-1}) = \frac{X_3(T_{co} - X1)(T_{sk} - X_2)}{3.6 \times 10^6} \quad (80)$$

$$\text{Skin blood flow (kg m}^{-2}\text{ s}^{-1}) = \frac{X_4 + X_5(T_{co} - X1)}{3600(1 + X_6(X_2 - T_{sk}))} \quad (81)$$

Their obtained parameters X_1 to X_6 vary hugely by individual subject, for example, the perspiration parameter X_3 between 10 and 120, the basal blood flow parameter X_4 between 0.08 and 7.6, the vasoconstriction parameter X_6 between 0.006 and 0.5. It is unlikely that a physiological parameter would actually differ by a factor of close to 100 between individuals, and thus these parameters may be a

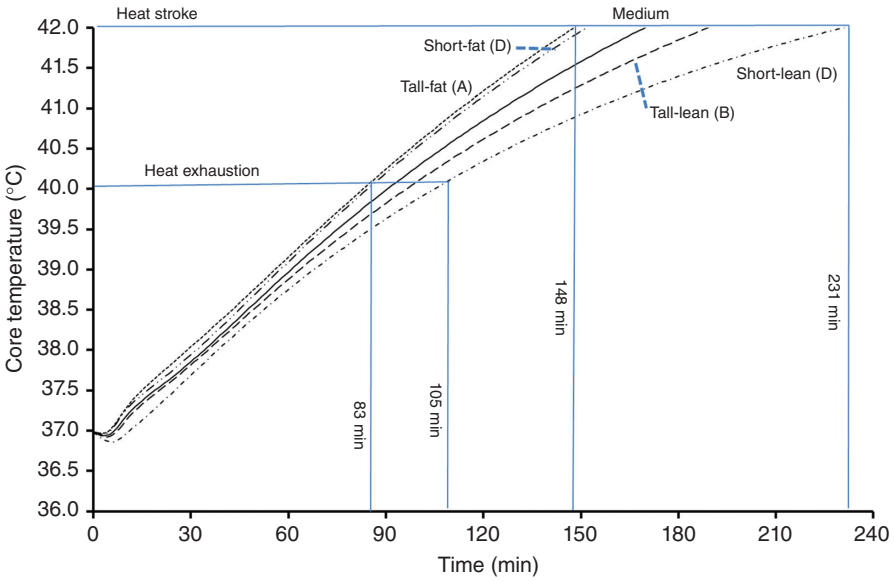

Figure 18 Simulation results for subjects with different anthropometric characteristics using the Yokota individualized model (273). Reproduced with permission from Journal of Thermal Biology.

reflection of mathematical tuning rather than underlying physiology.

Validation of the individualization

All references included in the previous section report improved predictive power of the individualized models indicating the importance of individualization measures. An illustration of the impact of the different somatic forms on predicted body core temperatures was provided by Yokota et al. (273) in Figure 18. Havenith (98,100) reported improvement in predictions expressed as a reduction of the mean squared error (MSE). The level of improvement varied with the climate type from 30% (warm, humid, and relative work load) to 71% (warm humid and absolute work load). The highest reduction was obtained for absolute work load scenarios (i.e., when different individuals exercised at the same power (in watts). Individual differences were "smoothed out" in conditions of relative work load, allowing less to be contributed additionally by individualization measures. Over all five tested conditions (neutral, hot/dry, and warm/humid; the latter with absolute and relative workloads); however, MSE was reduced by 60% due to model individualization measures.

Fiala et al. (57,59) validated the individualized FPC model (incorporating equations described in the aforementioned sections) using measured data obtained for individuals and for groups of athletes featuring different personal characteristics (81). The seminude unacclimatized subjects were exposed to steady environmental conditions of 28°C while exercising on a treadmill at levels up to 13 met (90% $VO_{2,max}$).

In Figure 19 (left), the measured group-average rectal temperature response is compared with rectal temperatures predicted by the model (fit.M) using the average personal characteristics representing the group of athletes (unacclimatized males, 1.80 m body height, 71.6 kg weight, 21.3 years, 60 $mL \cdot kg^{-1} \cdot min^{-1}$ maximum oxygen uptake). The right-hand diagram of Figure 19 refers to the response of a single athlete (smallest/lightest individual with 1.72 m, 62.7 kg, 19 years). For comparison also rectal temperatures predicted for a standard-fit male (s.fit.M) and female (s.fit.F) with the corresponding anthropometric characteristics are plotted in both diagrams. While predictions using the individualized model (fit.M) reproduce measured rectal temperatures well, that is, typically within experimental standard deviation, large discrepancies resulted for the standard-fit persons. In the latter case, predicted rectal temperatures exceeded 40/41°C toward the end of the exposures which underlines the need for considering individual characteristics in simulations especially for conditions of high-intensity exercise. Further examples are discussed in Refs. 55,59, and 57. Overall, the individualized model produced improved predictions of the body core temperature with RMSD values typically within 0.2 K.

Most of the other individualized models mentioned focus on less stressful (i.e., comfort range) conditions or the cold and often only used single, relatively small datasets for comparison. Zhou et al. (276) validated their 'individualized Chinese' person in the Fiala-based model, mainly focusing on mean skin temperature calculation. They observed that in low-stress conditions, the mean error was approximately halved compared to the "standard Fiala" model.

Integration of models with physiological data (noninvasive) for real time monitoring

In cases of extreme heat stress, relying on heat stress standards (ISO 7243, ISO 7933) can be too uncertain. For such cases, that is, where exposures are short and intense, or where specialist protective clothing is worn, the ISO standards

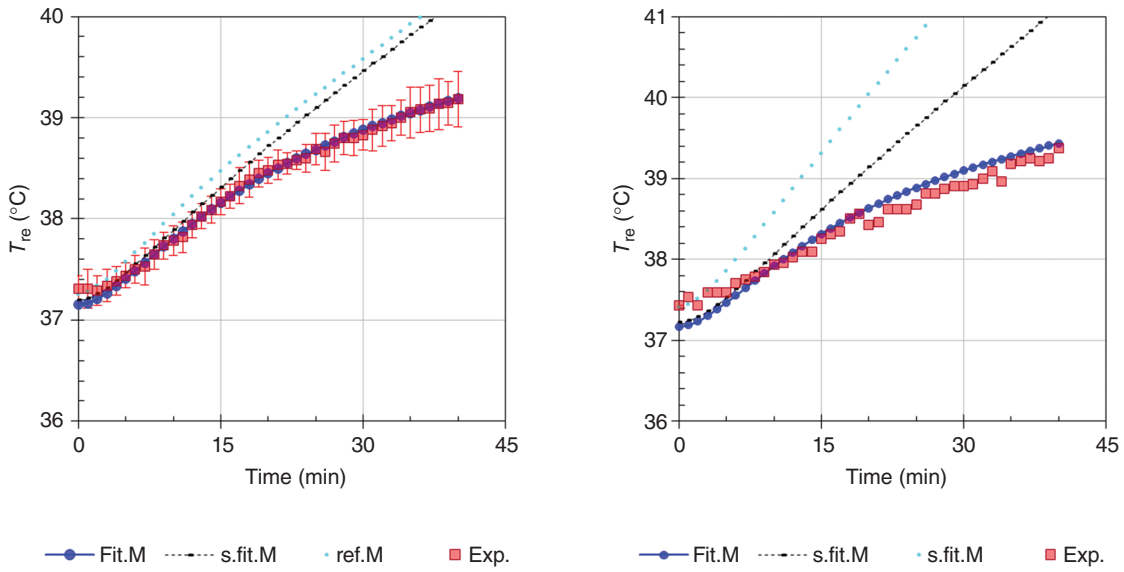

Figure 19 Comparison of predicted and measured group-average (left) and individual (right) rectal temperature responses. Left: group of athletes (n = 6) exercising at 11.7 met; right: single athlete exercising at 13.2 met. Fit.M: fit male (VO_{2max} =60 mL·kg^{-1}·min^{-1}), s.fit.M: standard-fit male (40 mL kg^{-1}·min^{-1}), s.fit.F: standard-fit female (40 mL kg^{-1}·min^{-1}), ref.M: *Reference Model* (40 mL kg^{-1}·min^{-1}).

typically recommend physiological measurements for monitoring the exposed persons.

Internal temperature and heart rate are the ultimate heat-stress indicators (179, 183, 221, 222). While heart rate is easy to measure with existing technologies, body core temperature still requires invasive measurement, usually esophageal, rectally, or intestinally, for example, with a radio pill. In the field, the first two methods are impractical and/or have low acceptance by the people under surveillance. Radio pills seem to be more acceptable (though not on a regular basis), but are very costly and must be ingested hours before (any emergency) operation. Hence, researchers and practitioners have been looking for other, noninvasive measurements of core temperature (40, 41, 211).

Noninvasive determination of core temperature (NICT) has been a challenge for physiological research and related technical developments for decades (40, 41, 211). NICT has become central also to the development of new intelligent PPE systems, personal monitoring, and heat stress warning systems for military and civilian applications (24, 26, 57, 59, 133, 188). The idea with this research is that the actual core temperature is predicted/assessed using noninvasive sensors, ideally integrated in the clothing. A number of empirical prediction equations have been developed using single (e.g., insulated skin temperature; 211) or multiple sensor data (40, 41, 191). The main outcome was that these empirical regression equations work well within the specific conditions for which they were developed, but that no universal equations across the climate/clothing/work spectrum could be obtained with sufficient predictive power (40).

More recently, alternative approaches to the empirical regression equation approach have been proposed (24, 59, 92, 93, 272). Using accessible, real time physiological data, they use various models to predict in real time the body core temperature.

Rather than predicting core temperature from other measures, Gribok et al. (93) investigated ways of 20-min-forward prediction of core temperature evolution, to allow early warning. They use Butterworth filtering and autoregressive modeling for this purpose. Problematic for such approaches are sudden changes of climate or activity level. Buller et al. (23), proposed a model to estimate core temperature, heat production, and heat loss from the body using real-time physiological measurements of heart rate, accelerometer, and skin heat flux using a dynamic Baysian Network model (Fig. 20) and the Kalman filter to enable forward predictions. By comparing

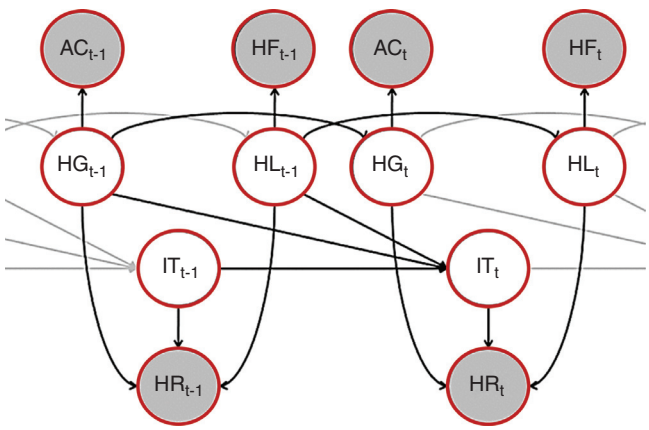

Figure 20 Physiology-based Dynamic Bayesian Network for thermoregulation. Formula temperature, formula gain, formula loss, formula rate, formula from accelerometry, and formula flux. White nodes represent latent variables and gray nodes are observed variables (23). Reproduced with permission from IEEE.

their parameters to daily energy expenditure data from doubly labeled water measurements, they obtained a correlation of $r^2 = 0.73$ for their energy expenditure predictions. Core temperatures were predicted with a RMSD of 0.28 (±0.16) over two validation conditions with a stated accuracy within ± 0.5°C in 83% of analyzed cases, which may not be reliable enough to protect individuals in high heat-stress conditions.

Yokota et al. (272), presented a model for predicting core temperature based on measured heart rate and environmental conditions. Heart rate was used to determine the metabolic rate as input into their physiological model:

$$M = [0.68 + 4.69(\mathrm{HR}_{\mathrm{ratio}} - 1) - 0.052(\mathrm{HR}_{\mathrm{ratio}} - 1)(T_{\mathrm{a}} - 20)]58.1A_{\mathrm{D}} \quad (82)$$

With

$$\mathrm{HR}_{\mathrm{ratio}} = \frac{\text{Current heart rate}}{\text{Resting heart rate}} \quad (83)$$

Equation (82) (second part) takes into account the thermal component of heart rate, linked to body temperature, caused by environmental stress. This model assumes that upon entering a hot climate the heat-induced HR increases instantly, while in reality this increase is a slow drift upward. Hence, the correction [second part of Eq. (82)] will cause an underestimation of metabolic rate. They validated the model with five laboratory studies, using individualized curves, and observed RMSD values between 0.05°C and 0.31°C for the various datasets.

In 2013, Buller et al. (24) followed this work up with a paper describing the use of the Kalman filter in the estimation of human body core temperature from sequential heart rate observations as a single parameter. Using a Bland-Altman analysis, they obtained an overall bias of −0.03°C (±0.32°C) with 95% of predictions falling within ±0.63°C. They concluded that the method was accurate enough to provide a practical indication of the thermal strain in the work place. Closer analysis of the results, however, showed that for individual validation conditions, the discrepancies can be much larger than the above mean values suggest. Furthermore, the dataset has only a limited amount of data at very high core temperatures, and thus most of these statistics are based on the lower core temperature values, where the deviation is not relevant in any case.

These two issues should not be considered as specific criticisms of the Buller et al. studies, as they tend to apply to most of the studies discussed here. Richmond et al. (209, 211) and Davey et al. (40) have specifically addressed the issue of prediction quality in different climatic conditions, and concluded that it may be difficult to come up with a universal NICT model for different clothing, climate, and exercise conditions.

An alternative approach was proposed by Fiala et al. (55, 59), in which noninvasive sensor information is processed using sophisticated numerical simulation of human bioheat transfer and thermoregulation (i.e., an adapted FPC model). The basic underlying idea is that the normal BCs in the model, i.e. the environmental conditions, are replaced by alternative BCs at the level of the skin and its microclimate.

Standard mathematical models of human heat transfer and thermoregulation (see previous sections) incorporate calculations of the environmental heat exchange as an integral part of the simulation process. Accurate calculations, however, require detailed knowledge of the prevailing environmental conditions and related parameters including surface convection coefficients, human view factors (for radiant heat exchanges), and detailed information on clothing properties—most of which are, as scene-dependent data, difficult to obtain in the field. From the mathematical point of view, environmental heat exchange represents BC at the surface of the body that, in principle, can be replaced by alternative BC formulations. Any measured body surface temperature, for example, can be interpreted as an "integral" of the various partial influences from the environment. Measured surface heat fluxes or temperatures may thus be considered as incorporating the environmental information required as BCs—taking away the need for detailed knowledge of scene-specific factors and parameters. The skin BC's can be obtained from a sensor system integrated in the clothing's inner layer.

In their study, Fiala et al. (59) adapted the original FPC model to enable flexible BCs definitions at the body surface. As illustrated in Figure 21, this approach accepts, apart from traditional BC definitions (standard model input like air temperature, humidity, etc.), also alternative BCs definitions (extended model input) using, for example, skin temperatures or heat fluxes as model input for the skin boundary. The type of BCs can be defined individually for each skin sector of the model depending on what information is available. This way the model was "connected" to—and used in conjunction with—different wearable sensors to predict the body core temperature of subjects exposed to different environmental and personal conditions and types of clothing.

Extensive datasets for heat exposures with subjects wearing sensors integrated in the protective clothing were used for validating this approach (40, 59). Apart from seminude subjects, the performance of the proposed method was tested also for subjects who underwent internal heat strain due to exercise while wearing different types of protective clothing (57). The tests were carried out using dedicated climate chamber experiments in which the body core temperature and other physiological and perceptual responses were measured in subjects undergoing periods of rest and exercise under very different combinations of environmental and clothing conditions (40, 41). In the simulation study (57), the researchers compared three methods: (i) using standard environmental BC's (Ehx), (ii) using nine measured local skin temperatures ($T_{\mathrm{sk,m}}$), and (iii) using only skin temperatures of the central body parts ($T_{\mathrm{sk,c}}$), that is, the trunk and the upper arm (five-point average). In all simulations, experimental metabolic rates were used as a further model input. An example of a simulated exposure to determine noninvasively the body core

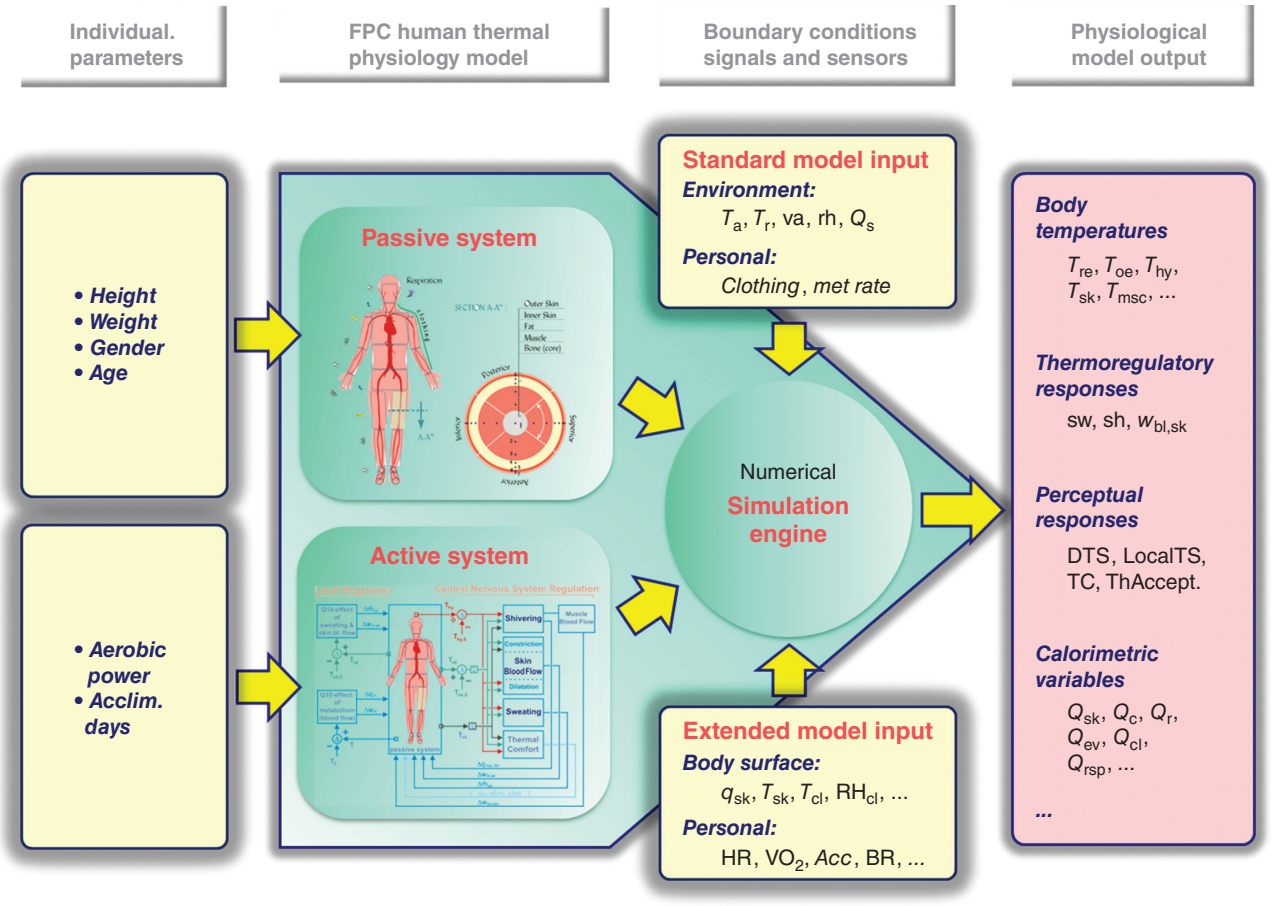

Figure 21 Schematic diagram of the "individualized" FPC model adapted for use with different types of peripheral sensors and boundary conditions at the body/skin surface to predict the body core temperature and other physiological responses. Reproduced from (55) with approval of the copyright holder.

temperature of exercising subjects is provided in Figure 22. Other exposures and scenarios simulated using different BC methods are discussed elsewhere (55, 57, 59).

Testing this in scenarios with and without directional (asymmetric) radiation, the first point to become obvious was the problem to define a complex thermal environment (directional radiation, wind direction, and changing activity levels) in terms of its BC's accurately. This was very time consuming, especially for the directional radiation component. Using the skin BC's simplified this substantially, with the five-point measurement working well in the absence of directional radiation. But as to be expected, with directional radiation sensor placement became more sensitive. Both sensor methods improved upon the environmental BC method, especially in uncompensable conditions.

The presented method proved to be a robust predictor of the rectal temperature under a broad range of exposure scenarios, environmental conditions, exercise intensities, type of clothing, and presence or absence of high intensity radiation sources. The average RMS deviations were 0.1°C and 0.2°C for group average and individual responses, respectively. It was thus concluded that the proposed numerical method is applicable without a need for adaptations to any specific exposures or types of clothing (59). In all simulations, the metabolic rate was an important input parameter; and the RMS deviations mentioned here, were obtained using actually measured metabolic rates. Although various research efforts are currently dedicated to determining this in simple ways (e.g., motion sensors), the accuracy of these methods remains a limiting factor, and direct measurement is not a realistic option in the field.

Heat Stress Indices Used by the Weather Services and Epidemiologists

In the previous sections, heat stress and strain indices were discussed that were mainly developed for the assessment of the direct, short-term risk of exposure to heat-related stressors. For application in other contexts, a number of different indices and models have been developed, related to heat stress and strain too (125):

- *Public weather service*. The issue is how to inform and advise the public on thermal conditions, discomfort and risk, on short time scales (weather forecast) for outdoor

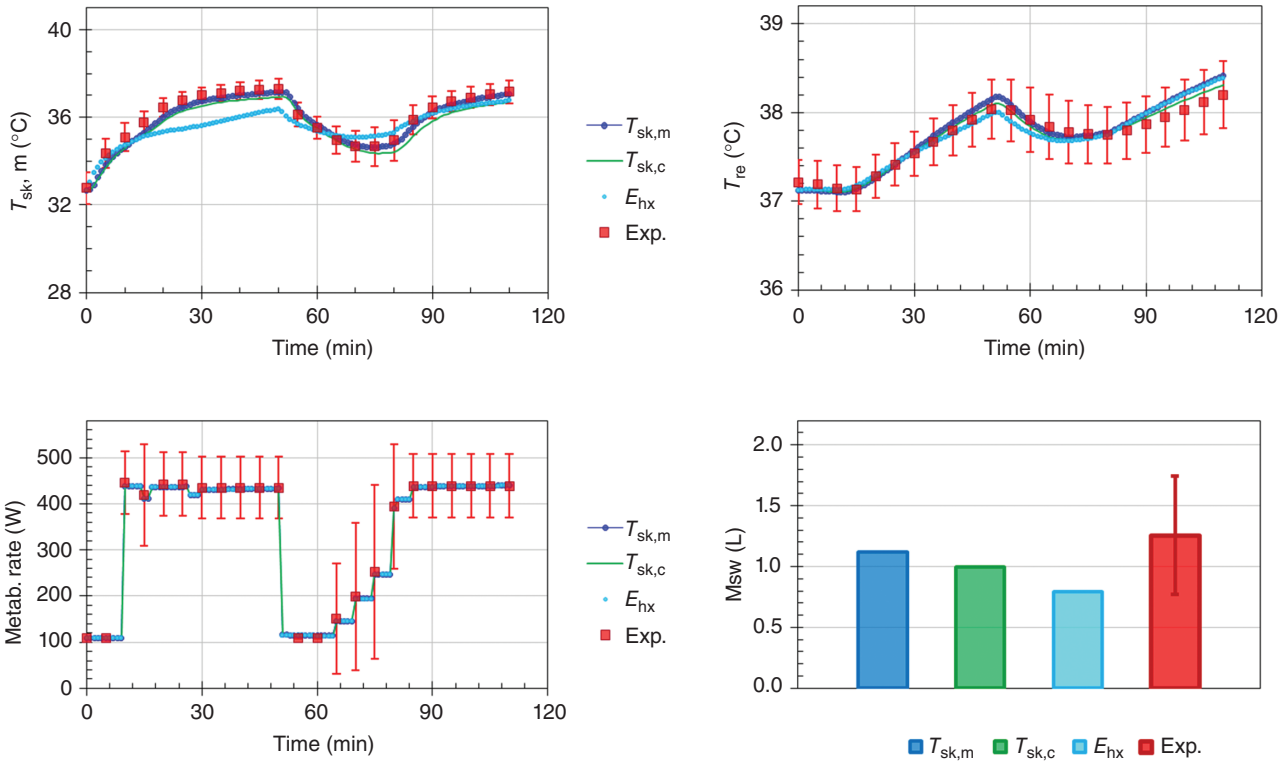

Figure 22 Measured and predicted responses of subjects ($n = 20$) wearing a permeable suit and exposed for 110 min to hot environmental conditions of 40.4°C, 23.4% RH, 0.4 m/s. The group-average rectal temperature (T_{re}) and total body weight loss (M_{sw}) were predicted from different configurations of skin temperature sensors ($T_{sk,m}$ and $T_{sk,c}$) and environmental conditions (Ehx) as input boundary conditions.

activities, appropriate behavior, and climate therapy. Currently, various national meteorological services around the world use a plethora of indices in their public weather advice.

Public Health System (PHS):

- *PHS*. To mitigate the adverse health effects of extreme weather events (heat waves and cold spells), it is necessary to implement appropriate disaster preparedness plans. This requires warnings about extreme thermal stress so that interventions can be released to save lives and reduce health impacts.

- *Precautionary planning*. This refers to a wide range of applications in public and individual spheres, such as urban and regional planning, and in the tourism industry.

- *Climate impact research in the health sector*. The increasing awareness of climate change and the related health impacts requires epidemiological studies based on cause-effect-related approaches.

Weather services across the world have developed a number of heat indices, distinct from the earlier discussed indices. Most of these indices are rather basic, trying to combine numerically certain weather station data into a single number, usually the temperature of a reference environment that integrates the effects of temperature and humidity, ideally with addition of wind and radiation in others. Weather services tend to calculate these indices for geographical grids with resolutions down to 5 km (123) or even less in special applications (e.g., urban heat island). This implies that large amounts of calculations for all grid points (some calculate worldwide) are required, which does not allow complex mathematical routines like those employed in physiological simulation models (123). Hence, most models used in meteorology are either based on simple relationships between temperature and humidity, or use the results of complex physiological models (56,230,231) but in the form of simple regression equations as a function of relevant climatic parameters, thereby realizing a fast lookup or calculation for individual grid points.

The apparent temperature

The apparent temperature (AT) is a measure of relative discomfort from combined heat and humidity. AT is defined as the temperature, at a reference humidity level, that produces the same level of discomfort as the actual environment characterized by the actual ambient temperature and humidity. Thus, AT is an adjustment to the ambient temperature (T) based on the level of ambient humidity. An absolute humidity at a dew point of 14°C is chosen as a reference (though small adjustments to the reference are made with increasing temperature). If the ambient vapor pressure is higher than the reference then

the AT will be higher than the actual ambient temperature and vice versa. The deviations from ambient temperature are estimated by the Steadman mathematical model of the human heat balance (232). AT is valid over a wide range of temperatures. A simplified hot weather version of the AT, known as the heat index (see next section), is used by the National Weather Service (NWS) in the United States.

The Australian Bureau of Meteorology uses an approximation of the value provided by Steadman's complete model which includes the effects of temperature, humidity, windspeed, and radiation. Under Australian conditions the effect of (direct and diffuse) solar radiation produces a maximum increase in the AT of about 8°C when the sun is at its highest elevation in the sky. Two equations for calculating AT are in use, one including solar radiation [Eq. (84)], and one without [Eq. (85)].

$$\mathrm{AT} = T_a + 0.348e - 0.70\mathrm{ws} + \frac{0.70Q}{\mathrm{ws} + 10} - 4.25 \quad (84)$$

$$\mathrm{AT} = T_a + 0.33e - 0.70\mathrm{ws} - 4.00 \quad (85)$$

where: T_a = dry bulb temperature (°C), e = water vapor pressure (hPa), ws = meteorological wind speed at an elevation of 10 m ($m \cdot s^{-1}$), and Q = net solar radiation absorbed per unit area of body surface ($W \cdot m^{-2}$).

It should be noted that when using the term AT one must keep in mind that there are several different versions of AT. For example, Almeida et al. (1) investigating heat-related mortality, used the formula:

$$\mathrm{AT}\ (°\mathrm{C}) = -2.653 + 0.994T_a + 0.0153T_{dp}^2 \quad (86)$$

with T_{dp} = dew point temperature (°C), based on Steadman's model (230, 231) and Kalkstein and Valimont's work (135), in an attempt to represent the effect of the typical temperature exposure that is commonly experienced during the warmer months.

The heat index

The heat index is another example of the calculation of an index using a regression equation that is based on results produced by a heat budget model, that is, the Steadman model (230, 231). The regression analysis was performed by Rothfusz, as reported in a 1990 NWS Technical Attachment (SR 90-23) (USA) (217). The original Rothfusz equations use Fahrenheit as units, (http://www.hpc.ncep.noaa.gov/html/heatindex_equation.shtml) but are converted to degrees Celsius here for both input and output:

$$\begin{aligned}\mathrm{HI} = &-8.78469476 + 64.4557644 \cdot T_a + 93.54195356 \cdot \mathrm{RH} \\ &- 233.78568 \cdot T_a \cdot \mathrm{RH} - 19.6929504 \cdot T_a^2 \\ &- 26.2797244 \cdot \mathrm{RH}^2 + 141.550848 \cdot T_a^2 \cdot \mathrm{RH} \\ &+ 46.42944 \cdot T_a \cdot \mathrm{RH}^2 - 9.16992 \cdot T_a^2 \cdot \mathrm{RH}^2\end{aligned} \quad (87)$$

Table 8 Effects of the Heat Index (Shade Values) (http://www.hpc.ncep.noaa.gov/html/heatindex_equation.shtml)

Celsius	Notes
27-32°C	Caution: fatigue is possible with prolonged exposure and activity. Continuing activity could result in heat cramps
32-41°C	Extreme caution: heat cramps and heat exhaustion are possible. Continuing activity could result in heat stroke
41-54°C	Danger: heat cramps and heat exhaustion are likely; heat stroke is probable with continued activity
over 54°C	Extreme danger: heat stroke is imminent

where T_a is the ambient temperature in °C and RH is relative humidity (%). HI (°C) is the heat index expressed as apparent temperature. For RH ≤ 13% and 26.7 ≤ T_a < 44.5°C, the following adjustment is subtracted from HI:

$$\mathrm{Adjustment} = \left[\frac{(13 - \mathrm{RH})}{7.2}\right]\sqrt{\frac{\left[17 - \left|\left(1.8T_a - 63.\right)\right|\right]}{17}} \quad (88)$$

while for RH > 85% and 26.7°C < T_a < 30.5°C, the following adjustment is added to HI:

$$\mathrm{Adjustment} = 0.02\,(\mathrm{RH} - 85)\left(55 - 1.8T_a\right)/1.8 \quad (89)$$

These regression equations are not appropriate when conditions of temperature and humidity warrant a heat index value lower than around 26°C. In those cases, a simpler formula is applied to calculate values consistent with Steadman's results. This regression is not valid for extreme temperature and relative humidity conditions beyond the range of data considered by Steadman. An interpretation of the HI values is given in Table 8.

It should be noted though that Rothfusz' simplified approach also introduced diverse problems compared to the full Steadman model. They include the need for adjustments (in a range of 0.7°C) to correct estimation errors and the loss of the effect of wind and radiation. Regarding the latter, exposure to high levels of solar radiation may raise heat index values by up to 8°C which is not included in Rothfusz' regression equation.

Humidex

The Canadian Meteorological service developed an alternative to the heat index: the humidex (short for "humidity index"). Apart from weather forecasting, humidex has also been used in epidemiological studies looking at mortality and morbidity (31).

Table 9 Range of Humidex versus Degree of Comfort or Discomfort

Less than 29°C	Little or no discomfort
30-34°C	Noticeable discomfort
35-39°C	Evident discomfort
40-45°C	Intense discomfort; avoid exertion
Above 45°C	Dangerous discomfort
Above 54°C	Heat stroke probable

The current formula for determining the humidex was developed by Masterton and Richardson of Canada's Atmospheric Environment Service in 1979 (171). It describes how hot the weather feels to an average person, when combining the effect of heat and humidity. Humidex differs from the heat index in being related to the dew point rather than relative humidity. Humidex is supposedly a "sensory index" representing an "equivalent temperature" approach, that is, it provides values that can be interpreted as a temperature of a dry climate that "feels the same as" the actual climate. For example, if the actual temperature is 32°C at 70% relative humidity, humidex indicates that this feels approximately like a dry temperature of 45°C.

The humidex formula is as follows:

$$\text{Humidex} = T_{db} + \left[0.5555\left(P_a - 10\right)\right] \quad (90)$$

Or

$$\text{Humidex} = T_{db} + 0.5555\left(6.11e^{5417.7530\left(\frac{1}{273.16} - \frac{1}{T_{dp}+273}\right)} - 10.\right) \quad (91)$$

with T_{db} = dry bulb temperature (T_a), P_a = vapor pressure (hPa), and T_{dp} = dew point temperature (°C).

Variations of the aforementioned Canadian version of humidex with regards to both the exact mathematical formulation and the interpretation of the results are in use throughout the world. Humidex is a simpler index than HI (it did not involve a thermoregulatory model) but, in essence, both indices only incorporate the influence of air temperature and humidity but neglect the effect of solar radiation, air speed, clothing and physical activity.

The interpretation of humidex values is presented in Table 9.

Heat budget models in weather forecasting

In addition to simpler indices also complete heat balance and even sophisticated thermophysiological models (discussed earlier) have been used for weather forecast purposes. Both take all mechanisms of the human environmental heat exchange into account and are therefore relevant to individual exposures and experiences. Most of the approaches used in meteorology are linked to a reference environment in which the overall thermal load on an (average) person would be the same as under the actual conditions. Some approaches started out by using the Fanger comfort model (53), predicting population's average thermal sensation, that is, the so-called predicted mean vote (PMV), using outdoor climate parameters, clothing insulation, and metabolic rate as model input. While this approach has become very popular for assessing indoor climates, its range was too limited for outdoor applications.

In his "Klima-Michel" model, Jendritzky et al. (128) extended Fanger's PMV and heat balance model to PMV* by introducing latent heat fluxes according to Gagge's et al. SET* approach (69). Jendritzky furthermore adapted the model for use in meteorology by considering outdoor-climate-specific radiation components. Another enhancement of Fanger's model to wide-ranging conditions was achieved by introducing adaptable clothing insulation that varies depending on climate between 0.5 and 1.75 clo (baseline 1.0 clo for July). The output of the "Klima-Michel" model, adopted by the German Meteorological Service (DWD), is the so-called perceived temperature (PT). PT is the air temperature of a reference environment in which the perception of heat or cold would be the same as under the actual outdoor weather conditions (124, 229). The reference climate represents calm air environment with a mean radiant temperature equal to the air temperature and 50% relative humidity.

The standard effective temperature SET* is a further approach used both for indoor and outdoor climate assessment applications. SET* defines an equivalent air temperature of an isothermal environment at 50% RH (69) based on Gagge's two-node model (67). In contrast to Fanger who assumes a "comfortable" mean skin temperature and sweat evaporation rate, the SET* approach calculates skin temperature (and skin wittedness) explicitly for the climate and clothing that is adjusted to the physical activity of concern. Pickup and deDear have enhanced the SET*-concept specifically for outdoor climate settings using their OUT_SET* index (203).

Another index that has become popular among meteorologists is the physiologically equivalent temperature (PET) developed by Höppe (111). PET (°C) is based on the MEMI human heat budget model (112)—an enhanced variant of Gagge's two node model (67). PET provides the air temperature of a reference environment in which the heat load and physiological strain would be the same as in the actual climate. The reference environment is defined in similar terms as discussed above with SET* being calculated for a standard person and all climates, but using a fixed clothing insulation of 0.9 clo and activity level of 1.5 Met, thus referring this index to an office environment.

Indices based on synoptic approaches

A synoptic approach to weather classification for the weather service defines which weather types (air mass type) can be identified in a given locality. It has been shown that there is

an association of mortality (134) with specific weather types (air masses). For heat-stress assessment, this is mainly used in mortality evaluation and heat health warning systems that are discussed in the next section.

Heat stress indices used by epidemiologist/public health

Apart from the daily weather forecast in which an indication of the expected level of heat stress is provided, special heat health warning systems have been developed with the aim of warning the public and the health services of increases in the risk to health due to heat stress above a certain threshold. The latter is usually based on an expected increase in mortality and morbidity. Most of the research in this area follows a rather basic approach to climate models, usually using just a single climate parameter, that is, temperature. This may work well in the cold, given that vapor pressures are consistently low and solar radiation not very strong, but on the heat-stress side, though a strong correlation with temperature is present, other climate parameters are of importance too. The predictive power of mortality and morbidity in the heat increases with the inclusion of vapor pressure or relative humidity in the models (45, 155), though the use of rh can lead to negative regression coefficients for this parameter in the equation (45, 155) which seems counter intuitive and has on occasion led to the erroneous conclusion that a high RH is beneficial. The negative correlation is for the major part caused by the link between temperature, humidity, and relative humidity. In many climate regions, the absolute humidity or vapor pressure shows only small variations during the day (in absence of precipitation), but this implies that RH goes down when temperature goes up, so RH is lowest in the hottest part of the day, leading to the negative coefficient. In reality, assuming equal air temperature, mortality would have a positive correlation with both absolute and relative humidity (98, 99, 123, 127).

Table 10 gives an overview of threshold criteria for the release of hot weather warnings in different countries (148). As discussed, for this purpose most countries use a simple temperature threshold. Some combine temperature and humidity, or the heat index and only southern Germany uses an analytical model for heat stress, the Klima-Michel heat budget model (124, 128, 243).

Kalkstein extended the synoptic approach mentioned earlier to health warning systems in the 1980s. Heat health warning systems that use such methods have now been set up in several cities in the United States, such as Cincinnati, Dayton, New Orleans, Philadelphia, Phoenix, and Washington, DC (148). The synoptic procedure classifies days that are considered to be meteorologically homogeneous, that is, have the same air mass type. This is accomplished by aggregating days in terms of seven meteorological variables (air temperature, dew point temperature, visibility, total cloud cover, sea-level air pressure, wind speed, and wind direction). Typically these data are collected four times each day (132).

UTCI

Through an initiative of Commission 6 of the International Society of Biometeorology (126) and the European Union COST-action 730 (125), a new climatic index, the "UTCI" or Universal Thermal Climate Index, was developed. The biometeorological world identified a need for a universal index that would cover the whole range of climate conditions and regions from cold to hot, and could be used in applications such as weather forecasting, climate change impact modeling, epidemiological studies of climate related mortality and morbidity, etc. When fully developed, the UTCI model should account for the following features (123):

- be based on the most advanced multinode thermophysiological models as reference for obtaining the key results from systematic simulations;
- include the capability to predict both whole body thermal effects (hypothermia and hyperthermia; heat and cold discomfort), and local effects (facial, hands, and feet cooling and frostbite);
- represent a temperature-scale index, (i.e., the air temperature of a defined reference environment providing the same physiological response); and
- require minimal computer time to allow world-wide grid calculations for meteorologists.

Several multinode models of human physiology as well as various two-node models (60, 62, 64, 116) were considered for their suitability to develop the UTCI model. In the intermodel comparisons, the models were evaluated by comparing regarding predicted body core and skin temperatures, calorimetric variables as well as thermoregulatory responses. Based on the results of intermodel comparisons between a limited number of models, and due to issues of suitability and availability (i.e., whether the COST-action would have access to the detailed model code and be allowed to use it for the UTCI work without licensing issues) the experts of the COST-action 730, WG1 on Thermophysiological Modeling agreed to use the Fiala multinode model (56, 58, 60, 63) as an adequate approach for the purposes of the COST-action 730.

It was considered important to ensure that the model selected for use to develop UTCI was able to reproduce the thermal and regulatory behaviors of an average person over the spectrum of atmospheric environments of interest. For that purpose, the original Fiala model was adapted and extended for purposes of the COST-action 730 as part of the Action activities. The multinode model was furthermore subjected to extensive validation tests against appropriate experimental observations obtained from human exposures to non-moderate BCs including (but not restricted to) cold and extreme cold ambient temperatures, increased air velocities, hot, dry, and humid environments, and conditions in which

Table 10 Threshold Criteria for Releasing Hot Weather Warnings

Country	Criteria for releasing the warning	Reference temperature
Temperature threshold		
Azerbaijan	40°C in more than 30% of the territory—42°C in one region	Not specified
Belarus	35°C	Air temperature
Czech Republic	29°C medium heat stress; 33°C high heat stress	Maximum air temperature
Greece	38°C	Maximum air temperature for 3 consecutive days
Latvia	33°C	Air temperature
Malta	40°C	Maximum air temperature
Portugal (district of Lisbon)	Ícaro index-2005 (Nogueira & Paixão, 2008 (193)). Daily maximum temperature > 32°C and other parameters derived from local temperature—mortality relationship	Maximum air temperature, 3 day forecast
Serbia and Montenegro	35-20 °C	Maximum and minimum air temperature
Spain		Maximum air temperature
Temperature and humidity threshold		
Romania	Temperature humidity index: (ITU) ≥80 ITU = *T*(°F) – (0.55 – 0.55*RH/100)*(*T*(°F) – 58) RH: relative humidity	Minimum air temperature
The former Yugoslav Republic of Macedonia	Increasing heat index (apparent temperature)	Maximum temperature
Turkey	Temperature > 27°C and relative humidity > 40%	
Complex index threshold		
Southwestern Germany	Maximum perceived temperature > 26°C	
Synoptic air masses		
Rome (Cegnar & Kalkstein, 2000; Kalkstein, 2000)	Dry tropical air mass No. of deaths = –45.92 – 0.08*TS + 2.05*DIR + 1.61*ATmin+1 + 0.75*ATmin+2 TS time of season (days since 14 May) DIR consecutive days of oppressive air mass (dry tropical or moist tropical plus) ATmin + 1 minimum apparent temperature forecast for tomorrow ATmin + 2 minimum apparent temperature forecast for the day after tomorrow AT apparent temperature derived from temperature, humidity, and wind speed Moist tropical air mass No. of deaths: –4.84 – 0.13*TS + 0.82*CH + 1 CH + 1: cooling hours (hours * degrees above 20°C) forecast for tomorrow	Warning based on air mass arrival time, on excess deaths expectation (threshold = 2), and duration
Philadelphia Hot Weather Health Watch/Warning System Kalkstein et al. 1996; Sheridan and Kalkstein 1998)	Offensive air mass presence Number of excess deaths predicted	

Note. Information collated from (148).

the human heat balance and the perceived outdoor temperature are affected by solar radiation (205).

Having selected the "UTCI-Fiala model" as the basis for the development, the next step was to develop a procedure to use this model to translate actual climate conditions into a UTCI value. It was decided to use the principle of a reference condition (similar to the idea was used in the wind chill index and Apparent Temperature) to which actual conditions were compared:

The UTCI is defined as the air temperature (T_a) *of the reference condition causing the same physiological model response as the actual condition.* The offset, that is, the

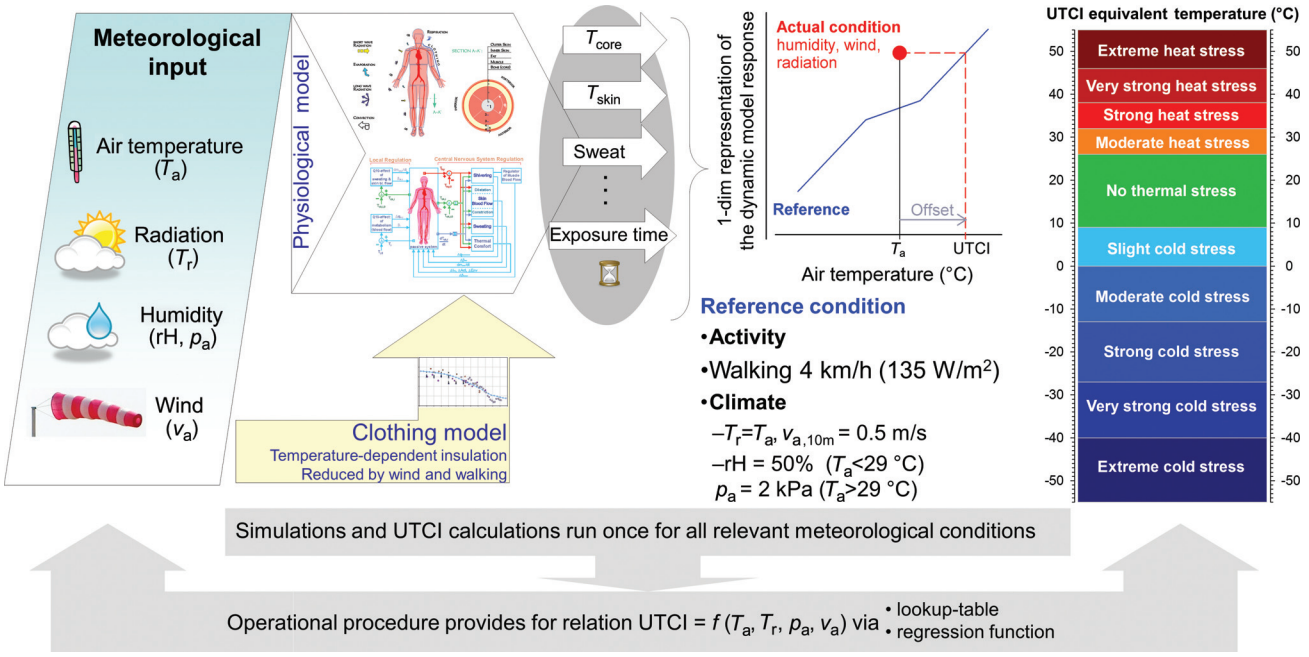

Figure 23 Concept of UTCI derived as equivalent temperature from the dynamic multivariate response of the thermophysiological UTCI-Fiala model (56), which was coupled with a clothing model (101). Reproduced from (20) with permission from Journal of Industrial Health.

deviation of UTCI from air temperature depends on the actual values of air and mean radiant temperature (T_{mrt}), wind speed (v_a), and humidity [expressed as water vapor pressure (vp) or relative humidity (RH)] (Fig. 23). This may be written in mathematical terms as:

$$\mathrm{UTCI} = f\left(T_a; T_{mrt}; \mathrm{va}; \mathrm{vp}\right) = T_a + \mathrm{Offset}\left(T_a; T_{mrt}; \mathrm{va}; \mathrm{vp}\right) \quad (92)$$

Applying this characterization required the identification of both the reference condition and the dynamic model response. To convert climate impact to a single value and to facilitate the interpretation and understanding of UTCI, reference conditions must be (1) defined in terms conforming to most people's experiences, and (2) relevant across the whole spectrum of climate zones to which UTCI is going to be applied. Therefore, the nonmeteorological variables metabolic rate MET and the thermal properties of clothing (insulation, vapor resistance, and air permeability) are of great importance. ISB Commission on UTCI had defined in 2000 a representative outdoor activity to be that of a person walking with a speed of 4 km/h (1.1 m/s). So, the rate of metabolic heat production was assumed to be 2.3 MET (135 W m^{-2}) for the reference person. The climate for the reference environment was decided to be:

– a meteorological wind speed (v_a) of 0.5 m/s at 10 m height (approximately 0.3 m/s at 1.1 m),

– a mean radiant temperature (T_{mrt}) equal to air temperature, and

– vapor pressure (vp) that represents relative humidity of 50%; at high air temperatures (>29°C) the reference humidity was taken as a constant vapor pressure at 20 hPa, as higher values would only rarely occur in natural environments.

As clothing has a strong impact on the physiological responses, a separate clothing model was developed for the UTCI that describes the clothing behavior of people based on the ambient temperature (72). Also, the impacts of wind and the activity on the clothing insulation and vapor resistance were incorporated (102, 105).

In comparing the model responses in actual conditions to those in the reference conditions, a challenge is that the model produces a multidimensional physiological response that needs to be matched to the similar multidimensional physiological response of the reference condition. Taking, for example, body core temperature as sole comparison criterion would work in extreme heat or cold (hyper- or hypothermia), but would not work in the zone where thermoregulation keeps the body core temperature stable. In the comfort area, for example, skin temperature (53) or vasodilation-vasoconstriction levels could be used, but, for example, in the heat, these may plateau and thus would not be suitable. Hence, the comparison needs to be based on a multidimensional physiological data footprint (21). This was achieved by a cluster analysis of the data produced by the model over a wide range of climatic conditions (21). Performing simulations on 926 reference conditions and over 10^5 different nonreference climatic combinations produced an extensive data set for this purpose. Data at 3 time points in 2 h

simulations were used (2 h were deemed a relevant exposure time maximum for this application). The cluster analysis (principal component analysis) produced a principal component based on 7 variables, using their values at 30 and 120 min: rectal and mean skin temperature, face temperature, sweat production, skin wettedness, skin blood flow, and shivering. These variables are integrated in a single value using the weighting factors obtained in the principle component analysis, and it is this PC value that is used to compare conditions, that is, translate any condition into the relevant reference condition.

The final requirement (low computational load) was not possible to achieve if running the physiological model for detailed geographical grids (e.g., 10 km grid width for a whole country). The solution to this was to run the model for all possible climate combinations, calculate all the UTCIs and to develop a statistical model to determine UTCI directly from the climate parameters (21).

The different values of UTCI are categorized in terms of thermal stress and strain. Table 11 presents the labeled stress categories and a list of physiological criteria.

The applicability of UTCI has been compared with selected biometeorological indices (e.g., TE, WBGT, HSI, WCT, PT, PET, SET*, PST, and PhS). The main finding of comparisons made for various sets of data (global, regional, local, daily, and momentary data) was that UTCI better expresses biothermal conditions for humans than other indices (16, 20).

Validation—General Considerations

Following the development of any model or index, the validation is essential to testing the quality and reliability of the predictions. The first and foremost criterion is that data used for validation shall be independent of the data used to develop the model. Using the same data for validation and development would only verify the functionality of the developed algorithms with respect to the original data, but would not produce a valid indicator of the model's general predictive power. A problem that researchers often meet is the paucity of well-documented datasets in the public domain. The desire to use as many data as possible for model development leaves them with only few data left for validation.

In the past, diverse approaches to split available data for development and validation have therefore been employed. One of them (first principles) is to use knowledge or understanding of the underlying physiological and/or physical process from the literature as a basis for model development without any specific parameter fitting using concrete datasets. In this case, any available data can be used for validation (98, 100, 170). Another technique is to split available data 50/50, that is, use half of the data for model development and half for validation. This split however should not be a random split of data points, as when split randomly the data, for example, from the same subject and test could then be found in both datasets thus preventing the datasets from being independent. For this reason, each dataset has to comprise the complete data obtained for individual tests and subjects, with no subject present in both. The 50/50 split unfortunately requires a large database. Other recent methods, which can be used well especially in empirical modeling or parameter estimation, include the so-called "boot strap," "leave one out," and "k-fold cross-validation" techniques, in which the model is developed based on the data from all but one individual, and then the equation/algorithm is validated on the set of data not used in the development of the model (50, 215). This is then permutated over all individuals and/or test conditions of the database, so the variation in the parameter estimates can be analyzed together with the goodness of the fit. For complex physiological models, these approaches are impractical however.

Also the comparisons of the model predictions with real data can be performed in various ways. One method is to qualitatively compare the shape of the time based development of variables between model and validation dataset. Many studies, especially those looking at, for example, clothing and comfort evaluations, focus fully on the qualitative comparison of the patterns of such curves (54, 220, 237, 252). Another method is to check whether the model curves fall within the standard deviation in the validation datasets, and argue that if this is the case, the model thus predicts within the natural individual variation within a group (200). Yet other modelers look at the time-series curves qualitatively, but then also compare either all data points or the final data points only (assuming they are the points with the highest heat strain and thus most important) using a correlation between predicted and measured data. In that case, the correlation coefficient is used as indicator of the goodness of fit (77-79,179,180,182,200). This can be extended by calculating the regression line between predicted and actual data, which provides the r^2 value, or the explained variance (%) of the model. This method works particularly well when comparing model improvements (98,100). However, the r^2 value on its own only provides information on the overall performance, and does not indicate how the model performance may vary over conditions. Various studies (179,180,182) show the r^2 values and plots of the residual distribution, but do not provide residual statistics. The latter is important to judge the relevance of the prediction error, and the standard error of the estimate (or prediction; SEE or SEP) can provide an indication of the size of the typical model deviation (98, 100, 170). However, even that is not sufficient if the goal is predictions for individual cases, rather than predictions over a large dataset. While r^2 may be high, and SEE low, these may be governed by data points in a safe range, and the more extreme, high risk, exposures may still have considerable deviations. Especially in very large datasets, often the ratio of low stress and strain data to those with high strain can be very high, allowing the low strain data to dominate the performance statistics. Where individual cases need to be simulated it is relevant to evaluate the high strain data points separate for their

Table 11 Translation of UTCI Equivalent Temperatures into Levels of Thermal Stress

UTCI (°C) range	Stress category	Physiological responses
Above +46	Extreme heat stress	Increase in T_{re} time gradient Steep decrease in total net heat loss Averaged sweat rate >650 g/h, steep increase
+38 to +46	Very strong heat stress	Core to skin temperature gradient < 1K (at 30 min) Increase in T_{re} at 30 min
+32 to +38	Strong heat stress	Dynamic Thermal Sensation (DTS) at 120 min >+2 Averaged sweat rate > 200 g/h Increase in T_{re} at 120 min Latent heat loss >40 W at 30 min Instantaneous change in skin temperature > 0 K/min
+26 to +32	Moderate heat stress	Change of slopes in sweat rate, T_{re} and skin temperature: mean (T_{skm}), face (T_{skfc}), hand (T_{skhn}) Occurrence of sweating at 30 min Steep increase in skin wettedness
+9 to +26*	No thermal stress	Averaged sweat rate > 100 g/h DTS at 120 min < 1 DTS between −0.5 and +0.5 (averaged value) Latent heat loss >40 W, averaged over time Plateau in T_{re} time gradient
+9 to 0	Slight cold stress	DTS at 120 min < −1 Local minimum of T_{skhn} (use gloves)
0 to −13	Moderate cold stress	DTS at 120 min < −2 Skin blood flow at 120 min lower than at 30 min (vasoconstriction) Averaged T_{skfc} < 15°C (pain) Decrease in T_{skhn} T_{re} time gradient < 0 K/h 30 min face skin temperature < 15°C (pain) T_{msk} time gradient < −1 K/h (for reference)
−13 to −27	Strong cold stress	Averaged T_{skfc} < 7°C (numbness) T_{re} time gradient < −0.1 K/h T_{re} decreases from 30 to 120 min Increase in core to skin temperature gradient
−27 to −40	Very strong cold stress	120 min T_{skfc} < 0°C (frostbite) Steeper decrease in T_{re} 30 min T_{skfc} < 7°C (numbness) Occurrence of shivering T_{re} time gradient < −0.2 K/h Averaged T_{skfc} < 0°C (frostbite) 120 min T_{skfc} < −5°C (high risk of frostbite)
Below −40	Extreme cold stress	T_{re} time gradient < −0.3 K/h 30 min T_{skfc} < 0°C (frostbite)

*It can be noted that with respect to the averaged dynamic thermal sensation *UTCI* values between 18 and 26 C may comply closely with the definition of the "*thermal comfort zone*" supplied in the Glossary of Terms for Thermal Physiology (2003) as: *The range of ambient temperatures, associated with specified mean radiant temperature, humidity, and air movement, within which a human in specified clothing expresses indifference to the thermal environment for an indefinite period.*

predictive performance, as, for example, done in Refs. 210 and 211.

Very similar to this method is the expression of goodness of fit in terms of the root mean square error or deviation (RMSD) (89, 96-98, 150, 249):

$$\mathrm{RMSD} = \sqrt{\frac{1}{n}\sum_{i=1}^{n}(\text{observed} - \text{predicted value})^2} \quad (93)$$

A summary statistic that provides an indication of the systematic error or discrepancy between a predicted quantity and the corresponding observation is the BIAS estimator (244):

$$\mathrm{BIAS} = \frac{1}{n}\sum_{i=1}^{n}(\text{observed} - \text{predicted value}) \quad (94)$$

It is important not to use this on its own, as significant overestimations can be cancelled out by significant underestimations in other parts of the simulation and result in low bias. Hence, a combination of bias and RMSD or SEE provides a more complete picture.

The so-called LoA or Bland-Altman method (24,211) follows, in principle, a similar philosophy. Using this graphical technique, the deviations between predicted and measured values are plotted against the mean of the two (15). The plot provides then a good visual insight on how the deviations vary for different ranges of the studied variable, so, for example, whether these deviations get higher with increasing heat strain levels. The LoA values, representing the 95 percentile of the deviation data, indicate the error made across the spectrum of studied conditions.

As with other techniques, however, data independence is an issue also with the LoA method and correlation, when time-series data are used. For correlation or regression of predicted and actual point comparison, strictly spoken all data points should be independent. This suggests only one data point per experiment could be used, as done in studies where only the end points are compared (98, 100). Given the paucity of data, this view may reduce the number of available points too much. This then requires a judgment of how many points provide a good balance of independence while still providing a good size validation set. This can be done by looking at the serial correlation of the data using the Durbin Watson statistic (48, 209, 210). Trials on this performed by Richmond et al. (209, 210) suggested that one data point every 20 min of an experiment would be acceptable, with one every 10 min being borderline. Though using higher frequency data may not change the overall correlation, it would inflate significance levels dramatically and incorrectly exaggerate the reliability of the validation.

When choosing the method of how to quantify the discrepancies between model predictions and measured data, it is also important to keep in mind the aim of the modeling. The measures discussed earlier (RMSD, LoA) provide information on the goodness of the fit as averaged over the time-series data. If a model is developed, for example, to predict exposure limits for the body core temperature (T_c) to prevent heat illness, the performance of the model to predict T_c below the limit (e.g., 38.5°C) is of secondary importance while the accuracy of predicting T_c in excess of that limit is relevant for validation. If only the sole value of RMSD or LoA is considered, without graphical representation, this information may be lost.

An alternative is to consider only the relevant range of data in the validation, for example, by taking into account only the final values (100), or the critical period (high body temperature) of an exposure. Richmond et al. (210, 211) looked at the predictive capacity of their empirical models in terms of exposure limits (39°C actual core temperature as limit) by splitting the data at that core temperature in "positives/negatives/false positives/false negatives" (Fig. 24). For their application, setting heat-stress limits, the performance at low core temperatures is irrelevant and their approach provides a solution to this issue.

A different type of validation is where models are programmed based on a listing of the code, or, for example, translated into a different computer language. The first happens, for example, where codes are taken from publications or ISO standards (119, 120). The second, for example, where older languages (Basic, FORTRAN) receive less support requiring translation into, for example, C++ (107). For such cases, the model outcomes need to be checked and for this reference input and output data should be provided for validation in the publication or standard.

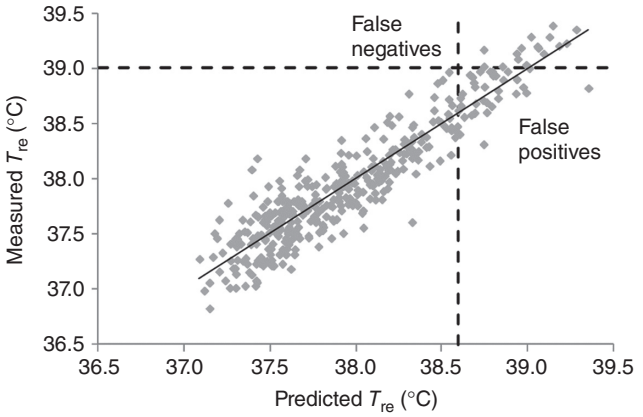

Figure 24 Validation of model prediction using the quality of prediction at high risk core temperatures, using concept of False Positives and False Negatives (209, 210), assuming 38.7°C is used as cut off criterion for the predicted value of core temperature and 39.0°C for actual core temperature as the limit value for risk. Modified and reproduced with permission from copyright holder (209).

Conclusion

A large number of tools, models, and indices for the assessment of human exposures to heat has been developed over the last century, ranging from simple physical instruments designed to mimic the human heat exchange with the environment, to complex thermophysiological models that simulate external and internal body heat transfer and allow detailed simulation of different work load, clothing, and climate scenarios.

Despite the advances in computing power that have enabled even complex models to run on handheld devices, simple climate indices such as WBGT are still most popular in the field, while the more complex models are more confined to research. The latter however are undergoing significant development and advancements, including, for example, expansions to simulate responses of individuals rather than group responses or the integration of simulation models into intelligent wearable monitoring devices for real-time risk assessment of heat strain using noninvasive sensor information. Although their acceptance still seems limited, thermophysiological models have found their way into different application areas including, for example, biometeorology and various technical disciplines.

References

1. Almeida SP, Casimiro E, Calheiros J. Effects of apparent temperature on daily mortality in Lisbon and Oporto, Portugal. *Environ Health* 10: 9-12, 2010. doi: 10.1186/1476-069X-9-12.
2. Al-Othmani MN, Ghaddar K, Ghali A. Multi-segmented human bioheat model for transient and asymmetric radiative environments. *Int J Heat Mass Transfer* 51(23-24): 5522-5533, November 2008. ISSN 0017-9310, ttp://dx.doi.org/10.1016/j.ijheatmasstransfer.2008.04.017.
3. Arkin HL, Xu X, Holmes KR. Recent developments in modeling heat transfer in blood perfused tissues. *IEEE Trans Biomed Eng* 41.2: 97-107, 1994.
4. Armstrong LE, Casa DJ, Millard-Stafford M, Moran DS, Pyne SW, Roberts WO. Exertional heat illness during training and competition, ACSM position stand. *Med Sci Sports Exerc* 39(3): 556-572, 2007. doi: 10.1249/MSS.0b013e31802fa199
5. Ashley CD, Luecke CL, Schwartz SS, Islam MZ, Bernard TE. Heat strain at the critical WBGT and the effects of gender, clothing and metabolic rate. *Int J Ind Ergonom* 38(7): 640-644, 2008.
6. Avolio AP. Multi-branched model of the human arterial system. *Med Biol Eng Comput* 18: 709-718, 1980.
7. Azer NZ, Hsu S. The prediction of thermal sensation from a simple model of human physiological regulatory response. *ASHRAE Trans* 83(I): 88-102, 1977.
8. Bedford T. Environmental warmth and its measurement. *Med Res Council* Memo 17. HMSO, London, 1946.
9. Belding HS. The search for a universal heat stress index. In: Hardy JD, editor. *Physiological and Behavioural Temperature Regulation*. Springfield IL: CC Thomas, 1970.
10. Belding HS, Hatch TF. Index for evaluating heat stress in terms of resulting physiological strain. *Heat Pip Air Condit* 27: 129-36, 1955.
11. Bernard TE. Heat stress and protective clothing: An emerging approach from the United States. *Ann Occup Hyg* 43(5): 321-327, 1999.
12. Bernard TE, Caravello V, Schwartz SW, Ashley CD. WBGT clothing adjustment factors for four clothing ensembles and the effects of metabolic demands. *J Occup Environ Hyg* 5(1): 1-5, 2007.
13. Bernard TE, Hanna WM. Environmental effects on WBGT and HSI using a computer simulation. *Int J Ind Ergonom* 3(2): 103-113, December 1988. ISSN 0169-8141, http://dx.doi.org/10.1016/0169-8141(88)90013-3.
14. Binkley HM, Beckett J, Casa DJ, Kleiner DM, Plummer PE. National athletic trainers' association position statement: Exertional heat illnesses. *J Athl Train* 37: 329-343, 2002.
15. Bland JM, Altman DG. Measuring agreement in method comparison studies. *Stat Methods Med Res* 8(2): 135-60, 1999. doi:10.1191/096228099673819272
16. Blazejczyk K, Epstein Y, Jendritzky G, Staiger H, Tinz B. Comparison of UTCI to selected thermal indices. *Int J Biometeorol* 56(3): 515-535, 2012.
17. Bligh J. Regulation of body temperature in man and other mammals. In: Shitzer A, Eberhart RC, editors. *Heat Transfer in Medicine and Biology – Analysis and Applications*. New York and London: Plenum Press, 1985, Vol. 1, Chap. 2.
18. Botsford JH. A wet globe thermometer for environmental heat measurement. *Am Ind Hyg Assoc J* 32.1: 1-10, 1971.
19. Brake DJ, Bates GP. Limiting metabolic rate (thermal work limit) as an index of thermal stress. *Appl Occup Environ Hyg* 17.3: 176-186, 2002.
20. Bröde P, Błazejczyk K, Fiala D, Havenith G, Holmér I, Jendritzky G, Kampmann B. The Universal Thermal Climate Index UTCI compared to ergonomics standards for assessing the thermal environment. *Ind Health* 51(1): 16-24, 2013.
21. Bröde, P, Fiala D, Błażejczyk K, Holmér I, Jendritzky G, Kampmann B, Tinz B, Havenith G. Deriving the operational procedure for the Universal Thermal Climate Index (UTCI). *Int J Biometeorol* 56: 491-494, 2012.
22. Budd GM. Wet-bulb globe temperature (WBGT)—its history and its limitations. *J Sci Med Sport* 11(1): 20-32, 2008.
23. Buller MJ, Castellani J, Roberts WS, Hoyt RW, Jenkins OC. Human thermoregulatory system state estimation using non-invasive physiological sensors. In: *Engineering in Medicine and Biology Society, EMBC, 2011 Annual International Conference of the IEEE*, 3290-2393, 2011.
24. Buller MJ, Tharion WJ, Cheuvront SN. Estimation of human core temperature from sequential heart rate observations. *Physiol Meas* 34(7): 781, 2013. doi:10.1088/0967-3334/34/7/781.
25. Candas V, Libert JP, Hoeft A, Vogt JJ. The required wettedness and the sweat rate. In: *New Trends in Thermal Physiology*. New York: Masson Publ., 1978, p. 114-115.
26. Cegnar T, Kalkstein LS. Development of heat watch/warning system in Rome. In: de Dear RJ et al., editor. *Biometeorology and Urban Climatology at the Turn of the Millennium: Selected Papers from the Conference ICB-ICUC'99 Sydney, 8-12, November 1999*. Geneva: World Meteorological Organization (WMO/TD No. 1026, WCASP-50), 2000.
27. Charny CK, Weinbaum S, Levin RL. An evaluation of the Weinbaum-Jiji bioheat equation for normal and hyperthermic conditions. *ASME J Biomech Eng* 112: 80-87, 1990.
28. Chen MM, Holmes KR. Microvascular contributions in tissue heat transfer. *Ann N Y Acad Sci* 355: 137-150, 1980.
29. Cheuvront SN, Montain SJ, Goodman DA, Blanchard L, Sawka MN. Evaluation of the limits to accurate sweat loss prediction during prolonged exercise. *Eur J Appl Physiol* 101(2): 215-224, 2007.
30. Colin J, Timbal J, Houdas Y, Boutelier C, Guieu J. Computation of mean body temperature from rectal and skin temperatures. *J Appl Physiol* 31(3): 484-489, 1971.
31. Conti S, Minelli G, Solimini R, Toccaceli V, Vichi M, Beltrano C, Perini L. Epidemiologic study of mortality during summer 2003 in italian regional capitals: results of a rapid survey. In: Kirch W, Menne B, Bertollini R, editors. *World Health Organization. Regional Office for Europe & Institute of Medicine (U.S.). Roundtable on Environmental Health Sciences, Research, and Medicine, Extreme Weather Events and Public Health Responses* (1st ed). Berlin: Springer, 109-120, 2005.
32. Cook EL. Epidemiological approach to heat trauma. *Milit Med* 116: 317-322, 1955.
33. Craig FN. Relation between heat balance and physiological strain in walking men clad in ventilated impermeable envelope. *Fed Proc* 9: 26, 1950.
34. Cropper PC, Yang T, Cook MJ, Fiala D, Yousaf R. Coupling a model of human thermoregulation with computational fluid dynamics for predicting human-environment interaction. *J Build Perform Simul* 1: 1-11, 2010.
35. Crosbie RJ, Hardy JD, Fessenden E. Electrical analog simulation of temperature regulation in man. *IRE Trans Biomed Electron* 8.4: 245-252, 1961.
36. d'Ambrosio Alfano FR, Malchaire J, Palella BI, Riccio G. WBGT index revisited after 60 years of use. *Ann Occup Hyg* 58(8): 955-970, 2014 doi:10.1093/annhyg/meu050.
37. d'Ambrosio Alfano FR, Palella BI, Riccio G. On the problems related to natural wet bulb temperature indirect evaluation for the assessment of hot thermal environments by means of WBGT. *Ann Occup Hyg* 56(9): 1063-1069, 2012.
38. Daanen H, Heerlen MC. Anthropometric Data. In: *Manual of the ARB5 Program.* Arbouw Foundation, P.O. Box 8114, Amsterdam, The Netherlands, Chap. 3, 1990, pp. 3-9.
39. Daanen H, Robinette KM. CAESAR: The Dutch data set, TNO-report TM-01-C026, TNO Human Factors, Kampweg 5, P.O. Box 23, 3769 ZG Soesterberg, The Netherlands, 2001.
40. Davey S, Richmond V, Griggs K, Gerrett N, Havenith G. The use of non-invasive measures to predict thermal strain: How accurate are universal models? In: Cotter JD, Lucas SJE, Mündel T, editors. *Proceedings International Conference on Environmental Ergonomics*, 2012, p. 263.
41. Davey S, Richmond V, Griggs K, Havenith G. Decision algorithm for the heat stressed worker: Empirical analysis. Prospie EU Project, Deliv. 3.2 Report: 1-98, 2011.
42. de Freitas CR, Grigorieva EA. A comprehensive catalogue and classification of human thermal climate indices. *Int J Biometeorol*, 1-12, 2014.
43. Departments of the Army, Navy and Air Force. Occupational and Environmental Heat stress control and heat casualty management. Report TB Med 507/AFPAM 48-152 (I) Headquarters, Department Of The Army and Air Force Technical Bulletin, 7 March 2003.
44. Deurenberg P, Ge K, Gaj-Hautvast J, Jingzhong W. Body mass index as predictor for body fat: Comparison between Chinese and Dutch adult subjects. *Asia Pac J Clin Nutr* 6: 102-105, 1997.
45. Díaz JR, García F, Velázquez de Castro E, Hernández C, López AO. Effects of extremely hot days on people older than 65 years in Seville (Spain) from 1986 to 1997 *Int J Biometeorol* 46-3: 145-149, 2002. DOI: 10.1007/s00484-002-0129-z
46. Droog RPJ, Kingma BRM, van Marken Lichtenbelt WD, Kooman JP, Van der Sande FM, van Steenhoven AA, Frijns AJH. Mathematical modelling of thermal and circulatory effects during hemodialysis. *Artif Organs* 36(9): 797-811, 2012. doi: 10.1111/j.1525-1594.2012.01464.x
47. DuBois D, DuBois EF. A formula to estimate the approximate surface area if height and weight be known. *Arch Intern Med* 17: 863-871, 1916.
48. Durbin J, Watson GS. Testing for serial correlation in least squares regression. II. *Biometrika* 38: 159-178, 1951.
49. Eberhart EC. Thermal models of single organs. In: Shitzer A, Eberhart RC, editors. *Heat Transfer in Medicine and Biology – Analysis and Applications*. New York London: Plenum Press, 1985, Vol. 1, Chap. 12.
50. Efron B, Tibshirani R. *An Introduction to the Bootstrap*. Boca Raton; London; New York; Washington D.C.: Chapman & Hall/CRC, 1993.
51. Ellis K. Human body composition: In vivo methods. *Physiol Rev* 80(2): 649-680, 2000.

52. Epstein Y, Stroschein LA, Pandolf KB. Predicting metabolic cost of running with and without backpack loads. *Eur J Appl Physiol Occup Physiol* 56 5: 495-500, 1987.
53. Fanger PO. *Thermal Comfort - Analysis and Applications in Environmental Engineering*. New York; London; Sidney; Toronto: McGraw-Hill, 1970.
54. Ferreira Domingos CM. Improvement of a physiological human model. Master thesis Environmental Engineering University of Lisbon, 2014.
55. Fiala D, Havenith G. Modelling human heat transfer and temperature regulation. In: Gefen A, Epstein Y, eds. The Mechanobiology and Mechanophysiology of Military-Related Injuries, Stud Mechanobiol Tissue Eng Biomater, Springer Berlin Heidelberg, 2015, (In Press). DOI 10.1007/8415_2015_183
56. Fiala D, Havenith G, Bröde P, Jendritzky G. UTCI-Fiala multi-node model of human heat transfer and temperature regulation. *Intl J Biometeorol* 56(3): 429-441, 2012.
57. Fiala D, Davey S, Psikuta A. Decision algorithms for the heat stressed worker: Numerical analysis. Prospie EU Project, Deliv. 3.2 Report: 1-50, 2011.
58. Fiala D, Psikuta A, Jendritzky G, Paulke S, Nelson DA, van Marken Lichtenbelt WD, Frijns AJH. Physiological modeling for technical, clinical and research applications. *Front Biosci* S2: 939-968, 2010.
59. Fiala D, Havenith G, Daanen H. Dynamic thermophysiological model of a worker. Prospie EU Project, Report Deliv. 3.1, 1-58, 2010.
60. Fiala D, Lomas KJ, Stohrer M. A computer model of human thermoregulation for a wide range of environmental conditions: The passive system. *J Appl Physiol* 87: 1957-1972, 1999.
61. Fiala D, Bunzl A, Lomas KJ, Cropper PC, Schlenz D. A new simulation system for predicting human thermal and perceptual responses in vehicles. In: Schlenz D, editor. *PKW-Klimatisierung III: Klimakonzepte, Regelungsstrategien und Entwicklungsmethoden*. Expert Verlag Renningen, Haus der Technik Fachbuch, 2004, Renningen, Germany, Vol. 27, pp. 147-162.
62. Fiala D, Lomas KJ, Stohrer M. First principles modelling of thermal sensation responses in steady state and transient boundary conditions. *ASHRAE Trans* 109 (1): 179-186, 2003.
63. Fiala D, Lomas KJ, Stohrer M. Computer prediction of human thermoregulatory and temperature responses to a wide range of environmental conditions, *Int J Biometeorol* 45(3), 143-159, 2001.
64. Fiala D, Lomas KJ. Application of a computer model predicting human thermal responses to the design of sports stadia. *Proceedings of the CIBSE National Conference, Harrogate*, 1999, pp. 492-499.
65. Fiala D. *Dynamic Simulation of Human Heat Transfer and Thermal Comfort*, PhD Thesis De Montfort University, 1998.
66. Fu M, Weng W, Yuan H. Numerical simulation of the effects of blood perfusion, water diffusion, and vaporization on the skin temperature and burn injuries. *Numer Heat Tr A-Appl* 65(12): 1187-1203, 2014.
67. Gagge AP. A two-node model of human temperature regulation in fortran. In: Parker Jr. JF, West VR, editors *Bioastronautics Data Book*. Washington DC: NASA SP-3006, 1971, pp. 247-262.
68. Gagge AP. An effective temperature scale based on a simple model of human physiological regulatory response. *Ashrae Trans* 77: 247-262, 1971.
69. Gagge AP, Fobelets AP, Berglund PE. A standard predictive index of human response to the thermal environment. *ASHRAE Trans* 92: 709-731, 1986.
70. Gagge AP, Nishi Y, Gonzalez RR. Standard effective temperature. *Symposium Thermal Comfort and Moderate Heat Stress*. London: CIB Commission W45, Building Research Establishment, 1972.
71. Gagge AP, Nishi Y, Heat exchange between human skin surface and thermal environment. *Comprehensive Physiology*, 2011.
72. Gagge AP, Rapp GM, Hardy JD. The effective radiant field and operative temperature necessary for comfort with radiant heating. *ASHRAE Trans* 73(1): 63-66, 1967.
73. Gisolfi CARL, Robinson S. Central and peripheral stimuli regulating sweating during intermittent work in men. *J Appl Physiol* 29: 761-768, 1970.
74. Givoni B. Estimation of the effect of climate on man: Development of a new thermal index. Technion-IIT, Building Research Station, 1963.
75. Givoni B. *Man Climate and Architecture*, London: Applied Science Publishers Ltd, 1976.
76. Givoni B, Goldman RF. Predicting metabolic energy cost. *J Appl Physiol* 30 3: 429-433, 1971.
77. Givoni B, Goldman RF. Predicting rectal temperature response to work, environment, and clothing. *J Appl Physiol* 32(6): 812-822, 1972.
78. Givoni B, Goldman RF. Predicting heart rate response to work, environment, and clothing. *J Appl Physiol* 34(2): 201-204, 1973.
79. Givoni B, Goldman RF. Predicting effects of heat acclimatization on heart rate and rectal temperature. *J Appl Physiol* 35(6): 875-879, 1973.
80. Goldman RF. Heat stress in industrial protective encapsulating garments, In: Levine SP, Martin WF, editors. *Protecting Personnel at Hazardous Waste Sites*. Ann Arbor, MI: Ann Arbor Science Publishers, 1984, pp. 295-355.
81. Goldman RF. Standards for human exposure to heat. In: Mekjavic IB, Banister EW, Morrison JB, editors. *Environmental Ergonomics*. Philadelphia: Taylor & Francis, 1988, pp. 99-138.
82. Goldman RF, Kampmann B. The Handbook on Clothing. Biomedical Effects of Military Clothing and Equipment Systems, Report NATO Research Study Group 7, 2007.
83. Gonzalez RR. SCENARIO revisited: Comparisons of operational and rational models in predicting human responses to the environment. *J Therm Biol* 29-7: 515-527, 2004.
84. Gonzalez R, Berglund L, Gagge A. Indices of thermoregulatory strain for moderate exercise in the heat. *J Appl Physiol* 44: 889-899, 1978.
85. Gonzalez RR, Cheuvront SN, Goodman DA, Blanchard LA, Berglund LG, Sawka MN. Corrections to the Shapiro Equation used to Predict Sweating and Water Requirements. Report New Mexico State Univ Las Cruces Dept of Biology T-07, 2008.
86. Gonzalez RR, Cheuvront SN, Montain SJ, Goodman DA, Blanchard LA, Berglund LG, Sawka MN. Expanded prediction equations of human sweat loss and water needs. *J Appl Physiol* 107: 379-388, 2009.
87. Gonzalez RR, Cheuvront SN, Ely BR, Moran DS, Hadid A, Endrusick TL, Sawka MN. Sweat rate prediction equations for outdoor exercise with transient solar radiation. *J Appl Physiol* 112: 1300-1310, 2012. First published January 12, 2012; doi:10.1152/japplphysiol.01056.2011.
88. Gonzalez, RR, Kenefick RW, Muza SR, Hamilton SW, Sawka MN. Sweat rate and prediction validation during high-altitude treks on Mount Kilimanjaro. *J Appl Physiol* 114(4): 436-443, 2013.
89. Gonzalez RR, McLellan TM, Withey WR, Chang SK, Pandolf KB. Heat strain models applicable for protective clothing systems: Comparison of core temperature response. *J Appl Physiol* 83: 1017-1032, 1997.
90. Gordon CC, Churchill T, Clauser CE, Bradtmiller B, McConville JT, Tebbetts I, Walker RA. 1988 anthropometric survey of U.S. army personnel: methods and summary statistics. Technical Report Nattick/TR-89/044, Yellow Springs, Ohio, 1-638, 1989.
91. Gordon RG, Roemer RB, Horvath SM. A mathematical model of the human temperature regulatory system - transient cold exposure response. *IEEE Trans Biomed Eng* 23: 434-444, 1976.
92. Gribok AV, Buller MJ, Hoyt RW, Reifman J. Individualized short-term core temperature prediction in humans using biomathematical models. *IEEE Trans Biomed Eng* 55-5: 1477-1487, 2008.
93. Gribok AV, Buller MJ, Hoyt RW, Reifman J. A real-time algorithm for predicting core temperature in humans. *IEEE Trans Inf Technol Biomed* 14-4: 1039-1045, 2010.
94. Haldane JS. The influence of high air temperatures No. I. *J Hyg* 5.04: 494-513, 1905.
95. Han TS, Lean MEJ. Anthropometric indices of obesity and regional distribution of fat depots. In: PerBjorntorp, editor. *International Textbook of Obesity*. John Wiley & Sons Ltd, 2001, pp. 51-65.
96. Haslam RA, Parsons KC. An evaluation of computer-based models that predict human responses to the thermal environment. *ASHRAE Trans* 94: 1342-1360, 1988.
97. Haslam RA, Parsons KC. Using computer-based models for predicting human thermal responses to hot and cold environments. *Ergonomics* 37(3): 399-416, 1994.
98. Havenith G. Individual Heat Stress Response. PhD Thesis, Catholic University Nijmegen, Netherlands, Ponsen and Looijen press, Wageningen, ISBN 90-9010979, 1997.
99. Havenith G. Heat balance when wearing protective clothing. *Ann Occup Hyg*, 43-5: 289-296, 1999, ISSN 0003 4878.
100. Havenith G. Individualized model of human thermoregulation for the simulation of heat stress response. *J Appl Physiol* 90: 1943-1954, 2001.
101. Havenith G, Fiala D, Blazejczyk K, Richards M, Bröde P, Holmér I, Rintamäki H, Benshabat Y, Jendritzky G. The UTCI-clothing model. *Int J Biometeorol* 56-3: 461-470, 2012.
102. Havenith G, Heus R, Lotens WA. Clothing ventilation, vapour resistance and permeability index: Changes due to posture, movement and wind. *Ergonomics* 33-8: 989-1005, 1990.
103. Havenith G, Inoue Y, Luttikholt VGM, Kenney WL. Age predicts cardiovascular, but not thermoregulatory, responses to humid heat stress. *Eur J Appl Physiol* 70-1: 88-97, 1995.
104. Havenith G, Luttikholt VGM, Vrijkotte, TGM. The relative influence of body characteristics on humid heat stress response. *Eur J Appl Physiol Occup Physiol* 70-3: 270-279, 1995.
105. Havenith G, Nilsson H. Correction of clothing insulation for movement and wind effects, a meta-analysis, *Eur J Appl Physiol* 92: 636-640, 2004.
106. Hensel H. Thermoreception and temperature regulation. *Monographs of the Physiological Society*, London: Academic Press, 1981.
107. Hensley DW, Mark AE, Abella JR, Netscher GM, Wissler EH, Diller KR. 50 years of computer simulation of the human thermoregulatory system. *J Biomech Eng* 135-2: 021006, 2013.

108. Hertig BA, Belding HS. Temperature: Its measurement and control in science and industry. *Evaluation and Control of Heat Hazards*, 1963, Part 3, Chap. 32, Reinhold Publishing Corp London.
109. Hill, LO, Griffith W, Flack M. The measurement of the rate of heat-loss at body temperature by convection, radiation, and evaporation. In: *Philosophical Transactions of the Royal Society of London. Series B, Containing Papers of a Biological Character*, Royal Society, London, 1916, pp. 183-220.
110. Hodgdon JA, Beckett MB. Prediction of percent body fat for US Navy women from body circumferences and height (No. NAVHLTHRSCHC-84-29). Naval Health Research Center SAN DIEGO CA. 1984.
111. Höppe P. The physiological equivalent temperature – a universal index for the biometeorological assessment of the thermal environment. *Int J Biometeorol* 43: 71-75, 1999.
112. Höppe P Die energiebilanz des menschen. *Wiss Mitt Meteorol Inst Uni München* 49, 1984.
113. Houdas Y, Ring EFJ. *Human Body Temperature. Its Measurement and Regulation*. New York, London: Plenum Press, 1982.
114. Houghton FC, Yaglou CP. Determining equal comfort lines. *J ASHVE* 29: 165-176, 1923.
115. Hsia TC. A prototype segmental model for blood flow and heat transfer in the limb.*Comp Progr Biomed* 4: 219-225, 1975.
116. Huizenga C, Zhang H, Arens E. A model of human physiology and comfort for assessing complex thermal environments. *Build Environ* 36-6: 691-699, 2001.
117. ISO 7243:1989, *Hot Environments – Estimation of the Heat Stress on Working Man, Based on the WBGT-Index (Wet Bulb Globe Temperature)*. Geneva: International Standards Organisation, 1989.
118. ISO 7726:1998, *Ergonomics of the Thermal Environment – Instruments for Measuring Physical Quantities*. Geneva: International Standards Organisation, 1998.
119. ISO 7933:1989, *Hot environments – Analytical Determination and Interpretation of Thermal Stress Using Calculation of Required Sweat Rate (Replaced by 2004 Version)*. Geneva: International Standards Organisation, 1989.
120. ISO 7933:2004, *Ergonomics of the Thermal Environment – Analytical Determination and Interpretation of Heat Stress Using Calculation of the Predicted Heat Strain*. Geneva: International Standards Organisation, 2004.
121. ISO 8996:2004, *Ergonomics of the Thermal Environment – Determination of Metabolic Rate*. Geneva: International Standards Organisation, 2004.
122. Ionides M, Plummer J, Siple PA. Office of the quartermaster general (US). Report from Climatology and Environmental Protection Section, September 1945.
123. Jendritzky G. Towards a universal thermal climate index UTCI for assessing the thermal environment of the human being. Memorandum of Understanding for the implementation of a European Concerted Research Action designated as COST 730. *160th CSO Meeting* December, 2004.
124. Jendritzky G, Birger Tinz B. The thermal environment of the human being on the global scale. *Glob Health Action*, 2009. Published online 2009 November 11. doi: 10.3402/gha.v2i0.2005
125. Jendritzky G, de Dear R, Havenith G. UTCI—Why another thermal index? *Int J Biometeorol*, 56-3: 421-428, 2012.
126. Jendritzky G, Maarouf A, Fiala D, Staiger H. An update on the development of a Universal Thermal Climate Index. *15th Conf. Biomet. Aerobiol. and 16th ICB02, 27 Oct-1 Nov 2002*, Kansas City: AMS, 2002, pp. 129-133.
127. Jendritzky G, Nübler W. A model analysing the urban thermal environment in physiologically significant terms. *Arch Met Geoph Biokl B*, 29: 313-26, 1981.
128. Jendritzky G, Sönning W, Swantes HJ. Ein objektives Bewertungsverfahren zur Beschreibung des thermischen Milieus in der Stadt- und Landschaftsplanung ('Klima-Michel-Modell') [An objective assessment procedure to specify the thermal environment in urban and landscape plannung ('Klima-Michel model')]. *Beiträge Akad Raumforschung Landesplanung Hannover*; 28: 1-85, 1979.
129. Jiji LM, Weinbaum S, Lemons DE. Theory and experiment for the effect of vascular microstructure on surface tissue heat transfer - part II model formulation and solution. *ASME J Biomech Eng* 106: 331-341, 1984.
130. Jones BW, Ogawa Y. Transient interaction between the human and the thermal environment. *ASHRAE Trans* 98: 189-196, 1992.
131. Journeay, WS, Reardon FD, Jean-Gilles S, Martin CR, Kenny GP. Lower body positive and negative pressure alter thermal and hemodynamic responses after exercise. *Aviat Space Environ Med* 75(10): 841-849, 2004.
132. Kalkstein LS. A new approach to evaluate the impact of climate on human health. *Environ Health Perspect* 96:145-150, 1991.
133. Kalkstein LS. Climate–health showcase projects: international heat/health watch-warning systems. In: de Dear RJ et al., editor. *Selected Papers from the Conference ICB-ICUC, Sydney, 1999*. Geneva: World Meteorological Organization/United Nations Environment Programme (WCASP-50), 2000, pp. 127-129.
134. Kalkstein, LS, Davis RE, Weather and human mortality: An evaluation of demographic and interregional responses in the Unites States, *Ann Assoc Am Geogr* 79: 44-64, 1989.
135. Kalkstein LS, Valimont KM. An evaluation of summer discomfort in the United States using a relative climatological index. *Bull Am Meteorol Soc* 67: 842-848, 1986.
136. Kampmann B, Piekarski C. The evaluation of workplaces subjected to heat stress: can ISO 7933 (1989) adequately describe heat strain in industrial workplaces? *Appl Ergon* 31-1: 59-71, 2000.
137. Kähkönen E. Comparison and error analysis of instrumentation and methods for assessment of neutral and hot environment on the basis of ISO standards. Kuopio, Finland: Kuopio University Publications, 1993.
138. Keller KH, Seiler L. An analysis of peripheral heat transfer in man. *J Appl Physiol* 30-5: 779-786, 1971.
139. Kenney WL. WBGT adjustments for protective clothing. *Am Ind Hyg Assoc J* 48: A576-A577, 1987.
140. Kenney WL, Mikita DJ, Havenith G, Crosby P. Simultaneous derivation of dry and evaporative heat exchange coefficients for military outerwear. In: H.Tokura, editor, *2nd International Symposium on Clothing Comfort Studies in Mt. Fuji (Japan)*, November 30-December 2, 1991, p. 227-244.
141. Kenney WL, Mikita DJ, Havenith G, Puhl SM, Crosby P. Simultaneous derivation of clothing specific heat exchange coefficients. *Med Sci Sports Exerc* p. 283-289, 1993.
142. Kerslake D. McK. Errors arising from the use of mean heat exchange coefficients in the calculation of the heat exchanges of a cylindrical body in a transverse wind. In: JHHardy, editor, *Temperature, Its Measurement and Control in Science and Industry*, (3rd ed.), 1963, Part 3, Reinhold Publishing Corp London.
143. Kerslake D McK. The stress of hot environments. *CUP Archive*, 1972, Vol. 29, Monographs of the Physiological Society Cambridge University Press, Cambridge, UK.
144. Kerslake D McK, Waddell JL. The heat exchanges of wet skin. *J Physiol* 141-1: 156-163, 1958.
145. Kitney RI. The analysis and simulation of the human thermoregulatory control system. *Med Biol Eng* Jan. 74, 57-65, 1974.
146. Kohler E. Physiologische Reaktionen in Bereich der Hitzetoleranzgrenze bei einer ruhenden Versuchsperson (Physiological reactions in resting test subjects at the limit of their heat tolerance). Dissertation, Universitaet Tuebingen, Tuebingen, 1976, p. 29.
147. Kondo N, Nishiyasu T, Inoue Y, Koga S. Non-thermal modification of heat-loss responses during exercise in humans. *Eur J Appl Physiol* 110-3: 447-458, 2010.
148. Koppe C, Kovats S, Jendritzky G, Menne B, Breuer DJ. Heat waves: Risks and responses. Regional Office for Europe: World Health Organization, 2004.
149. Kraning KKII, Belding HS, Hertig BA. Use of sweating rate to predict other physiological responses to heat. *J Appl Physiol* 21-1: 111-117, 1966.
150. Kraning KKII, Gonzalez RR. A mechanistic computer simulation of human work in heat that accounts for physical and physiological effects of clothing, aerobic fitness, and progressive dehydration. *J Therm Biol* 22-4: 331-342, 1997.
151. Kubaha K, Fiala D, Lomas KJ. Predicting human geometry-related factors for detailed radiation analysis in indoor spaces. *Proceedings of the IBPSA 8th Int Building Simulation Conference*, Eindhoven, Netherlands, 2003, Vol. 2, pp. 681-688.
152. Kubaha K, Fiala D, Toftum J, Taki AH. Human projected area factors for detailed direct and diffuse solar radiation analysis. *Int J Biometeorol* 49: 113-129, 2004.
153. Kubaha K. Asymmetric radiation and human thermal comfort. PhD Thesis, De Montfort University, UK, 2005.
154. Kuk JL, Lee SJ, Heymsfield SB, Ross R. Waist circumference and abdominal adipose tissue distribution: Influence of age and sex. *Am J Clin Nutr* 81: 1330-1334, 2005.
155. Kunst AE, Looman CW, Mackenbach JP. Outdoor air temperature and mortality in the Netherlands: A time series analysis: *Am J Epidemiol* 137: 331-341, 1993.
156. Kuznetz LH. A two-dimensional transient mathematical model of human thermoregulation. *Am J Physiol* 6-3: R266-R277, 1979.
157. Lee DHK. Proprioclimates of man and domestic animals. *UNESCO Arid Zone Res Ser* 10: 102-125, 1958.
158. Lemieux H, Blier PU, Tardif JC. Does membrane fatty acid composition modulate mitochondrial functions and their thermal sensitivities? *Comp Biochem Physiol A Mol Integr Physiol* 149(1): 20-29, 2008.
159. Libert JP, Candas V, Vogt JJ. Effect of rate of change of skin temperature on local sweating rate. *J Appl Physiol* 47: 306-311, 1979.
160. Libert JP, Vogt JJ, Candas V, Hoeft A. Influence des conditions hygrothermiques ambiantes sur le rendement evaporatoire de la sudation thermique. *J Physiol* 70: 717-735, 1975.

161. Lind AR, Effect of individual variation on upper limit of prescriptive zone of climates. *J Appl Physiol* 28-1: 57-62, 1970.
162. Lind AR, Hellon RF. Assessment of physiological severity of hot climates. *J Appl Physiol* 11-1: 35-40, 1957.
163. Lorenz M, Fiala D, Spinnler M, Sattelmayer T. A coupled numerical model to predict heat transfer and passenger thermal comfort in vehicle cabins. *SAE Technical Paper 2014-01-0664*, SEA International, Warrendale, PA, USA, doi:10.4271/2014-01-0664, 2014.
164. Lotens WA. How well does WBGT predict heat strain – Estimates from a mathematical model, Report TNO Institute for Perception, IZF C-12, 1986.
165. Lotens WA. Predictive thermal modelling. In: Holmes GT, Marsh PL, Vanggaard L, Doucet J, Behmann FW, editors. *Handbook on Clothing: Biomedical Effects of Military Clothing and Equipment Systems* (No. NATO-AC/243-D/7). Belgium: North Atlantic Treaty Organization Brussels, 1988.
166. Lotens WA. Heat transfer from humans wearing clothing. Delft University of Technology, PhD Thesis, 1993.
167. Machle W, Hatch TF. Heat: Man's exchanges and physiological responses. *Physiol Rev* 27.2: 200-227, 1947.
168. Malchaire J. Validation des indices de contrainte thermique pour la prédiction des astreintes et des durées limites d exposition. Rapport final de recherché CECA 7247.22.01 Luxembourg, 1986.
169. Malchaire J, d'Ambrosio Alfano F. Document presented to ISO TC159/SC5/WG1, 2014.
170. Malchaire J, Piette A, Kampmann B, Mehnert P, Gebhardt HJ, Havenith G, Den Hartog E. Development and validation of the predicted heat strain model. *Ann Occup Hyg* 45-2: 123-135, 2001.
171. Masterton JM, Richardson FA. Humidex, a method of quantifying human discomfort due to excessive heat and humidity. Downsview, Ontario: CLI 1-79, Environment Canada, Atmospheric Environment Service, 1979.
172. McArdle B, Dunham W, Holling HE, Ladel WSS, Scott JW, Thomson ML, Weiner JS. The prediction of the physiological effects of warm and hot environments. Med Res Council, London RNP Report 47/391, London, 1947.
173. McKarns, JS, Brief RS. Nomographs give refined estimate of heat stress index. *J Occup Environ Med* 8-10: 557, 1966.
174. Mehnert P, Malchaire J, Kampmann B, Piette A, Griefahn B, Gebhardt HJ. Prediction of the average skin temperature in warm and hot environments. *Eur J Appl Physiol* 82(1-2), 52-60, 2000.
175. Minard D. Prevention of heat casualties in Marine Corps recruits. *Milit Med* 126: 1961, 261-272.
176. Missenard A. A thermique des ambiences: équivalences de passage, équivalences de séjours. *Chaleur Indust* 276: 1948, 159-72 (in French).
177. Mitchell D. Human surface temperature: Its measurement and its significance in thermoregulation. PhD Thesis, University of Witwatersrand, Johannesburg, 1971.
178. Mitchell D, Atkins AR, Wyndham CH. Mathematical and physical models of thermoregulation. In: Bligh, Moore editors. *Essays on Temperature Regulation* North-Holland Publ. Col., 1972, pp. 37-54.
179. Moran DS, Epstein Y. Evaluation of the environmental stress index (ESI) for hot/dry and hot/wet climates. *Ind Health* 44: 2006, 399-403.
180. Moran, DS, and Pandolf KB. Wet bulb globe temperature (WBGT)–to what extent is GT essential?. *Aviat Space Environ Med* 70(5): 480-484, 1999.
181. Moran, DS., Pandolf KB, Shapiro Y, Laor Y, Heled Y, Gonzalez RR. Evaluation of the environmental stress index for physiological variables. *J Therm Biol* 28(1): 43-49, 2003.
182. Moran DS, Pandolf KB, Shapiro Y, Heled Y, Mathew WT, Gonzalez RR. An environmental stress index (ESI) as a substitute for the wet bulb globe temperature (WBGT). *J Therm Biol* 26(4): 427-431, 2001.
183. Moran DS, Shitzer A, Pandolf KB. A physiological strain index to evaluate heat stress. *Am J Physiol* 275: 129-134, 1998.
184. Murakami S, Kato S, Zeng J. Combined simulation of airflow, radiation and moisture transport for heat release from a human body. *Build Environ* 35: 489-500, 2000.
185. Nadel ER, Bullard RW, Stolwijk JAJ. Importance of skin temperature in the regulation of sweating. *J Appl Physiol* 31: 80-87, 1971.
186. NASA. In: Webb Associates, editor. *Anthropometric Source Book, Volume I: A Handbook of Anthropometric Data.* Athropol. Res. Proj. Staff, *NASA Reference Publication 1024*, N79-11734. Ohio: Yellow Springs, 1978, pp. I-1–IX-58.
187. NASA. In: Webb Associates, editors. *Anthropometric Source Book, Volume II: Anthropometry for Designers*. Athropol. Res. Proj. Staff, *NASA Reference Publication 1024*. Ohio: Yellow Springs, 1978, pp. 1-421.
188. Hoyt RW, Buller MJ, Gunga HC, Werner A, Sattler F, Koch J, Nevola VR, Ledderhos C, Valk P, Varoneckas G, Convertino VA, Freund BJ, Van Albert S, Smrcka P, Hana K, Kaspar J, Fiala R, Ondruska V, Eminger K, Hanousek J. Real-Time Physiological and Psycho-Physiological Status Monitoring. NATO RTO Tech. Rep. RTO-TR-HFM-132 AC/323(HFM-132)TP/283, ISBN 978-92-837-0093-7, 2010.
189. Nelson DA, Charbonnel S, Curran AR, Marttila EA, Fiala D, Mason PA, Ziriax JM. A high-resolution voxel model for predicting local tissue temperatures in humans subjected to warm and hot environments. *J Biomech Eng* 131(4): 1003, doi:10.1115/1.3002765, 2009.
190. NHANES III survey data. National Health and Nutrition Examination Survey, survey data charts also available on http://www.halls.md./, 1999. Accessed on Jul 2015
191. Niedermann R, Wyss E, Annaheim S, Psikuta A, Davey S, Rossi RM. Prediction of human core body temperature using non-invasive measurement methods. *Int J Biometeorol* 58(1): 7-15, 2014.
192. NISHI Y, GAGGE AP. Moisture permeation of clothing - a factor governing thermal equilibrium and comfort, *ASHRAE Trans* 76: 137-145, 1970b.
193. Nogueira P, Paixão E. Models for mortality associated with heatwaves: Update of the Portuguese heat health warning system. *Int J Climatol* 28(4): 545-562, 2008.
194. Novieto, Divine T. Adapting a human thermoregulation model for predicting the thermal response of older persons. Thesis deMontfort University, 2013.
195. Novieto, Divine T, Zhang Y. Thermal comfort implications of the aging effect on metabolism, cardiac output and body weight. *Adapting to Change: New Thinking on Comfort symposium, 9-11 April*, NCEUB, *Cumberland Lodge. Windsor, UK*, 2010.
196. Nunneley SA, Stribley RF. Fighter index of thermal stress (FITS): guidance for hot-weather aircraft operations. *Aviat Space Environ Med* 50(6): 639-642, 1979.
197. Pandolf KB, Givoni B, Goldman RF. Predicting energy expenditure with loads while standing or walking very slowly. *J Appl Physiol* 43: 577-581, 1977.
198. Pandolf, KB, Haisman MF, Goldman RF. Metabolic energy expenditure and terrain coefficients for walking on snow. *Ergonomics* 19(6): 683-690, 1976.
199. Pandolf KB, Stroschein LA, Drolet LL, Gonzalez RR, Sawka MN. Prediction modeling of physiological responses and human performance in the heat. *Comput Biol Med* 16(5): 319-329, 1986.
200. Pandolf KB, Stroschein LA, Gonzalez RR, Sawka MN. Prediction modeling of physiological responses and soldier performance in the heat. Army Research Inst of Environmental Medicine Natick MA No. USARIEM-M28-89, 1986.
201. Paquette S, Gordon C, Bradtmiller B. Anthropometric Survey (ANSUR) II Pilot Study: Methods and summary statistics. *Technical report NATICK/TR-09/014,* U.S. Army Natick Soldier R&D Center, Natick, Ohio: Yellow Springs, 2009, pp. 1-88.
202. Pennes HH. Analysis of tissue and arterial blood temperatures in the resting human forearm. *J Appl Physiol* 1: 93-122, 1948.
203. Pickup J, de Dear R. An outdoor thermal comfort index (OUT_SET*) - Part I - The model and its assumptions. In: de Dear R, Kalma J, Oke T, Auliciems A, editors. *Biometeorology and Urban Climatology at the Turn of the Millennium. Selected Papers from the Conference ICB-ICUC'99 (Sydney 8-12 Nov. 1999)*. Geneva: WMO, WCASP 50, 2000, pp. 279-283.
204. Psikuta A. Development of an 'artificial human' for clothing research. PhD Thesis De Montfort University, 2009.
205. Psikuta A, Fiala D, Laschewski G, Jendritzky G, Richards M, Blazejczyk K, Mekjavic I, Rintamäki H, de Dear R, Havenith G. Validation of the Fiala multi-node thermophysiological model for UTCI application. *Intl J Biometeorol* 56(3): 443-460, 2012.
206. Psikuta A, Richards M, Fiala D. Single-sector thermophysiological human simulator. *Physiol Meas* 29(2): 181-192, 2008.
207. RadTherm: Technical Documentation. Thermo Analytics Inc., 2006.
208. Richards M, Fiala D. Modelling fire-fighter responses to exercise and asymmetric IR-radiation using a dynamic multi-mode model of human physiology and results from the Sweating Agile thermal Manikin (SAM). *Eur J Appl Physiol* 92(6): 649-653, 2004.
209. Richmond V. Monitoring heat strain during work in challenging environments. Thesis Loughborough University, Environmental Ergonomics Research Centre, 2012.
210. Richmond V, Davey S, Griggs K, Havenith G. Prediction of core body temperature from multiple variables. *Annals of Ocup Hygiene* in press, 2015.
211. Richmond VL, Wilkinson DM, Blacker S, Horner FE, Carter J, Havenith G, Rayson MP. Insulated skin temperature as a measure of core body temperature for individuals wearing CBRN protective clothing. *Physiol Meas* 34(11): 1531, 2013.
212. Robinette KM, Blackwell S, Daanen H, Boehmer M, Fleming S, Brill T, Hoeferlin D, Burnsides D. Civilian American and European Surface Anthropometry Resource (CAESAR). United States Air Force Research Laboratory, Final Report, AFRL-HE-WP-TR-2002-0169, 2002.

213. Robinson S, Meyer FR, Newton JL, Tsao CH, Golgersen LO. Relations between sweating, cutaneous blood flow and body temperature in work. *J Appl Physiol* 20: 575-582, 1965.
214. Robinson S, Turrell ES, Gerking SD. Physiologically equivalent conditions of air temperature and humidity. *Am J Physiol* 143: 21-32, 1945.
215. Rodriguez JD, Perez A, Lozano JA. Sensitivity analysis of k-fold cross validation in prediction error estimation. *IEEE Trans Pattern Anal Mach Intell* 32(3): 567-575, 2010.
216. Romanovsky, AA. Thermoregulation: Some concepts have changed. Functional architecture of the thermoregulatory system. *Am J Physiol Regul Integr Comp Physiol* 292(1): R37-46, 2007. doi:10.1152/ajpregu.00668.2006
217. Rothfusz LP. The heat index equation (or, more than you ever wanted to know about heat index). *Report SR90-23,* Scientific Services Division, Fort Worth, Texas: National Oceanic and Atmospheric Administration, National Weather Service, Office of Meteorology, 90-23, 1990.
218. Rowell LB, Wyss CR. Temperature regulation in exercising and heat-stressed man. In: Shitzer A, Eberhart RC, editors. *Heat Transfer in Medicine and Biology - Analysis and Applications*. New York and London: Plenum Press, 1985, p. 53-78.
219. Rugh JP, Lustbader J. Application of a sweating manikin controlled by a human physiological model and lessons learned. *6th International Thermal Manikin and Modelling Meeting*, TBIS, Hong Kong, 2006.
220. Salloum M, Ghaddar N, Ghali K. A new transient bioheat model of the human body and its integration to clothing models. *Int J Therm Sci* 46-4: 371-384, 2007. ISSN 1290-0729, http://dx.doi.org/10.1016/j.ijthermalsci.2006.06.017.
221. Sawka MN, Latzka WA, Montain SJ, Cadarette BS, Kolka MA, Kraning KK, II, Gonzalez RR. Physiologic tolerance to uncompensable heat: Intermittent exercise, field vs laboratory. *Med Sci Sports Exerc* 33: 422-430, 2001.
222. Sawka MN, Pandolf KB. Physical exercise in hot climates: physiology, performance, and biomedical issues. In: Wenger CB, editor. *Medical Aspects of Harsh Environments*. Department of the Army, Office of the Surgeon General, Borden Institute, Washington, 2002.
223. Schickele E. Environment and fatal heat stroke; an analysis of 157 cases occurring in the Army in the US during World War II. *Military surgeon* 100(3): 235-256, 1947.
224. Severens NMW, van Marken Lichtenbelt WD, Frijns AJH, van Steenhoven AA, de Mol BAJM, Sessler DI. A model to predict patient temperature during cardiac surgery. *Phys Med Biol* 52: 5131-5145, 2007.
225. Shapiro Y, Moran D, Epstein Y, Stroschein L, Pandolf KB. Validation and adjustment of the mathematical prediction model for human sweat rate responses to outdoor environmental conditions. *Ergonomics* 38(5): 981-986, 1995.
226. Shapiro Y, Pandolf KB, Goldman RF. Predicting sweat loss response to exercise, environment and clothing. *Eur J Appl Physiol Occup Physiol* 48(1): 83-96, 1982.
227. Shitzer A. General analysis of the bioheat equation. In: Shitzer A, Eberhart RC, editors. *Heat Transfer in Medicine and Biology – Analysis and Applications*. New York London: Plenum Press, 1985, Vol. 1, Chap. 10.
228. Smith C. A Transient three-dimensional model of the human thermal system. PhD Thesis, Kansas State University, KS, USA, 1991.
229. Staiger H, Bucher K, Jendritzky G. Gefühlte temperatur. Die physiologisch gerechte bewertung von wärmebelastung und kältestress beim aufenthalt im freien in der maßzahl grad celsius. *Ann Meteorol Deutscher Wetterdienst, Offenbach* 33: 100-107, 1997.
230. Steadman RG. The assessment of sultriness. Part I: A temperature-humidity index based on human physiology and clothing science. *J Appl Meteorol* 18(7): 861-873, 1979. doi:10.1175/1520-0450(1979)018<0861:TAOSPI>2.0.CO;2 [1]
231. Steadman RG. The assessment of sultriness. Part II: Effects of wind, extra radiation and barometric pressure on apparent temperature. *J Appl Meteorol* 18(7): 874-885, July 1979.
232. Steadman RG. A universal scale of apparent temperature. *J Clim Appl Meteorol* 23(12): 1674-1687, 1984.
233. Smolander J, Ilmarinen R, Korhonen O. An evaluation of heat stress indices (ISO 7243, ISO/DIS 7933) in the prediction of heat strain in unacclimated men. *Int Arch Occup Environ Health* 63(1): 39-41, 1991.
234. Stolwijk JAJ. Mathematical Model of Thermoregulation. In: Hardy JD, Gagge AP, Stolwijk JAJ, editors. *Physiological and Behavioral Temperature Regulation*. Springfield, IL: Charles C, 1970, pp. 703-721.
235. Stolwijk JAJ. A mathematical model of physiological temperature regulation in man. NASA contractor report, NASA CR-1855, Washington DC, 1971.
236. Stolwijk JAJ, Hardy JD. Partitional calorimetric studies of responses of man to thermal transients. *J Appl Physiol* 21: 967, 1966.
237. Takada S, Kobayashi H, Matsushita T. Thermal model of human body fitted with individual characteristics of body temperature regulation, *Build Environ* 44-3: 463-470, 2009. ISSN 0360-1323, http://dx.doi.org/10.1016/j.buildenv.2008.04.007.
238. Tanabe S, Arens EA, Bauman FS, Zang H, Madsen TS. Evaluating thermal environments by using a thermal manikin with controlled skin surface temperature. *ASHRAE Trans* 100: 39-48, 1994.
239. Tanabe S, Kobayashi K, Nakano J, Ozeki Y, Konishi M. Evaluation of thermal comfort using combined multi-node thermoregulation (65MN) and radiation models and computational fluid dynamics (CFD). *Energ Buildings* 34(6): 637-646, 2002.
240. Thom EC. The discomfort index. *Weatherwise* 12: 57-60, 1959.
241. Tikuisis P, Ducharme MB. Finite-element solution of thermal conductivity of muscle during cold water immersion. *J Appl Physiol* 70: 2673-2681, 1991.
242. Tilley AR, Associates HD. The measure of man and woman: Human factors in design. In: *Whitney Library of Design*. New York: Imprint of Watson-Guptill Publications, 1993.
243. Tinz B, Jendritzky G. Europa- und weltkarten der gefühlten temperatur. In: Chmielewski F-M, Foken Th, editors. *Beiträge zur Klima- und Meeresforschung*. Berlin und Bayreuth, pp. 111-123, 2003.
244. van der Linden WJ. Equating error in observed-score equating. *Appl Psychol Meas* 30: 355-378, 2006.
245. van Marken Lichtenbelt WD, Frijns AJH, van Ooijen MJ, Fiala D, Kester AM, van Steenhoven AA. Validation of an individualised model of human thermoregulation for predicting responses to cold air. *Int J Biometeorol* 51: 169-179, 2007.
246. Varene P. Computation of respiratory heat exchanges. *J Appl Physiol* 61(4): 1586-1589, 1986.
247. Visscher TLS, Seidel JC. Time trends (1993-1997) and seasonal variation in body mass index and waist circumference in the Netherlands. *Int J Obes* 28(10): 1309-1316, 2004.
248. Vogt JJ, Candas V, Libert JP, Daull F. Required sweat rate as an index of thermal strain in industry. *Stud Environ Sci* 10: 99-110, 1981.
249. Wang F, Kuklane K, Gao C, Holmér I. Can the PHS model (ISO7933) predict reasonable thermophysiological responses while wearing protective clothing in hot environments? *Physiol Meas* 32 (2): 239, 2011.
250. Weinbaum S, Jiji LM, Lemons DE. Theory and experiment for the effect of vascular microstructure on surface tissue heat transfer - part I: Anatomical foundation and model conceptualization. *ASME J Biomech Eng* 106: 321-330, 1984.
251. Weinbaum S, Jiji LM. A new simplified bioheat equation for the effect of blood flow on local average tissue temperature. *ASME J Biomech Eng* 107: 131-139, 1985.
252. Weng WG, Han XF, Fu M. An extended multi-segmented human bioheat model for high temperature environments. *Int J Heat Mass Transfer* 75: 504-513, 2014, ISSN 0017-9310, http://dx.doi.org/10.1016/j.ijheatmasstransfer.2014.03.091.
253. Werner J. Temperature regulation during exercise: A review. In: Gisolfi CV, Lamb DR, Nadel ER, editors. *Exercise, Heat and Thermoregulation*. Dubuque: Brown & Benchmark, 1993, pp. 49-84.
254. Werner J, Buse M. Temperature profiles with respect to inhomogeneity and geometry of the human body. *J Appl Physiol* 65: 1110-1118, 1988.
255. WHO Interim report FAO/WHO/UNU Expert Consultation, Report on Human Energy Requirements. Geneva, WHO, 2004.
256. Winslow CEA, Herrington LP, Gagge AP. Physiological reactions of the human body to varying environmental temperatures. *J Physiol* 120-1, 1937.
257. Wissler EH. The effect of longitudinal conduction of heat on the cooling of the finger. US Army Medical Research Laboratory Report No. 363. Fort Knox, KY: US Army, 18 December, 1958.
258. Wissler EH. Steady-state temperature distribution in man. *J Appl Physiol* 16: 734-740, 1961.
259. Wissler EH. An analysis of factors affecting temperature levels in the nude human. *Temperature, its Measurement and Control in Science and Industry* Vol. III, Part 3, Biology and Medicine. Edited by James D. Hardy. New York: Reinhold; London: Chapman and Hall, 603-612, 1963.
260. Wissler EH A mathematical model of the human thermal system. *Bull Math Biophys* 26: 147-166, 1964.
261. Wissler EH Mathematical simulation of human thermal behavior using whole body models. In: Shitzer A, Eberhart RC, editors. *Heat Transfer in Medicine and Biology – Analysis and Applications*. New York London: Plenum, 1985, pp. 325-373.
262. Wissler EH, Pasche A. Diver response to hot water loss at depths greater than 300 meters: Experimental observations and theoretical interpretation. In: HOmhaaen, editor. *Proceedings of the XIIth Annual Meeting of the European Undersea Biomedical Society*, Bethesda, Md. (9650 Rockville Pike, Bethesda 20814): Undersea Medical Society, pp. 7-14, 1985.
263. Wissler EH. A review of human thermal models. In: Mekjavic IB, Banister EW, Morrison JB, editors. *Environmental Ergonomics*. New York: Taylor and Francis, 1988, pp. 267-285.

264. Wissler EH. Pennes' 1948 paper revisited. *J Appl Physiol* 85.1: 35-41, 1998.
265. Wölki D, van Treeck C, ibpsa.org. Individualization of a mathematical manikin model in terms of gender, age and morphological issues for predicting thermal comfort: A Preliminary Study 2013, *Proceedings of BS2013: 13th Conference of International Building Performance Simulation Association*, *International Building Performance Simulation Association*, Loughborough, UK, Chambéry, France.
266. Wölki D, van Treeck C, Zhang Y, Stratbücker S, Bolineni SR, Holm A. Individualisation of virtual thermal manikin models for predicting thermophysical responses. *Proceeding of the Indoor Air Conference*, International Society of Indoor Air Quality and Climate – ISIAQ, Santa Cruz, california, Austin; Texas, 2011.
267. Wulff W. The energy conservation equation for living tissue. *ISEE Trans BME* 21(6): 494-495, 1974.
268. Wyndham CH, Atkins AR. A physiological scheme and mathematical model of temperature regulation in man. *Pflügers Arch* 303: 14-30, 1968.
269. Xu X, Tikuisis P. Thermoregulatory modeling for cold stress. *Compr Physiol* 4: 1057-1081, July 2014.
270. Xu X, Werner J. A dynamic model of the human/clothing/environment system. *Appl Human Sci* 16: 61-75, 1997.
271. Yaglou CP, Minard D. Control of heat casualties at military training centers. *AMA Archives of Industrial Health* 16.4: 302-316, 1957.
272. Yokota M, Berglund L, Cheuvront S, Santee W, Latzka W, Montain S, Moran D. Thermoregulatory model to predict physiological status from ambient environment and heart rate. *Comput Biol Med* 38(11): 1187-1193, 2008.
273. Yokota M, Berglund LG, Bathalon GP. Monte Carlo simulations of individual variability and their effects on simulated heat stress using thermoregulatory modeling. *J Therm Biol* 35-3: 154-159, 2010. ISSN 0306-4565, http://dx.doi.org/10.1016/j.jtherbio.2010.02.002.
274. Yousaf R, Fiala D, Wagner A. Numerical simulation of human radiation heat transfer using a mathematical model of human physiology and computational fluid dynamics (CFD). In: Nagel EW, Kröner D, Resch M, editors. *High Performance Computing in Science and Engineering '07 Trans. High Performance Computing Center Stuttgart*. Heidelberg: Springer Berlin, 2007, Part 8, pp. 647-666
275. Zhang H, Huizenga Ch, Arens E, Yu T. Considering individual physiological differences in a human thermal model. *J Thermal Biology* 26 (4-5): 401-408, 2001. ISSN 0306-4565, http://dx.doi.org/10.1016/S0306-4565(01)00051-1.
276. Zhou X, Lian Z, Lan L. An individualized human thermoregulation model for Chinese adults. *Build Environ* 70: 257-265, 2013. ISSN 0360-1323, http://dx.doi.org/10.1016/j.buildenv.2013.08.031.
277. Zintl W. Physiologische Reaktionen im Bereich der Hitzetoleranzgrenze vor und nach Hitzeakklimation bei einer ruhenden Versuchsperson (Physiological reactions in resting test subjects at the limit of their heat tolerance before and after acclimatization to heat). Dissertation, Universitaet Tuebingen, 1979, pp. 56.
278. Zunis foundation website, http://www.zunis.org/index.html, accessed January 20, 2014.